IFJ PAN

Report on research activities 2014–2016

The Henryk Niewodniczański Institute of Nuclear Physics
Polish Academy of Sciences, Kraków, Poland

Report on research activities 2014–2016

The Henryk Niewodniczański
Institute of Nuclear Physics
Polish Academy of Sciences

Radzikowskiego 152
31–342 Kraków, Poland
http://www.ifj.edu.pl

Phone: +48-12-6628200
Fax: +48-12-6628458
e-mail: dyrektor@ifj.edu.pl

Report on research activities 2014–2016

October 2017

CONTENTS

INTRODUCTION

The Henryk Niewodniczański Institute of Nuclear Physics, Polish Academy of Sciences (IFJ PAN) counts among the topmost Polish research centres (the highest, A+ rank awarded after a nation-wide governmental assessment of all research institutions). IFJ PAN is a member of the Marian Smoluchowski Consortium which has been granted the status of a Leading National Research Centre, KNOW (Krajowy Naukowy Ośrodek Wiodący) for the years 2012–2017.

IFJ PAN was especially successful over the period 2014-2016, both in terms of fundamental research and the application of nuclear physics for the benefit of the society. The latter is due to the Cyclotron Centre Bronowice (CCB) which became operational on 15 October 2015. It is now a state-of-the-art proton therapy centre and a research laboratory, operating two proton cyclotrons: 60 MeV AIC-144 and 230 MeV Proteus C-235 from IBA Belgium. With two experimental halls and three treatment rooms, serviced by two rotating gantries with Pencil Scanning Beam as well as a horizontal line for eye treatment, CCB is a modern clinical centre for the treatment of cancer patients. Advanced dosimetry, quality assurance tools, Dual Energy Computed Tomography and Treatment Planning Systems are available both for cancer therapy and research in oncology and medical physics.

Understanding the structure of matter and interactions between its constituents down to the smallest possible scale is one of the most difficult tasks of modern science, and a driving force for the research carried out at IFJ PAN. This effort encompasses subnuclear, nuclear, and molecular physics, and extends towards the most distant parts of the Universe. Research conducted at IFJ PAN is by no means limited to "pure" physics. Quite the contrary: a number of on-going projects are interdisciplinary science, done together with chemists, environmental scientists, biologists, medical doctors, not to mention materials engineers. So profiled are also PhD studies at our Institute.

Progress in research would never be possible without international projects in the field of large research infrastructure (CERN, GSI, GANIL, LNL/LNS, ILL, to name just a few in Europe; RIKEN, ANL, JINR and other worldwide). Engineers at IFJ PAN are Europe's renowned specialists whose work at CERN has been acknowledged for years, who were recognised during the building of XFEL (European X-Ray Free Electron Laser), and who can now be met at the construction site of European Spallation Source.

Dear Reader, I invite you to take a closer look at the activities and accomplishments of our Staff and to share their enthusiasm in the quest for keys to the Nature's most interesting puzzles.

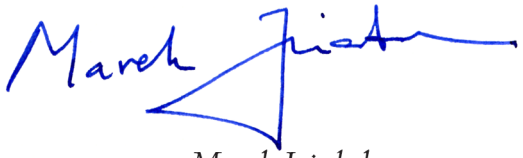

Marek Jeżabek
Director General

RESEARCH HIGHLIGHTS 2014–2016

I. DIVISION OF PARTICLE AND ASTROPARTICLE PHYSICS

The main aim of research at the Division of Particle and Astroparticle Physics is to explore the fundamental structure of the Universe by studying the basic constituents of matter – fundamental particles – and forces governing particle interactions. Since the 1970s, the Standard Model of particle physics has described the principal structure of matter. Matter is formed from fundamental quarks and leptons which interact via four forces that adhere to symmetry and invariance principles. However, the Standard Model is unable to describe 96% of the known Universe and unsolved problems and mysteries remain. The ambition of contemporary particle physics is to seek an explanation of well-established features of the Universe, not accounted for by the Standard Model, such as the nature of Dark Matter, matter-antimatter asymmetry, neutrino masses and many other issues. On the theoretical side, the effort is focused on extending the Standard Model by adding new interactions and new fundamental particles. This has to be verified by experimental findings, such as experimental evidence for the *Supersymmetry* theory. To further verify the Standard Model and to unveil the theory beyond the Standard Model, particle physicists use the most powerful particle accelerators, both man-made and natural – as offered by cosmic acceleration mechanisms. Research teams of our Division contribute to this worldwide effort aimed at gaining a deeper knowledge and better understanding of the Universe.

Our groups participate in leading particle and astro-particle physics projects undertaken by large international collaborations at world's best experimental facilities. We are involved in all phases of such projects: from initial design, optimization, and construction of detector systems, preparation of research programs, active participation in data analyses, to maintaining and upgrading novel detector systems. Our ongoing activities are fully in line with all current project requirements.

The high-energy front projects include the ATLAS and LHCb experiments at the CERN Large Hadron Collider (LHC), and cosmic-ray experiments, such as the Pierre Auger Project, the CROME experiment, and the H.E.S.S. and HAWC astronomical observatories. High-precision physics is performed by the Belle experiment at the KEKB (Tsukuba, Japan), the STAR experiment at the Brookhaven (BNL) Relativistic Heavy Ion Collider, and the H1 and ZEUS experiments at the HERA collider in Hamburg (DESY). In the area of neutrino physics we are involved in the T2K experiment at the Japan Proton Accelerator Complex, the ICARUS experiment at Gran Sasso (Italy), and the SUNLAB project. Among the above-listed projects, there are ongoing projects as well as some projects (Belle, ICARUS, H1 and ZEUS), which no longer collect data, but still analyse them.

Over the recent years we have witnessed further remarkable achievements reported by the LHC experiments. Following the spectacular discovery of the Higgs boson by the ATLAS and CMS experiments back in 2012, the research conducted by these two general-purpose experiments focused on measurements of properties of the newly discovered particle and on the search for particles and phenomena not described by the Standard Model. The IFJ PAN team of **The ATLAS Experiment Department** is actively contributing to this research. The present activities include detector operation and development, data collection and processing as well as physics analyses of this data. In 2015, the LHC has entered into a new high-energy frontier both for proton-proton and lead-lead collisions, providing the physics community with excellent opportunities for searches beyond the Standard Model. The thrust of the study pursued in the Department is fermion decays of the Higgs boson, and specifically decays to *tau* leptons and *b*-quarks. In parallel, we explore the physics of strongly interacting matter at extreme energy densities, where the Quark-Gluon Plasma phase of matter is formed, using the data on lead-lead and proton-lead collisions. The third domain of the activities of The ATLAS Experiment Department is the precise measurement of protons as they emerge from collisions at small angles, the so-called forward region, aimed at studying elastic and diffractive scattering processes. Our teams are also actively involved in the upgrades of the ATLAS detector for the high-luminosity LHC (HL-LHC) operations foreseen beyond the year 2020.

Another LHC experiment, the LHCb project, is focused on investigating the tiny difference between matter and antimatter by studying particles containing heavy quarks, the *c*- or *b*-quark. Our physicists at the **LHCb Experiment Department** are involved in this study. The activities of this group involve measurements of rare processes with an unprecedented accuracy as well as searches for processes violating the fundamental symmetry principles. Complementary studies of heavy flavour production and multiparticle correlations in the unique forward region at LHC, covered by the LHCb spectrometer, are also being performed. An upgrade of the LHCb detector system to follow the upgrade of the LHC accelerator, including its HL-LHC phase is already at an advanced stage. Members of our Department actively contribute to this LHCb upgrade.

Studies of rare processes in the flavour domain, performed at B-factories, provide an alternative way to seek effects beyond the Standard Model. Such a study is performed by the team of the **Department for Leptonic Interactions**, by their participation in the Belle and Belle II experiments at the High Energy Accelerator Research Organization (KEK) in Tsukuba, Japan. The team's effort is focused on rare decays of particles containing heavy quarks, using the unique data sample of 1000 fb^{-1} collected at the KEKB e^+e^- collider in the energy region of $\Upsilon(nS)$ (n = 1, 2, 4, 5) resonances. Of particular interest are measurements of semitauonic B decays which challenge the Standard Model predictions. In parallel, there is vigorous preparation of an upgraded detector, Belle II. This new detector, together with the upgrade of the e^+e^- accelerator facility, would allow us to collect 50 times more data than that from Belle, and to further extend studies of violation of symmetry between particles and antiparticles. The first data collection runs using the Belle II detector are planned in 2017.

Physicists at the **Department on Neutrino and Dark Matter Studies** explore the neutrino domain of particle physics. The main ongoing activity is within the T2K experiment (Tokai to Kamioka), focused on studies of neutrino oscillations, on precise measurements of the neutrino mixing parameters and on measurements of cross sections of various final states of neutrino interactions. The ICARUS experiment has now been terminated, but there is still ongoing activity with data analysis, eg. studies of atmospheric neutrinos. This year also marked the completion of the physics feasibility study for the Polish site of the next generation of neutrino experiments, the SUNLAB project (Sieroszowice Underground Neutrino Laboratory). The possibility of organising a small SUNLAB laboratory, with an extremely low radioactive background, remains open.

The very high-energy frontier is probed by cosmic-ray experiments using particles arriving from outer space, of energies much higher than the beam energy of the LHC. The group at the **Department of Cosmic Ray Research** participates in the Pierre Auger project, aimed at searching for yet unknown sources of cosmic rays of the highest energy ever observed. A hybrid detection technology is employed in order to increase the precision of the measurements and to extend the physics potential of the Project. Along with the Pierre Auger Project, members of this Department are engaged in feasibility studies of cosmic ray detection in the microwave range, performed within the CROME experiment. Recently, this team also initiated a new project within the area of "citizen science", namely the CREDO (Cosmic Ray Extremely Distributed Observatory) project.

The team of the **Department of Gamma-Ray Astrophysics** investigates cosmic sources of particles and radiation of high energy in an effort to understand the origin of cosmic rays and to explore the extreme environment of powerful cosmic accelerators. The Department's activities involve both theoretical modelling and observations of highest-energy gamma-ray sources. On the theoretical side, these studies concern particle acceleration processes in cosmic plasma systems, such as shocks waves of supernova remnants, pulsar wind nebulae or jets of active galaxies. For this purpose, high-performance supercomputers are used to perform large-scale *ab-initio* Particle-In-Cell numerical simulations. Astronomical observations are performed using ground-based facilities, such as the High Energy Stereoscopic System (H.E.S.S.) and the High-Altitude Water Cherenkov (HAWC). The team is also involved in a preparatory phase of the Cherenkov Telescope Array (CTA) project, a next-generation ground-based observatory which will provide unprecedented sensitivity for detection of gamma rays over a very broad energy range.

Along with ongoing involvement in the currently running accelerator projects, we are also looking into the more distant future by actively participating in some future developments. These include next-generation linear electron-positron colliders (ILC/CLIC) and post-LHC era circular colliders (FCC-Future Circular Colliders). The team at the **Department of Linear Colliders** is engaged in these activities.

Successful management of high-energy physics experiments requires large computing resources to store and analyse huge amounts of experimental data. Therefore, we are also heavily involved in a global collaboration to link distributed computer centres, within the WLCG (Worldwide LHC Computing Grid), and in particular in the development of the Polish Tier 2 at the ACK Cyfronet AGH and of the local Tier 3 facility at our Institute. Furthermore, the **"Cloud Computing for Science and Economy"** project (http://cc1.ifj.edu.pl.), financed from structural funds within the POIG grant of the European Commission and by the Polish Ministry of Science and Higher Education, was successfully completed in 2014. An individual-user cloud system has been in operation since the beginning of 2012. It has been extensively used for calculations by various research teams of the Institute and by external collaborators. The system provides resources within the available infrastructure in a self-service mode via an intuitive Web interface. Sharing computing resources among various groups greatly enhances multi-user efficiency of the infrastructure, at the same reducing maintenance costs by a large factor.

The Departments of our Division are well integrated and cooperate in computing, education, organization of conferences, seminars and outreach events. We also closely cooperate with other Divisions of our Institute, especially with the Division of Theoretical Physics, the Division of Nuclear Physics and Strong Interactions and the Division of Scientific Equipment and Infrastructure Construction.

In the following, we give more detailed descriptions of selected research highlights in which groups of our Division were strongly involved over the last few years, and their achievements.

SELECTED RESEARCH HIGHLIGHTS OF THE DIVISION OF PARTICLE AND ASTROPARTICLE PHYSICS

Recent measurements performed at the LHC have benefitted from increases in collision energy and volume of data collected. Using these data, we were actively involved in the **search for charged Higgs bosons** in the τ+jets final state using 14.7 fb^{-1} of proton-proton collision data recorded at $\sqrt{s}$ = 13 TeV **within the ATLAS experiment**. Experimental observation of charged Higgs bosons, $H^{\pm}$, which are predicted by several models with an extended Higgs sector, would indicate physics beyond the Standard Model. The results of this search for charged Higgs bosons were obtained with active participation of physicists from IFJ PAN. The search focuses on the τ+jets channel in top-quark-associated $H^{\pm}$ production with a hadronically decaying W boson and a τ lepton in the final state (Fig. 1). No evidence of any charged Higgs boson has been found so far. For the $m_{H^{\pm}}$ mass range 200 – 2000 GeV, upper limits have been set on the production cross section of a charged Higgs boson with the subsequent decay $H^{\pm} \rightarrow \tau\nu$ over the range 2.0 – 0.008 pb, as illustrated in Fig. 2.

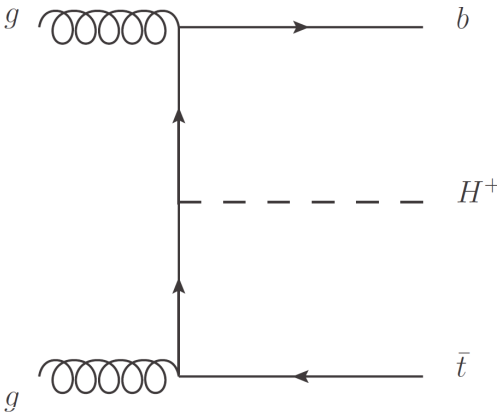

Fig. 1 *Feynman diagram of the leading-order for the production of a charged Higgs boson with mass $m_{H+}>m_{top}$, in association with a single top quark.*

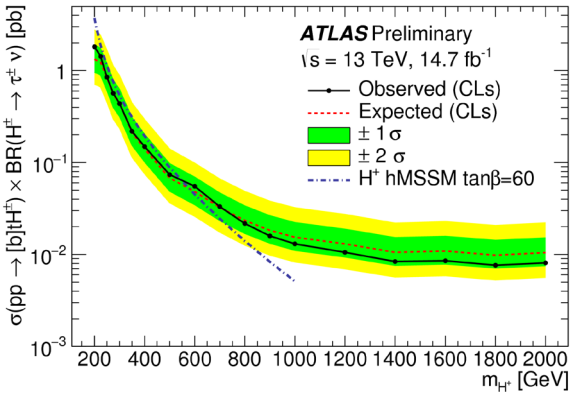

Fig. 2 *Observed and expected 95% CL exclusion limits for heavy charged Higgs boson production as a function of m_{H^+}. The prediction for $\sigma(pp \rightarrow [b]t\,H^+) \times BR(H^+ \rightarrow \tau\nu)$ as a function of the charged Higgs boson mass is also shown as a dotted-dashed line, for tanβ = 60 in the hMSSM benchmark scenario.*

Data collected by the ATLAS experiment during the 2015 heavy ion LHC run offer a new opportunity to probe properties of quark-gluon plasma (QGP) at unprecedently high temperatures and densities. In 2015, relativistic lead (Pb) ions were collided at the LHC at the largest energy ever obtained in the laboratory, providing lead-lead collisions at the centre-of-mass energy of 5.02 TeV per pair of interacting nucleons. Additionally, reference proton-proton data at energies of 5.02 and 13 TeV were also recorded. The ATLAS group at the IFJ PAN is actively involved in **the study of collective phenomena** in different collision systems. Collectivity is assessed by measurements of Fourier harmonics, v_n, of azimuthal angle distributions of the produced charged particles. First measurements from the ATLAS experiment of the azimuthal anisotropy of charged hadrons, both in small proton-proton and large Pb+Pb systems were performed. For Pb+Pb collisions at $\sqrt{s_{NN}}$ = 5.02 TeV, the second and higher-order Fourier harmonics (up to v_7) over wide ranges of transverse momenta, pseudorapidity and centrality were obtained (see Fig. 3). The measurements are based on the Scalar Product and Two Particle Correlation methods and are compared with results concerning Pb+Pb collisions at the lower LHC energy. The obtained results are crucial for understanding properties of the hot and dense system created in heavy-ion collisions.

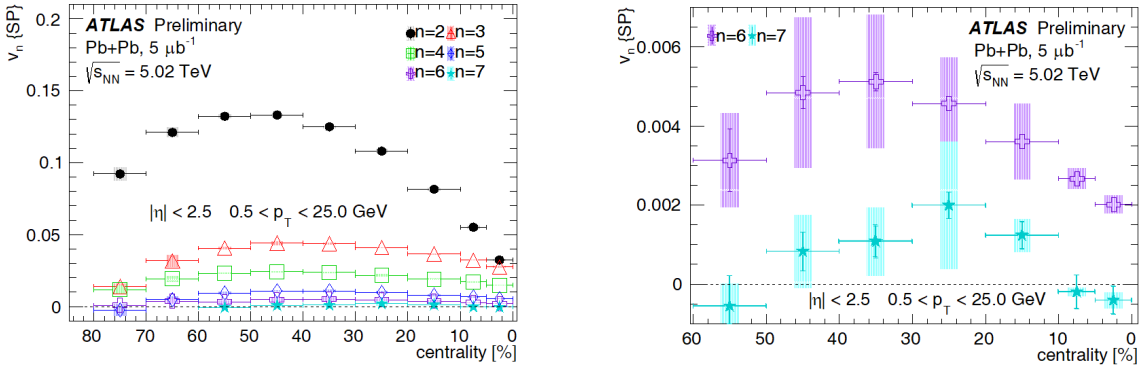

Fig. 3 *The left plot shows Fourier harmonics, v_n, as a function of centrality (increasing from left to right) for Pb+Pb collisions at 5.02 TeV. The right plot shows only v_6 and v_7 with a zoomed vertical scale.*

A study of **collectivity in proton-proton collisions** was also performed using the **ATLAS** data [Phys. Rev. Lett. **116** (2016) 172301]. Interestingly, measurements of the two-particle correlations (Fig. 4) show that the second order Fourier harmonic of particle azimuthal angle distributions, v_2 (or elliptic flow), in proton-proton collisions is approximately constant as a function of multiplicity. We also found that the transverse momentum dependence of v_n in the small proton-proton system is similar to that measured in Pb+Pb collisions.

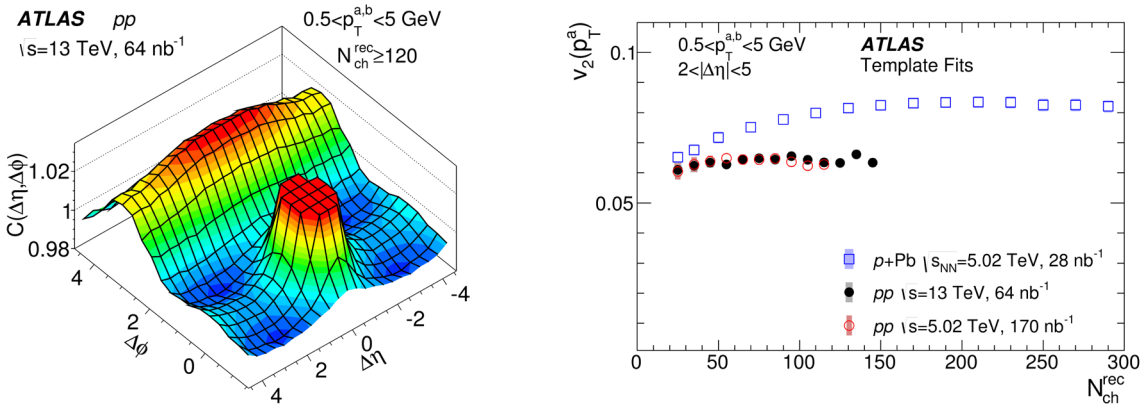

Fig. 4 *Two-dimensional correlation function, $C(\Delta\phi,\Delta\eta)$, for 13 TeV proton-proton collisions (left panel) and the Fourier harmonic v_2 in 13 TeV and 5.02 TeV proton-proton, and 5.02 TeV p+Pb collisions, as a function of multiplicity, N_{ch}^{rec} (right panel).*

The IFJ PAN group at the **LHCb** collaboration has contributed to **searches for very rare or forbidden processes that violate various fundamental symmetries of the SM**. Any experimental observation of such decays would provide a strong evidence of physics beyond the Standard Model. In particular, analyses of $\tau\to\mu\mu\mu$ and $\Lambda_b\to K\mu$ decays have been performed and other decay modes are being searched for. Angular distributions of decay products are a very sensitive probe of phenomena beyond the SM. Analysis of the $B^0\to K^{*0}\mu\mu$ decay showed an anomaly against theoretical predictions (Fig. 5). Possibly, with the data now being recorded, this puzzle will be resolved.

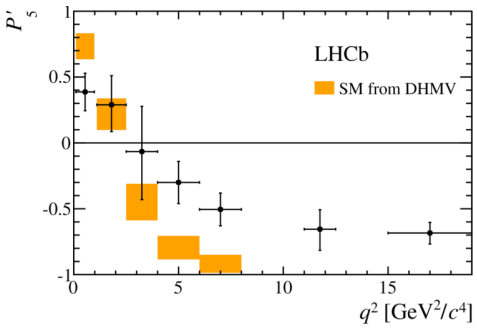

Fig. 5 *Distribution of the P_5' angular observable as a function of mass squared of the muon pair q^2 for $B^0 \to K^{*0}\mu\mu$ decay [JHEP* ***02*** *(2016) 104].*

The **Belle** collaboration continues to explore the data sample collected at the KEKB collider, which includes 742 million $\overline{B}B$ pairs produced in $\Upsilon(4S)$ decays. Hadronic B decays mediated by the b→c quark transition provide a good opportunity to **study the spectroscopy of charmed mesons**. Decays of the type $\overline{B} \to D_s^- KM, (M = \pi, K)$ allow one to study charmed resonances in the poorly known mass region above 2.5 GeV/c^2. Fig. 6 presents the effective mass distribution of the $D_s^- K_S^0 \left(D_s^- K^+\right)$ system measured in the decay. The $\overline{B}^0 \to D_s^- K_S^0 \pi^+ \left(B^+ \to D_s^- K^+ K^+\right)$ broad peak observed around 2.6 GeV/c^2 indicates the dominance of resonance production over this mass region, and may be assigned to radial excitations of the D mesons. Further studies of the observed structure could shed light on several puzzles of the b → c transitions that remain to be resolved.

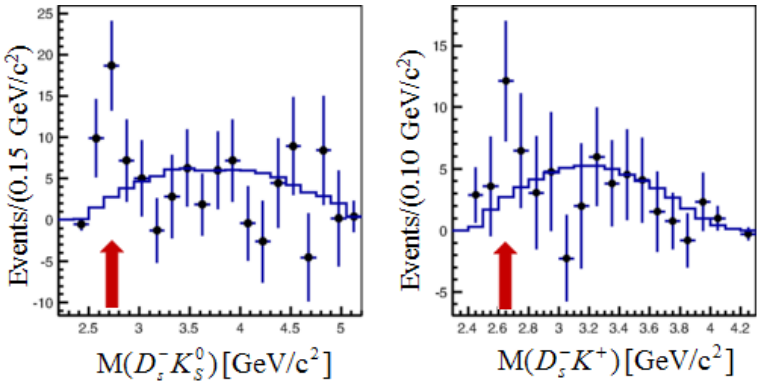

Fig. 6 *Hints of resonant structures in the invariant mass distributions of $D_s^- K_S^0$ for the $\overline{B}^0 \to D_s^- K_S^0 \pi^+$ (left) and $D_s^- K^+$ for $B^+ \to D_s^- K^+ K^+$ (right). Points with error bars represent data after background subtraction; the histograms show the phase-space distribution of the signal MC sample normalized to data luminosity [Phys. Rev. D* ***91*** *(2015) 032008].*

In 2016, the **H1** Collaboration published their final results of the **QCD instanton searches** [Eur. Phys. J. **C76** (2016) 381], where the contribution of IFJ PAN physicists was significant. No evidence for the production of QCD instanton-induced events has been observed. Upper limits on the cross-section for instanton-induced processes between 1.5 pb and 6 pb at 95% confidence level were obtained, depending on the kinematic domain in which instantons could be produced (Fig. 7). Compared to earlier publications, QCD instanton exclusion limits have been improved by one order of magnitude. For the first time these results challenge predictions based on perturbative instanton calculations with

parameters derived from lattice QCD. These limits may be used to assess the compatibility of theoretical assumptions such as that of the dilute instanton gas approximation with H1 data, or to test theoretical predictions of instanton properties such as their size and distance distributions.

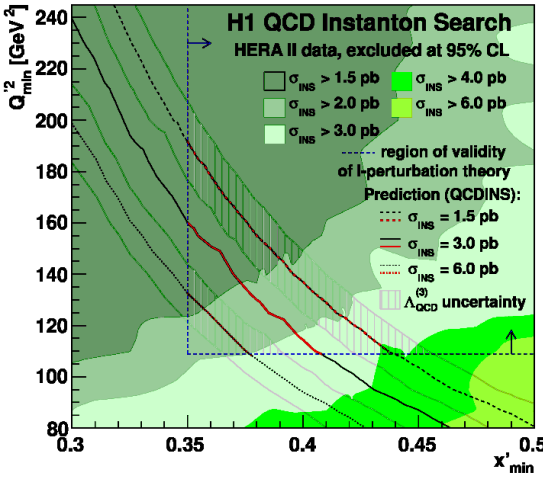

Fig. 7 *Upper limits on the instanton cross-section at 95% confidence level, as a function of x'min and* $Q'^2_{\min}$. *Also shown are isolines of the predicted fixed instanton cross-section and the effect of varying the QCD scale* $\Lambda^{(3)}_{QCD} = (339 \pm 17)$ *MeV defined in the* $\overline{MS}$ *scheme within uncertainties. The instanton cross section extrapolated beyond the indicated region of validity of instanton perturbation theory is also shown.*

The announcement by the T2K (Tokai to Kamioka, in Japan) long baseline neutrino experiment of **an indication for a strong violation of the CP symmetry for neutrinos** was one of the highlights of the most important particle physics conference ICHEP 2016. Considerable improvements in the performance of the J-PARC accelerators, in data taking and in data analysis were necessary for this achievement. The T2K experiment uses the accelerator muon neutrino and antineutrino beams produced at J-PARC in Tokai and registers their interactions by two near detectors, ND280 and INGRID, located at J-PARC and by the Super-Kamiokande far detector in Kamioka, at a distance of 295 km. Over the years 2014–2016 the proton beam power of the J-PARC Main Ring Synchrotron was doubled, resulting in extensive neutrino and antineutrino data samples of 7.48×10^{20} POT and 7.47×10^{20} POT, respectively. Over the same period several results on neutrino oscillations have been published by the T2K collaboration. Among the most important are the first direct observation of the appearance of electron neutrino in the muon neutrino beam with a statistical significance of 7.3 σ, precise measurement of the neutrino mixing parameter θ_{23} pointing to its maximum value, first analyses combining measurements of muon neutrino disappearance and electron neutrino appearance to estimate the four oscillation parameters, Δm^2_{23}, θ_{23}, θ_{13}, and δ_{CP}, and the neutrino mass ordering, a first-time indication of a tendency for strong violation of the CP symmetry for neutrinos and finally the first T2K measurement of muon-antineutrino oscillations. Results presented at ICHEP 2016 were based on the updated combined oscillation analysis in the framework of three neutrino flavours and, for the first time, also three antineutrino flavours, using the full data samples. T2K's new data follow earlier trends, i.e. a preference for maximal disappearance of muon neutrinos and a discrepancy between the electron neutrino and electron antineutrino appearance rates. T2K observes 32 electron neutrinos and 4 electron antineutrinos, while around 24 neutrinos and 7 antineutrinos are expected at no CP violation. As shown in Fig. 8, the actual T2K data yield a 90% confidence interval for δ_{CP} of $[-0.99\pi; -0.12\pi]$ ($[-0.67\pi; -0.24\pi]$) for the normal (inverted) neutrino mass ordering. The best fit points lie near the maximally CP violating value $\delta_{CP} = -0.5\pi$, with the CP conserving values ($\delta_{CP} = 0$ and $\delta_{CP} = \pi$) remaining outside of the T2K 90% confidence level interval.

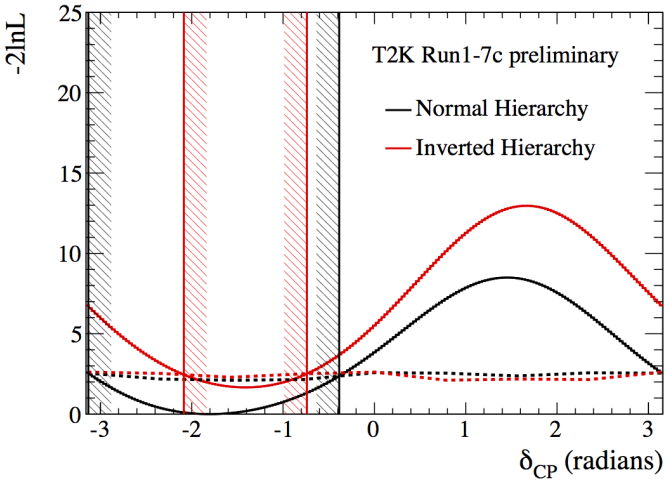

Fig. 8 *The measured allowed 90% CL intervals as a function of* δ_{CP} *and mass hierarchy with the full data set, presented at the ICHEP 2016 conference.*

First experimental characterization of microwave emission from cosmic ray air showers, obtained by the CROME (Cosmic-Ray Observation via Microwave) experiment, suggests that microwave emission is not dominated by molecular bremsstrahlung, as was previously believed. The observed microwave emission is consistent with MHz radio emission of air showers, amplified over directions close to the Cherenkov angle due to the time compression effect, with frequency shifted upwards into the GHz range. The MHz emission of air showers stems mainly from geomagnetic and Askaryan radio emission caused by the deflection of electrons and positrons of the shower disk in Earth's magnetic field and by the charge excess in the shower front, respectively. The CROME experiment was located in the centre of the KASCADE-Grande air shower array in Karlsruhe, Germany. It consisted of various radio antennas covering a wide range of frequencies from about 1 MHz up to 12 GHz. Of these frequencies the most important one was the C-band (3.4-4.2 GHz) offering measurements with the lowest noise and nearly perfect atmosphere transparency. Three C-band antennas were pointed along different directions (upward, and tilted by 15° towards the magnetic north and magnetic south) to observe parts of the sky with varying angles relative to the local geomagnetic field. The read-out of all antennas was triggered by the detection of high-energy air showers in the KASCADE-Grande array. Microwave signals were detected from over 30 showers of energies above 3×10^{16} eV, as shown in Fig. 9.

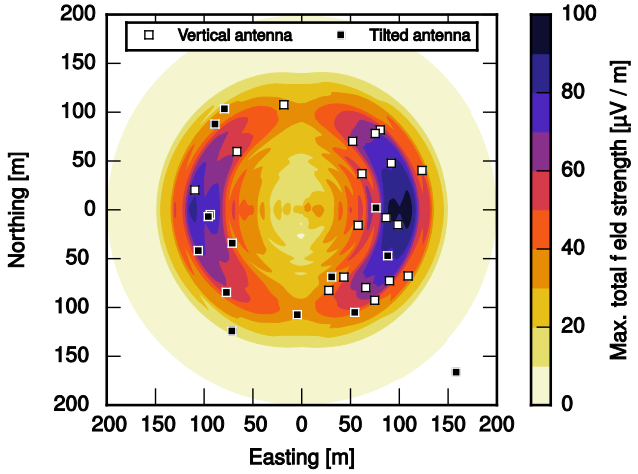

Fig. 9 *Positions at which the microwave signal was detected relative to the shower core at (0,0). The coloured contours indicate the maximum total field strength at ground level predicted by the CoREAS simulation for a typical vertical shower of energy* 10^{17} *eV [Phys. Rev. Lett.* ***113*** *(2014) 221101].*

The spatial and angular distributions of the observed microwave signal agree well with results of simulations of MHz emission of air showers performed by the CoREAS program. The structure of the Cherenkov-like ring, the east-west asymmetry and the polarisation pattern are qualitatively well reproduced by the data. In addition, most showers were detected at their forward direction with viewing angles of the emission region compatible with the Cherenkov angle in air, at altitudes above 3 km (close

to the expected maximum of shower development). Thus, the GHz observations are consistent with the known signatures of MHz radio emission of high-energy charged particles in an air shower, collimated within the Cherenkov angle cone.

The number of muons in air showers has been studied by the Pierre Auger Collaboration, using observations of inclined air showers. Such inclined showers allow the number of muons at ground level to be measured directly, since the electromagnetic component is mostly absorbed at the large atmospheric depth crossed by the shower. The analysis was based on 174 air showers with zenith angles between 62° and 80°, and of energies between 4×10^{18} and 5×10^{19} eV, recorded simultaneously with the surface detector array and the fluorescence detector of the Pierre Auger Observatory. The number of muons in each shower was derived by scaling a simulated reference profile of the lateral muon density distribution at ground level until it fitted the data. A deficit of average muon content $\langle R_\mu \rangle$ was shown in simulations, ranging from 30 to 80% at 10^{19} eV, depending on the nuclear interaction model. The calculated logarithmic gain of muons ($\mathrm{d}\langle \ln R_\mu \rangle / \mathrm{d} \ln E$) is compatible with model predictions – its value favours a transition from lighter to heavier elements in the considered energy range. Measurement of the muon number, combined with previous measurements of the depth of the air shower maximum, provides important insights into the consistency of hadronic interaction models. The hadronic and muonic components of air showers are less well understood than the electromagnetic component. Improvements in the description of the muon component are necessary to reduce systematic uncertainties in simulations of air showers. The study demonstrated that the mass composition of cosmic rays can be inferred from the muon number measured at ground level (Fig. 10). To fully explore this appproach, the apparent muon deficit in air shower simulations needs to be resolved and the uncertainty of the muon measurements to be further reduced. Improvement expected in the near future, such as upgrade of the detectors (AugerPrime), will significantly enhance the constraining power of muon measurement on mass composition.

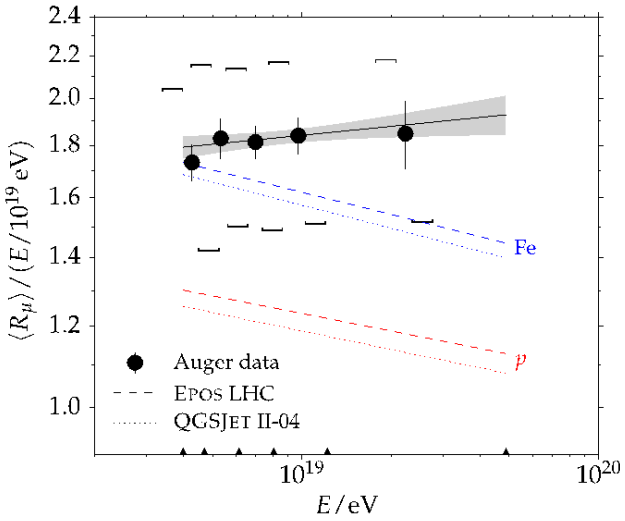

Fig. 10 *Average muon content $\langle R_\mu \rangle$ per shower energy E, as a function of energy in double logarithmic scale. Data (circles) are shown in bins of equal number of air showers, together with a fit (line); square brackets indicate the systematic uncertainty of measurement. Shown for comparison are theoretical predictions for air showers induced by protons and iron nuclei [Phys. Rev. D* **91** *(2016) 032003].*

Cosmic-Ray Extremely Distributed Observatory (CREDO) is a recently inaugurated, international project to organize the existing cosmic-ray infrastructure under one operational entity. This will enable efficient global analysis of cosmic-ray data to be performed, enhancing its sensitivity to extremely extended cosmic-ray phenomena presently missed by individual detectors or observatories. The meeting at which the CREDO Collaboration was inaugurated was held at IFJ PAN on August 30, 2016, with about 50 attendees from 9 countries. The CREDO science is focused on indirectly searching for Super Heavy Dark Matter by observing very large electromagnetic cascades initiated above Earth's atmosphere. Within the Super Heavy Dark Matter scenarios it is assumed that production of supermassive particles (of mass $\geq 10^{23}$ eV) could have occurred in the early Universe during the inflation phase. Such particles may annihilate or decay at present, leading to production of jets containing mainly photons, including such that have extremely high energies, of even 10^{20} eV, or higher. Such photons could reach the Earth unaffected or they might initiate electromagnetic cascades well above the Earth's atmosphere.

The latter option is presently a scientific *terra incognita*. Given the fundamental uncertainties about the physics in the above energy range, one cannot make any predictions about the properties of cascades initiated by extremely energetic photons or by other particles. Such cascades, called shortly super-preshowers, are considered within the CREDO strategy in a general manner, with no pre-assumptions about their properties, such as their spatial or temporal distributions, particle energy spectrum or shape of the shower front. The practical issue to be resolved by CREDO is to determine which types of super-preshowers may be observed on Earth with the presently available infrastructure. There is an obvious, though so far unprobed, „detection horizon" for super-preshowers. This "horizon" could be located anywhere between an obviously detectable air shower induced by a super-preshower composed of tightly collimated particles (not yet observed) or an obviously undetectable super-preshower composed of particles spread out so widely that only a few of them could reach the Earth (cf. Fig. 11).

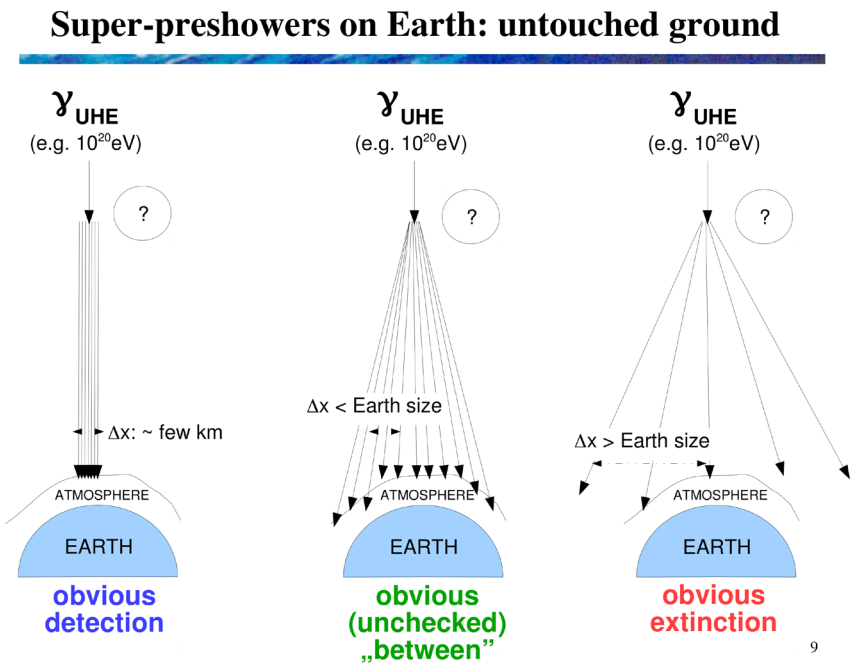

Fig. 11 *A qualitative illustration of the unprobed potential of detecting large electromagnetic cascades (super-preshowers) with the available cosmic-ray infrastructure organized in a global network. [P. Homola, plenary talk at the Pierre Auger Collaboration meeting].*

CREDO will probe this super-preshower „detection horizon", which should either lead to the observation of physical phenomena so far unseen or to setting upper limits to the existence of large electromagnetic cascades. In either case, constraints to theoretical models dealing with particles of the highest energies will emerge.

The **H.E.S.S.** (High Energy Stereoscopic System) observatory **discovered three extremely bright stellar-type sources of very high-energy gamma rays** in the Large Magellanic Cloud – a dwarf satellite galaxy of the Milky Way [Science **347** (2015) 406]. These sources are (see Fig. 12): the N157B nebula – the most powerful known source of pulsar wind, the old supernova remnant N132D – the brightest gamma-ray source, and the so-called superbubble 30 Dor C – a huge spherical shell in the interstellar medium blown by the winds of massive stars and supernovae. Their high-energy gamma-ray emission indicates that these objects are powerful accelerators of cosmic-ray particles. The pulsar wind nebula N157B is associated with the most energetic pulsar known. However, it is a less effective particle accelerator than the famous Crab pulsar. The enormous gamma ray brightness of N157B is due to the lower magnetic field strength and intense starlight from neighbouring star-forming regions. Efficient production of cosmic rays in such an old supernova remnant as N132D poses a serious challenge to the current theory of particle acceleration at shock waves. Superbubble 30 Dor C represents a new class of sources

in the very high-energy regime. Extreme physical conditions in this source lead to efficient acceleration of cosmic rays to very high energies.

The Centre of our Galaxy, the Milky Way, harbours the nearest super-massive black hole (Sgr A*). For over a decade this was a target of prime importance to the H.E.S.S. Observatory, which detects

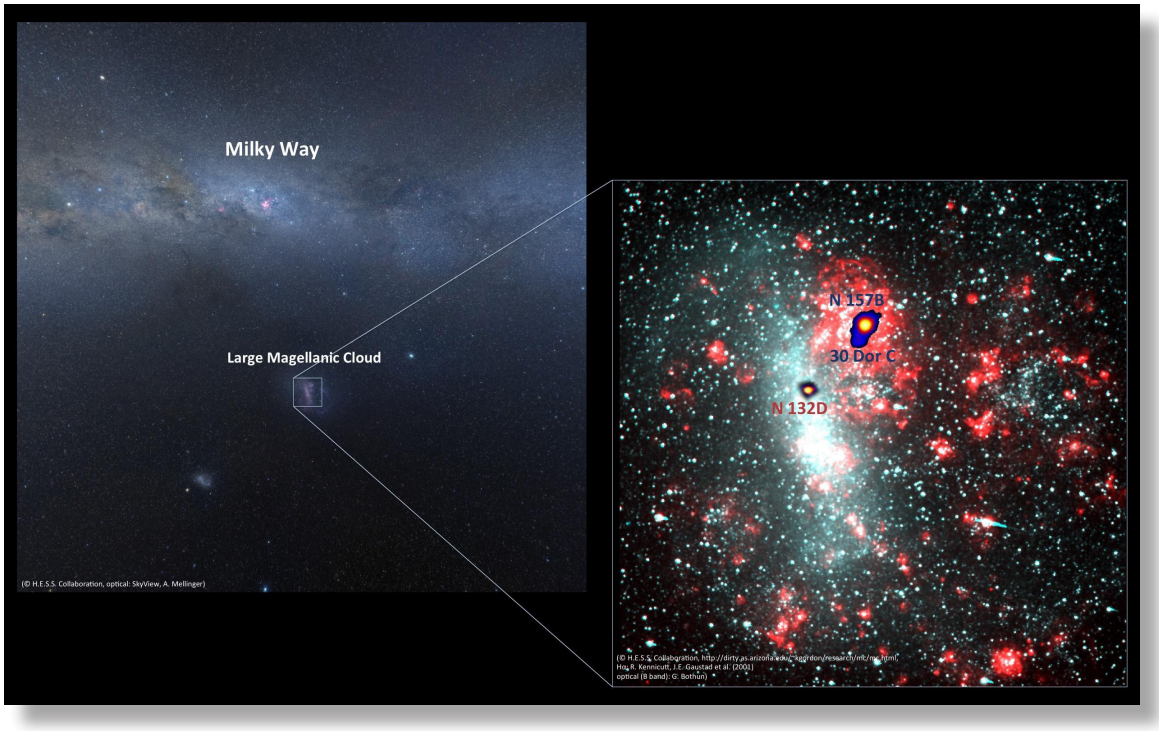

Fig. 12 *Optical image of the sky with the Milky Way and the Large Magellanic Cloud and a zoom into the LMC with optical and Hα images. Superimposed are H.E.S.S. sky maps of the three powerful cosmic particle accelerators discovered. (Milky Way image: ©H.E.S.S. Collaboration, optical: SkyView, A. Mellinger; LMC image: ©H.E.S.S. Collaboration, http://dirty.as.arizona.edu/~kgordon/research/mc/mc.html, Hα: R. Kennicutt, J.E. Gaustad et al. (2001), optical (B-band): G. Bothun).*

high-energy gamma rays. Gamma-ray photons can be produced in interactions of cosmic rays with ambient matter. Detailed analysis of a 10-year observational data set led in 2016 to a **discovery in the Galactic Centre of the source of cosmic rays with Peta-Electronvolt (PeV) energies,** a hundred times higher than those achieved in LHC at CERN [Nature **531** (2016) 476], see Fig. 13. This unprecedentedly violent particle accelerator is most likely the central black hole – Sgr A*. These results mark a significant step in the ongoing debate about the origin of cosmic rays – which so far has indicated supernova remnants as the prime sources of PeV Galactic cosmic rays.

The research group at the Department of Linear Collider of our Institute, studies various aspects of **measurements of the photon structure function for the future e^+e^- linear collider**, ILC/CLIC (International Linear Collider/Compact Linear Collider), within the FCAL (Forward CALorimeters) and CLICdp (CLIC detector and physics) collaborations. The planned maximum collision energy in the centre-of-mass system is 1 TeV at the ILC and 3 TeV at the CLIC. As the available energy will be higher than that in previous experiments, it is expected that it would be possible to examine the photon structure function in the range of lower Bjorken-x and higher scale of photon virtuality Q^2. In particular, at CLIC energies measurements can be performed over x down to ~10^{-4} and over Q^2 up to $10^5 GeV^2$. Measurements of photon structure functions are investigated using the so-called single-tag events arising from the deep-inelastic scattering (DIS) process in e^+e^- collisions, where the electron or the positron scatters on the almost real photon and can be detected if its polar angle is above some detection threshold. Simultaneously, there is a veto on the second tag anywhere in the detector. These studies are performed using the structure of the detectors prepared for future experiments. Monte Carlo simulations of DIS events are provided by different programs, such as PYTHIA, HERWIG,

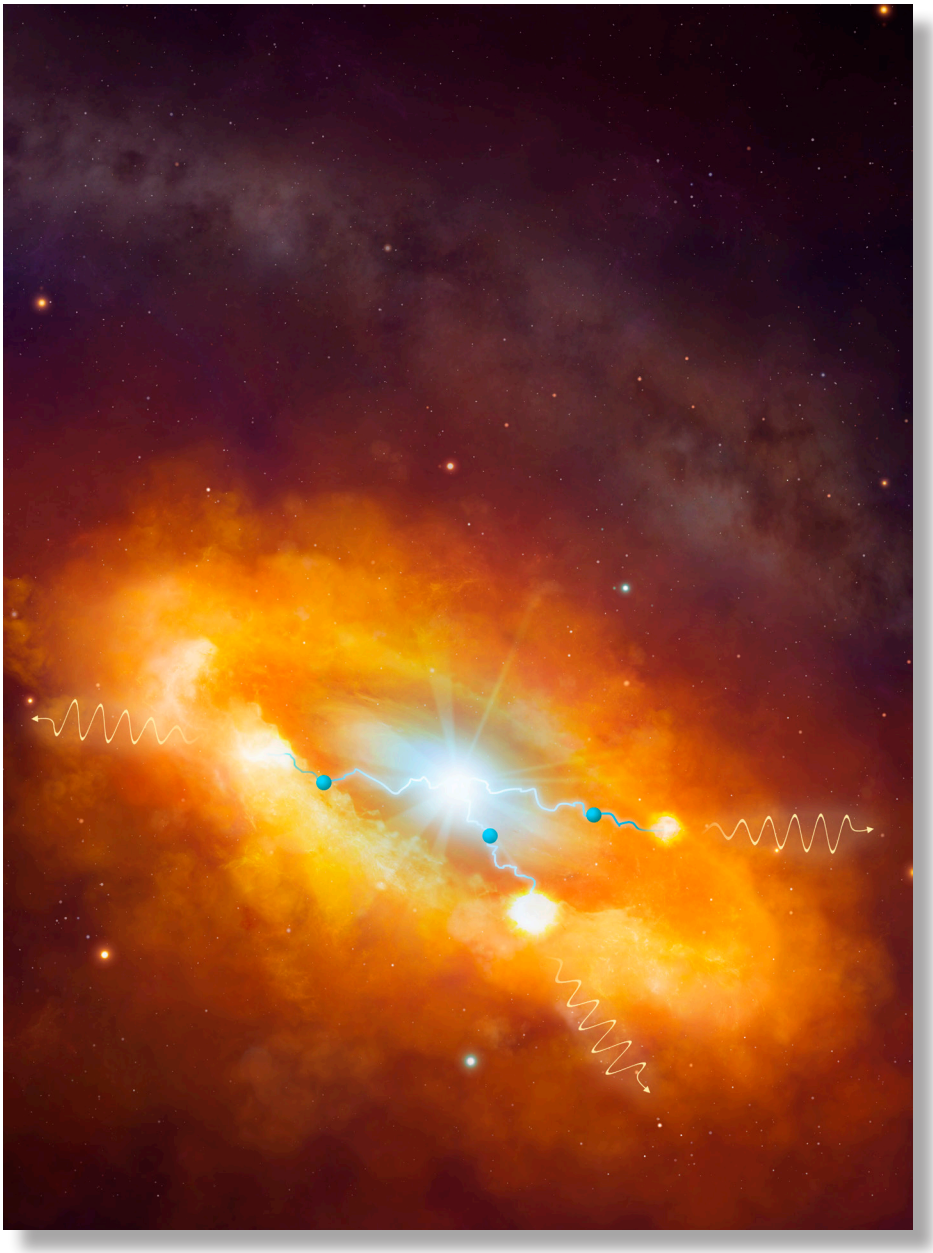

Fig. 13 *Cosmic Pevatron in the Galactic Centre. Artist's view of the gamma-ray emission production near the central supermassive black hole Sgr A*. Relativistic protons (blue spheres) injected by Sgr A* propagate diffusively until they interact with interstellar protons of the surrounding giant molecular clouds producing neutral pions that decay into gamma rays (yellow wave).* © ***Dr Mark A.*** *Garlick (Mark Garlick Words and Pictures Ltd, Quality Space Art and Animation)/ H.E.S.S. Collaboration.*

WHIZARD or TWOGAM, and using the global software ILCSoft. It is possible to track particles in the detectors (package Mokka) and reconstruct (package Marlin) the physical quantities from information provided by Mokka. The electron or positron tag is obtained from special forward detectors of the FCAL collaboration: BeamCal and LumiCal, and in the main part of the electromagnetic calorimeter (ECAL Endcap). Preliminary results of this research at limited statistics for ILC at $\sqrt{s_{ee}} = 500\,\mathrm{GeV}$ are presented in Fig. 14. They confirm the validity of such research in the future linear collider. These analyses are continued in order to increase the statistics and to account for systematic effects.

The IFJ PAN research and engineering staff was also actively involved in **designing, building and installation of the ATLAS Forward Proton (AFP) detector** which significantly extends the range of physics at ATLAS by tagging and measuring the momentum and emission angle of very forward protons. It will enable observation and measurement of a range of processes where one or both protons

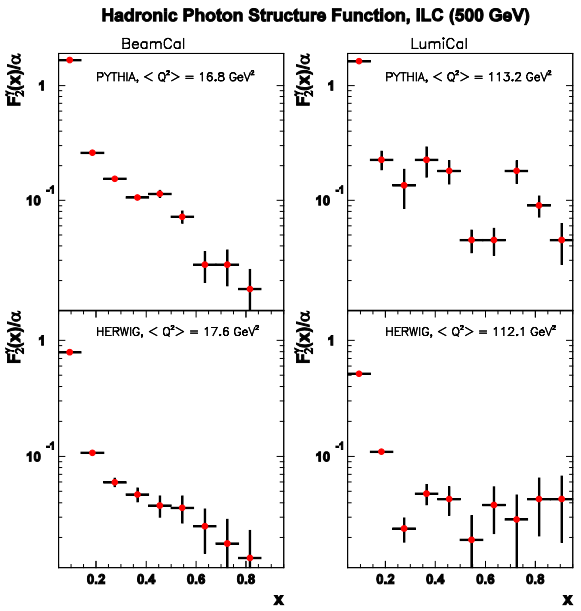

Fig. 14 *Values of $F_2^\gamma\left(x,Q^2\right)$ as a function of x as obtained from PYTHIA and HERWIG Monte Carlo generators and by ILCSoft global software. The points represent calculations with their statistical errors only. In this analysis electrons are tagged in the BeamCal and LumiCal detectors.*

remain intact, which otherwise would be difficult to study. Such processes are typically associated with elastic and diffractive scattering, where the proton radiates a virtual colourless "object," the so-called Pomeron, which is often thought of as a non-perturbative collection of soft gluons.

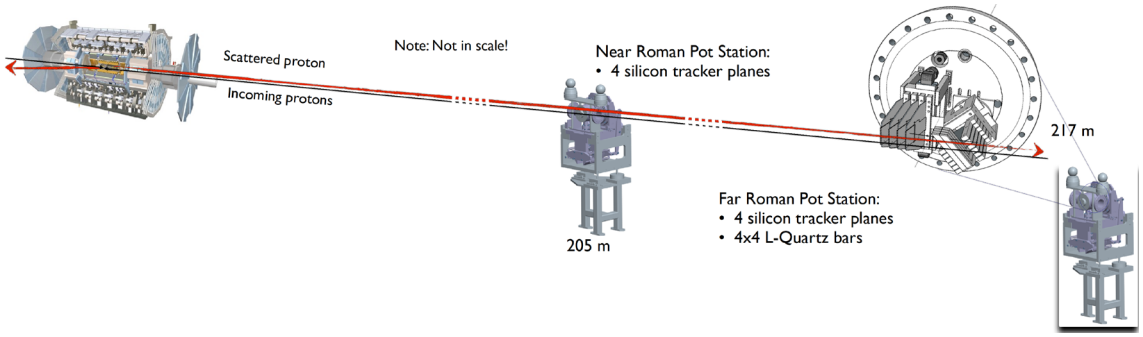

Fig. 15 *The 2016 layout of the AFP detector.*

A major step in the ATLAS forward physics program took place at the end-of-year 2015-2016 shutdown when the AFP tracking system (see Fig. 15) at one side ("one arm") of the interaction point was installed with a significant contribution of the IFJ PAN personnel. The full two-arm system, with both tracking and timing detectors at both sides of the interaction point, is planned to be completed during the extended end-of-year shutdown of 2016-2017.

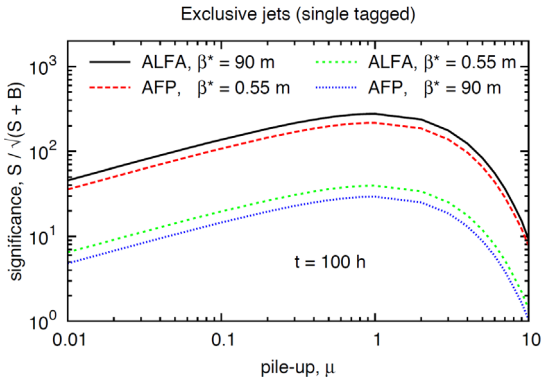

Fig. 16 *Statistical significance for 100 hours of data-taking as a function of pile-up.*

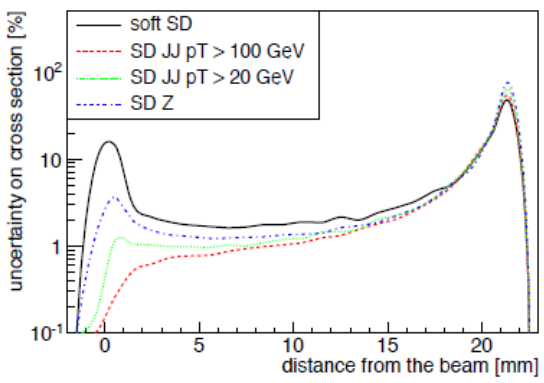

Fig. 17 *Relative error on the cross section due to a 100 μm absolute horizontal misalignment for several diffractive processes.*

The one-arm AFP detector has successfully collected the first proton-proton data in August 2016. These are currently analysed. The details of alignment-related effects on track reconstruction in AFP at the LHC were recently investigated. Propagation of the detector alignment-related effects into the uncertainties of the reconstructed track parameters and cross-sections were studied for different scenarios, as shown in Fig. 16. Feasibility studies of measurement of the central exclusive jet production at the LHC using the proton tagging technique were also performed at the centre-of-mass energy of 14 TeV and the ATLAS detector. The expected significance of the central exclusive dijet cross-section measurement for a data collection period of 100 h has been estimated, as shown in Fig. 17.

The **Belle II** spectrometer at the SuperKEKB e^+e^- collider with the designed peak luminosity of $8\times10^{35}\text{cm}^{-2}\,\text{s}^{-1}$ is a new generation B-factory that is under construction at KEK. To fully explore the potential of the new facility, precise measurements of the magnetic field inside the detector volume are mandatory. For this purpose, **a robotic device for precise magnetic field mapping has been designed at IFJ PAN**. The project consists of three sets of arrays of 3D Hall probes, two of them stationary, and one rotating inside the volume, to be used by vertex detectors. The rotating structure (Fig. 18) is driven by a piezoelectric motor, and servo-controlled using STM32 based electronics which is able to orient the probes with a precision better then $1/2^{12}$ of 360° rotation ($1/2^{10}$ is required by physics constrains). The robot is being constructed by the IFJ PAN team in cooperation with a Polish company Urbicum, providing an excellent opportunity for technology transfer from high-energy physics community to local industry.

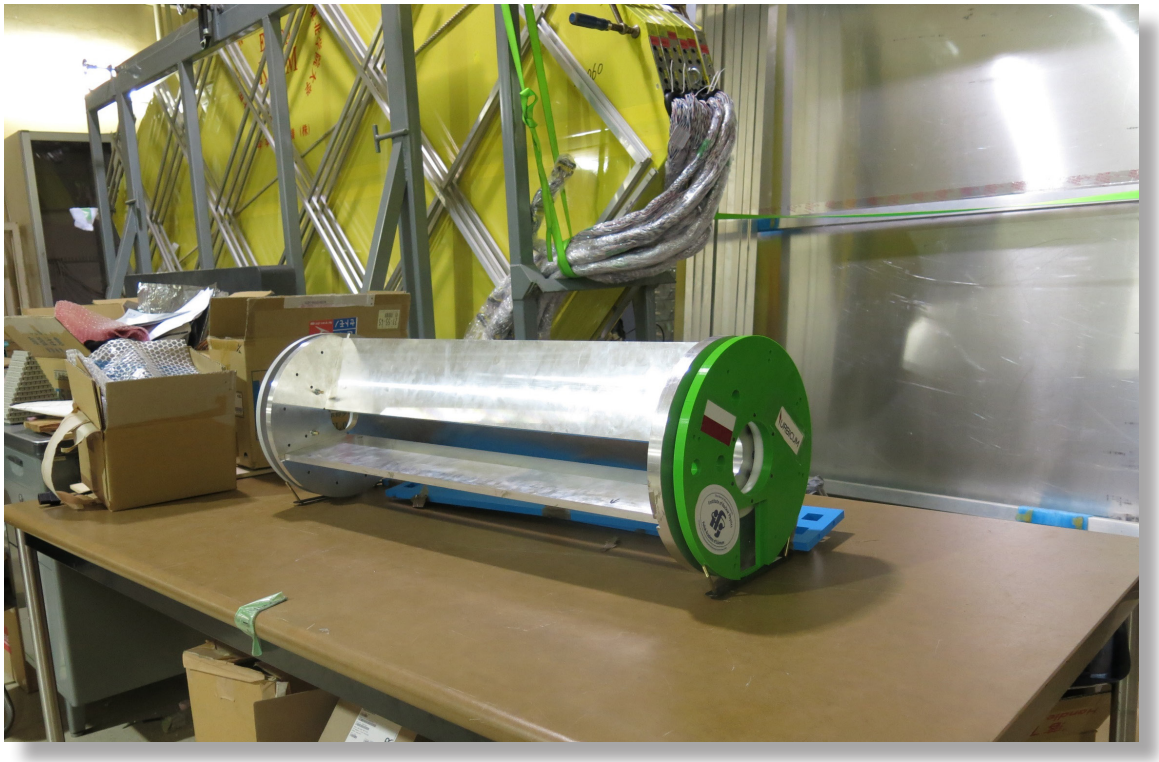

Fig. 18 *Rotating structure of the robotic device for precise magnetic field mapping, during tests at KEK.*

II. DIVISION OF NUCLEAR PHYSICS AND STRONG INTERACTIONS

Nuclear physics is fundamental to our understanding of the world. It explains the most basic questions about the physical universe and its origin. At our Institute research in experimental and theoretical nuclear physics is carried out at the **Division of Nuclear Physics and Strong Interactions, which consists of four Departments.** Investigations in the field of nuclear structure are the topic of the **Department of the Structure of Atomic Nucleus**. Within this area of research, stimulated by scientific interest and by society's needs, the general thrust is to measure and explain properties of atomic nuclei. More specifically, it is to develop a predictive understanding of nuclei and of their role in the Universe, as governed by fundamental quantum chromodynamics (QCD) and electroweak theory, and based on experimental data covering a wide range of nuclides. Of particular interest are those which lie in unexplored territories of the nuclear landscape.

Studies concerning nuclear reactions and the properties of strong interactions are the domain of the **Department of Nuclear Reactions and Hadronic Processes**. Here, of primary interest is gaining a profound knowledge of hadron-hadron interactions and of nuclear reactions – to understand the emergence of hadrons from quarks and gluons and the mechanism of formation of more complex structures such as atomic nuclei.

Investigations of the physics of strongly interacting matter at extreme energies and densities are undertaken at the **Department of Ultrarelativistic Nuclear Physics and Hadron Structure**. These investigations are mostly aimed at gaining information about the primordial quark-gluon plasma (QGP) which had existed in the Early Universe, just a few microseconds after the Big Bang, and turned into hadrons as the temperature decreased. Such information, unavailable from any astronomical observation, can be obtained only by studying heavy ion collisions at extremely high energies.

Theoretical studies addressing a broad variety of issues in nuclear physics are carried out at the **Department of Theory of Strong Interactions and Many-Body Systems**. Here, the research interest ranges from quantum chromodynamic (QCD) descriptions of ultrarelativistic nucleon-nucleon or nucleus-nucleus collisions to nuclear fission and nuclear shape transitions. These investigations are based on our belief that quantum chromodynamics, together with the theory of electroweak interactions, both of which are the main pillars of the Standard Model, will provide the basis for a general understanding of the emergence of hadrons from quarks and gluons, and of the formation and the structure of atomic nuclei.

Most of our investigations are realised through international collaborations, many of which are located around Large Scale Facilities in Europe, such as GSI (Darmstadt, Germany), GANIL (Caen, France), COSY (Jülich, Germany), LNL (Legnaro, Italy) or IPN (Orsay, France). A number of projects have also been located at other world-leading laboratories, such as CERN, ILL (Grenoble, France), ANL (Argonne, USA) or RIKEN (Wako, Tokyo, Japan). In many of these projects, the research staff of our Division plays a key role.

A brief description of our results in areas of research performed at our Division is given in the section below, while some highlights of the achievements of our Divisions are described in more detail in the last part of this chapter.

NUCLEAR STRUCTURE RESEARCH

We have studied nuclear structure over various regions of the nuclear chart by performing experiments with radioactive and stable beams and by combining several methods, such as discrete gamma-ray spectroscopy, high-energy gamma ray detection and charged particle or heavy-ion scattering. Our scientific accomplishments over the past three years were closely connected with the development in our Department of nuclear radiation detection systems in which cutting-edge technology is applied.

A successful attempt was made at LNL-INFN, Italy to Coulomb-excite low spin states, at the band-head of the superdeformed (SD) band in ^{42}Ca. Coincident γ–rays were measured with the AGATA Demonstrator (AD) – a prototype of a new generation of γ-ray spectrometers. This pioneering experiment provided the first evidence of triaxiality associated with the development of superdeformation in the A~40 mass region.

On the other hand, investigations of high-spin states in the ^{49}V nucleus, produced in the fusion-evaporation reaction ^{28}Si (^{28}Si,α3p), revealed the termination of the rotational band due to full angular momentum alignment at the spin of I = 31/2. This result emerged from a detailed analysis of the experiment performed earlier at IPHC, France with the Cracow Recoil Filter Detector (RFD), coupled to EUROBALL – the precursor of the latest γ-tracking detector arrays.

We are expecting a breakthrough in our high-spin investigations of A~40 nuclei, due to the availability of AGATA and PARIS γ-spectrometers and of the DIAMANT particle detector array, now operating at the GANIL accelerator centre in Caen, France. Currently we are involved in preparing elements of this setup which will be used in a forthcoming experiment aimed at discrete and continuum γ-spectroscopy of the superdeformed ^{44}Ti nucleus.

The pygmy dipole resonances (PDRs) are another type of collective excitations that were objects of our recent studies. Inelastic scattering of ^{17}O ions on a ^{140}Ce target was employed to investigate the PDR states in the ^{140}Ce nucleus at LNL-INFN, Italy. Use of a loosely bound ^{17}O beam prevented any background γ-radiation related to projectile excitation, thus enabling exclusive measurement and unambiguous determination of the E1 character of high energy (Eγ > 5MeV) γ-rays deexciting the PDR in ^{140}Ce nucleus. Our investigations of PDR excitations in nuclei over different mass regions, using hadronic probes, such as protons and alpha particles, are presently continued at RCNP Osaka.

We have investigated high-spin states, including long-lived isomers, in the neutron-rich nuclides $^{118\text{-}128}$Sn, ^{204}Hg and ^{207}Tl produced in fission or multinucleon transfer processes by studying the collisions of ^{48}Ca, ^{64}Ni and ^{208}Pb projectiles with thick targets made of ^{238}U and ^{208}Pb. This new information on isomer lifetimes and on their decay pattern was extracted from a large data set of γ-ray coincidences collected in experiments performed at the ATLAS accelerator at Argonne National Laboratory (USA), using the GAMMASPHERE Ge detector array.

High-spin structures have also been studied in neutron-rich nuclei, products of fission of ^{235}U and ^{241}Pu targets induced by an intense, highly collimated cold neutron beam from the nuclear reactor at ILL, France. Gamma rays were detected in the EXILL Ge detector array complemented by a set of fast $LaBr_3$ scintillators – FATIMA, used to determine lifetimes. In particular, striking changes in the coupling between the valence proton and excitations of the ^{132}Sn core, along the yrast line in the one-proton-valence ^{133}Sb nucleus were revealed. Also, a new isomeric state, the isomerism of which arises from the change of nuclear shape, was identified in ^{96}Y.

We have participated in testing the possibility of performing γ-spectroscopy studies of exotic fragments produced in fusion-fission and transfer-fission reactions induced by a ^{238}U beam on a ^{9}Be target. A proof-of-principle experiment was performed at the GANIL laboratory in Caen, France, using the VAMOS++ mass spectrometer to select products of interest with mass numbers A~130, and the AGATA Ge detector array placed at the target position, and the EXOGAM array located at the focal plane of the VAMOS++ spectrometer, to detect the associated prompt and delayed γ rays. This approach will enable further complex γ-spectroscopy of very exotic nuclides to be performed, including nuclides produced in nuclear reactions induced by radioactive beams provided by SPIRAL at GANIL.

Radioactive ion beams (RIB) provide access to nuclides located far from the β-stability line. Such secondary beams can be produced either by "*in-flight*" selection of residues of fragmentation reactions induced by heavy, relativistic projectiles impinging on light targets, or by the "*ISOL*" method, i.e. by separation and reacceleration of fission fragments produced by irradiation of thick uranium targets with light

ion beams. To study the structure of low lying states in ^{88}Kr, we used the *in-flight* facility *SIS-FRS* of GSI, Germany, applying a combined γ-ray and particle detector setup – PreSPEC. In this relativistic Coulomb excitation experiment the RIB of ^{88}Kr at 128 MeV/nucleon energy was scattered on a ^{197}Au target. A similar *RIB facility (RIBF)* operating at RIKEN, Japan, in conjunction with the DALI2 scintillator array and the ZeroDegree Spectrometer, was employed to investigate collective excitations in ^{104}Sn projectiles inelastically scattered at the energy of 150 MeV/nucleon on a hydrogen target.

At the REX-ISOLDE *"ISOL"* facility at CERN we applied cluster-transfer reactions induced by the RIB of ^{98}Rb at 2.85 MeV/nucleon on a ^{7}Li target to investigate α-and *triton*-transfer processes, giving access to *yrast* and near-*yrast* states in the neutron-rich nuclei ^{98,99}Sr, ^{99}Y or ^{100}Zr. The MINIBALL Ge detector array was used to measure the associated γ-spectra.

The above-described research is strongly linked with our work on detector development carried out at our Division. The main activity in this area is the development of novel multi-detector arrays PARIS, AGATA and GALILEO planned to be used in future European infrastructures, such as SPIRAL2 in France, FAIR in Germany or SPES in Italy.

The PARIS detector system is built as an international project, coordinated by our group. The aim is to develop and build an innovative calorimeter for high energy gamma photons. Ultimately, PARIS in 4π geometry will be composed of 24 clusters containing 9 *"phoswich"* type detectors, each of which consists of two scintillators, $LaBr_3$ and NaI, glued together. The complex signal of such a scintillators system is unfolded into its original components using fast digital electronics and pulse shape analysis. This solution assures excellent performance of the detector in terms of very high detection efficiency at high energy γ-radiation combined with very good energy and time resolution. The first prototype of the PARIS cluster was assembled and tested in the laboratory and in-beam conditions, fully confirming its expected performance. We initiated preparatory work to install the so-called PARIS Demonstrator, which consists of four such clusters, at GANIL.

AGATA is a state-of-art germanium spectrometer under construction within a European collaboration. Its principle of operation is based on the concept of complete reconstruction of trajectories of gamma rays scattered in a shell built of high purity germanium crystals.

Our group has developed and operates AGAVA, the VME interface between AGATA and other ancillary devices. So far AGAVA was successfully used to couple AGATA with the mass spectrometers PRISMA at LNL, FRS at GSI and VAMOS++ at GANIL. Coupling via AGAVA to other devices has also been successful.

Both AGATA and PARIS Demonstrator arrays will be used at GANIL in a series of approved experiments led by our group. Apart from the above-mentioned spectroscopy of ^{44}Ti, our pioneering experiments will enable us to study the structure of neutron-rich isotopes of B, C, N, O and F, produced in transfer reactions, or to observe γ-ray emission from states close to the threshold set by neutron binding energy in the ^{14}C nucleus.

INVESTIGATIONS OF NUCLEAR REACTIONS AND HADRONIC INTERACTIONS

Our groups have actively participated in three large collaborations: ANKE, WASA and PANDA. Within the ANKE collaboration differential cross sections and analysing powers for the pd → ppn charge exchange reaction were measured at various energies, ranging from 726 to 2400 MeV. Similar measurements were carried out for the dp → ^{3}He X reaction, at relatively low excess energies above the η meson and two-pion production thresholds.

Within the WASA collaboration we have continued the study of the Abashian-Booth-Crowe resonance structure in the double pionic fusion to ^{3}He. A correlation is seen between this effect and a resonance-like energy dependence in the total cross section. Differential cross sections are well described by the hypothesis of d^* resonance formation. The Charge Symmetry Breaking effect was studied in the dd → ^{3}Heπ^0 reaction.

In the course of preparation for the future PANDA experiment at FAIR, further tests were carried out of the central tracker detector prototype and of the read-out system based on a multipurpose

sampling ADC, as a universal tool for data processing. Signal processing procedures were developed to allow simultaneous determination of the position and energy of the particle.

Some members of our group conducted a series of measurements at the Warsaw Cyclotron, concerning elastic scattering of ^{20}Ne on ^{16}O and back-scattering off different isotopes of Zr and Ni. The ^{12}C(^{11}B,^{15}N)^{8}Be reaction was also studied.

The symmetry energy project at RIKEN was continued within the SPiRIT collaboration. It was extended by investigating pion production within exotic Sn fragmentation. Our main contribution to these experiments was in the construction of the KATANA trigger/veto system. The results of the LAND data analysis of the ASY-EOS experiment indicate a soft to linear density dependence of the symmetry energy.

Experiments on deuteron breakup on proton and deuteron targets at different beam energies performed at KVI, Groningen and Forschungszentrum, Jülich were analysed in the search for effects of three-nucleon forces. The BINA detector has been installed at the Cyclotron Centre Bronowice (IFJ PAN) and is now ready to continue such research in Kraków.

Measurements of the neutron electric dipole moment (nEDM), conducted with our participation at the unique solid deuterium-based source of ultra-cold neutrons at PSI Villigen, are approaching the end of their first data-taking stage. Their cumulative accuracy makes them the most sensitive single measurement of nEDM ever performed. An upgraded version of the apparatus, already under construction, will allow us to increase this sensitivity by a factor of five, at least.

Measurements of permanent electric dipole moments of charged particles in a storage ring experiment are under preparation at the Forschungszentrum Jülich, within the JEDI collaboration. A final design of the new EDM polarimeter is being prepared. Differential cross section and vector and tensor analysing powers in deuteron-induced reactions from a carbon target have been measured.

ULTRARELATIVISTIC NUCLEAR PHYSICS AND HADRON STRUCTURE STUDIES

Within this research area, hadronic and nuclear reactions at relativistic energies were studied within the NA49, SPS and LHC-ALICE experiments at CERN. Although the NA49 experiment had completed its data collection a few years ago, there is still on-going analysis of the rich data gathered in that experiment. In 2016, the IFJ PAN group joined, as a full member, the successor of NA49 – the NA61 experiment. Our activity will concentrate on studies of electromagnetic effects.

During the long shutdown of the LHC (LS1), the main activities in the ALICE experiment concentrated on analysis of data collected during Run 1. Of particular interest to us were ultraperipheral and diffractive PbPb interactions and investigations of long-range correlations of charged particles in nuclear collisions.

We were also involved in simulations of the Time Projection Chamber in view of its upgrade during LS2. As data collection in Run 2 began, we were engaged in gas gain calibration of the ALICE TPC, using ^{83}Kr sources.

THEORY

In the theoretical studies carried out in our Division we apply quantum chromodynamics (QCD) to investigate exclusive processes that occur in proton-proton or nucleus-nucleus collisions at ultrarelativistic energies. For example, the cross section for $c\bar{c}c\bar{c}$production was calculated in the collinear approximation including all Feynman diagrams. In a pioneering work, we showed that the contribution of single scattering mechanism is one order of magnitude smaller than the contribution of double parton scattering. This offers a unique possibility of studying double-parton scattering in the production of four charm quarks. As a follow-up of this observation, the role of double parton scattering was discussed in the context of jets with large rapidity distance between jets. The calculation was performed in the leading-order collinear approach. It was demonstrated that the relative contribution of such processes depends on the energy, transverse momenta and rapidity distance between jets.

The first calculation of distributions of photons from the Higgs boson decay was presented within the k_t-factorization approach. Both leading and higher-order processes were included. The results, obtained for different unintegrated gluon distribution functions, were compared with data of the ATLAS collaboration.

Another area of activity was exploration of correlation observables in the transverse momentum of jet pairs or their relative azimuthal angle. Calculations were performed in the k_t-factorization approach for large rapidity distance between the jets, with inclusion of both gluon and quark/antiquark-initiated processes.

Total and differential cross sections for the production of charm and bottom quarks/antiquarks and corresponding mesons were calculated. The possibility of measurement with the LHCb apparatus was considered for events including one and two mesons.

A particularly impressive achievement was the work on the production of $c\bar{c}c\bar{c}$ in the $2 \to 4$ process using the k_t-factorization approach – the Kimber-Martin-Ryskin unintegrated gluon distributions were used in this case.

The calculation of four-jet production was carried out considering both single and double parton scattering processes. The results were compared with experimental data obtained at the LHC. Very detailed studies were performed on how to enhance the relative contribution of double parton scattering by imposing cuts on rapidity distance between jets and relative azimuthal angle.

A study of correlation of jets of particles remote in rapidity was performed within the framework of k_t-factorization. Good agreement with experiment was achieved.

The calculation of dilepton invariant masses in the formalism with unintegrated gluon distributions was carried out, taking into account many unintegrated gluon distributions. The effect of gluon saturation was predicted, however, the LHCb experimental data do not show clearly the presence of this effect.

Calculations of the production of four jets was performed in the k_t-factorization formalism, including both single and double parton scattering effects. The results were compared with experimental data obtained by ATLAS and CMS collaborations. Good agreement was achieved.

The production of pairs of $D^0\,D^0$ mesons was considered again, taking into account fragmentation of gluons and evolution of the fragmentation function. This leads to many new processes both for single and double-parton scattering. Inclusion of those processes without modifying other parameters leads to a considerable enhancement of the cross section for di-meson production. These results are in conflict with the relevant LHCb data.

Very detailed studies of exclusive production of J/ψ in proton-proton and proton-antiproton collisions were made using several unintegrated parton-distribution functions taken from the literature. Based on this analysis, unique differential distributions in rapidity, transverse momentum and relative azimuthal angle between protons were obtained. The possibility of saturation effects and odderon exchange was considered.

The production of charged pion pairs in proton-proton and proton-antiproton scattering was investigated. The contribution from exclusive production of ρ^0 meson and contribution from the so-called Drell-Söding mechanism were calculated using a model with a tensor pomeron and an f_2 reggeon. The interference effect was studied in detail. The results were compared with predictions of the Lebiedowicz-Szczurek model. It was shown that the photon-induced contribution may be significant over certain phase space areas.

The contribution of photoproduction to the exclusive production of pairs of charged pions was calculated in the tensor pomeron and reggeon model. Both resonance and Drell-Söding mechanisms were considered.

The exact calculation of differential cross section for the $pp \to ppH^+H^-$ process was performed for the LHC and FCC, assuming photon-photon fusion. The results were confronted with results obtained in the equivalent photon approximation. The role of the Dirac and Pauli form factors was discussed.

The production of meson resonances in the $pp \to pp\,\pi^+\pi^-$ reaction was discussed in the framework of diffractive two-pomeron processes with tensorial pomeron/reggeon. The corresponding amplitudes were obtained and used in this calculation. By adjusting some model parameters we were able to describe some recent experimental data from RHIC and LHC accelerators.

Several differential distributions for the $pp \to pp\pi^+\pi^-$ reaction were calculated including continuum and resonance states within the tensor pomeron and reggeon model. The continuum contribution was found to be of size similar to that in the Lebiedowicz-Szczurek model. The $f_2(1270)$ resonance state was here considered for the first time.

The $pp \to pp\pi^+\pi^-\,\pi^+\pi^-$ reaction was studied with emphasis on diffractive mechanisms – so far, only sequential mechanisms with $\sigma\sigma$ and $\rho^0\rho^0$ were considered. The calculations were performed within the tensor pomeron model. Good agreement with SPS experimental data was achieved.

Different models of spin structure of the $pp \to pp$ reaction were discussed in the high energy region. We considered exchange of scalar, vector and tensor objects. It was shown that only exchange of tensor pomeron, which we had proposed over the last few years, is consistent with the experimental data.

A new approach to the production of charged lepton pairs was proposed and the first calculation was performed for muons. The results were compared with the outcome of the LPAIR program. Differences between the two approaches were discussed.

Two methods, collinear and k_t-factorization, were considered in the context of production of lepton pairs via fusion of two photons. Four classes of processes, which depend on what happens to the protons, were considered. The results of calculation were compared with recent result obtained by the CMS collaboration.

A special computer code for computing the production of neutrons emitted in the decay of nuclei electromagnetically excited in ultraperipheral collisions, was written. The code can be applied to high-energy collisions relevant for RHIC and LHC.

It was shown that the photoproduction mechanism studied in ultraperipheral production of the J/ψ meson can also be applied in the case of nonperipheral reactions, $b < R1 + R2$, leading to an enhancement of the cross section for small transverse momenta of the J/ψ mesons. Results of our calculations are in semi-quantitative agreement with the recent ALICE data for semi-central production of J/ψ mesons.

We proposed to investigate $\gamma\gamma \to \gamma\gamma$ elastic scattering in the peripheral ultrarelativistic heavy ion collisions. A pioneering calculation in the equivalent photon approximation in the impact parameter space with realistic photon fluxes was carried out. The predictions for LHC were presented. Very recently, the ATLAS collaboration confirmed our predictions and announced the first case of measurement of elastic photon-photon scattering.

A calculation of the cross section for production of two pairs of charged leptons in ultraperipheral ultrarelativisitic heavy ion collisions was performed. Only the double scattering (probably dominant) mechanism was included. The results for single e^+e^- production were compared with ALICE data.

The semiexclusive production of J/ψ mesons was investigated in detail. Differential distributions for different mechanisms were calculated. We included both electromagnetic and diffractive proton dissociation. The results were compared to the contribution of the purely exclusive process $pp \to pp\, J/\psi$.

A calculation of the pion $v1$-directed flow due to electromagnetic effects generated by the spectators was performed. The results were compared with experimental data obtained by the STAR collaboration. It was found that the time of pion emission depends of pion rapidities.

The hypothesis was tested that the signal observed in 2015 in the two-photon final state at the invariant mass of 750 GeV is a technipion,. Two specific models were considered. Processes initiated by photons were considered including leading and higher-order contributions.

A calculation of single-diffractive production of $c\bar{c}$and D mesons was performed for the first time in the k_t-factorization approach. Within this study, we have calculated the first unintegrated diffractive distribution functions (Kimber-Martin-Ryskin method) based on collinear diffractive parton distributions, which were obtained some time ago by the H1 collaboration.

Following a large amount of experimental data and theoretical analyses in the framework of sudden and eikonal approximations of reaction dynamics, we carried out an extensive investigation to understand the dependence of one-nucleon removal cross sections on the asymmetry of the neutron S_n and proton S_p separation energies within our framework of the SMEC model (Shell Model Embedded in the Continuum). Our analysis, performed for isospin mirror nuclei ^{24}Si, ^{24}Ne and ^{28}S, ^{28}Mg, and for a series of neon isotopes ($20 \leq A \leq 28$), clearly confirmed that nucleon spectroscopic factors which normalize the cross section, depend only on the one-nucleon separation energies, but not on their asymmetry. In the same framework (of SMEC), we have investigated the possible formation of a pygmy resonance in the vicinity of the neutron threshold in neutron-rich Ne isotopes. We have found that a small number of highly-lying states move towards the threshold if they are coupled to a continuum of scattering neutron states.

Collective motions and exotic shape transitions were studied – a description of the Poincaré and Jacobi shape transition was developed. The collective Hamiltonian was defined – its dynamic deformation parameters allow one to obtain realistic predictions of the mass and spin ranges where shape transitions may be observed for all known isotopes with Z = 16-100. The collective Hamiltonian and an investigation of high order symmetries were also developed in a 6-dimensional deformation space for ^{156}Gd.

Fission dynamics was described with a transport equation of the Langevin type in 4-dimensional collective coordinate space. We investigated the influence of various macroscopic models on fission observables. Also, a fully microscopic description of the spontaneous fission of ^{238}U with Energy Density Functionals was addressed.

Theoretical studies in order to precisely determine the Zemach radius of the electromagnetic structure of the proton have been continued at the RIKEN-RAL facility, within the FAMU Collaboration, by using laser-spectroscopy to measure the hyperfine-splitting (HFS) energy of the 1s state of the muonic hydrogen atom pμ. Measurements of the muon transfer rate to oxygen performed at RIKEN-RAL proved that this process strongly depends on pμ kinetic energy below 0.1 eV. Therefore, a hydrogen gaseous target with a small hydrogen admixture is a good choice for the future laser-spectroscopy experiment. Theoretical studies of the antiprotonic helium atoms p^-He^+ in helium targets were extended to solid ^{4}He.

Dynamic equations driven by a stable Lévy noise are characterized by a divergent variance and it is necessary to introduce a truncation to determine the correlation properties of the system. The Langevin equation with exponentially correlated noise resolves itself to a two-dimensional Fokker-Planck equation which can be solved by a method of characteristics. Its solutions also represent the Lévy stable distribution and its width, for a given time, is smaller than that for processes in the white noise limit.

The scattering theory was modified in order to include quantum tunnelling. A detailed analysis of the Gamow decay allowed us to understand how the reflection and transmission amplitudes affect the standard optical model. To understand differences between the theories, we examined the boundary condition imposed on S-matrix construction.

SELECTED RESEARCH HIGHLIGHTS OF THE DIVISION OF NUCLEAR PHYSICS AND STRONG INTERACTIONS

Low-energy multiple Coulomb excitation (COULEX) is known to be a very efficient method of extracting information on static electromagnetic moments of low lying, short-lived nuclear states. In particular, it can provide a value and a sign of the quadrupole moment-Q_0, which can be related to the shape and the size of the deformation of the nucleus.

The COULEX experiment was performed at the Laboratori Nazionali di Legnaro, INFN, Italy, which resulted in **the first experimental evidence for a 3-axial character of the superdeformed band in the A~40 mass region** [Phys. Rev. Lett. **117**, 062501 (2016)]. A ^{42}Ca beam at 170 MeV impinged on 1 mg/cm-thick ^{208}Pb and ^{197}Au targets. The γ rays from the excited nuclei were measured with three triple clusters of AGATA in coincidence with back-scattered projectiles, detected in the DANTE array consisting of three Micro-Channel Plate detectors, covering θ_{LAB} angles from 100 to 144 degrees. The γ transitions deexciting states in ^{42}C, populated up to $J^\pi = 4^+$ were observed, as shown in the spectrum of Fig. 1.

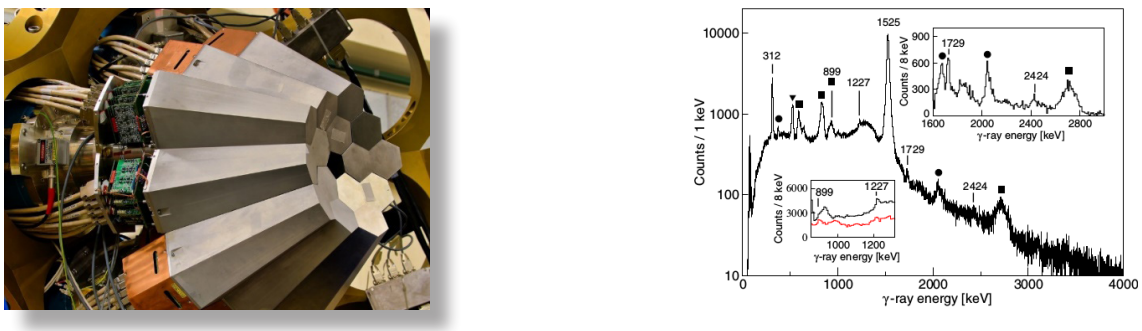

Fig. 1 *The AGATA array at LNL Legnaro (left) and the γ-ray spectrum (right) measured in the ^{42}Ca + ^{208}Pb Coulomb excitation experiment in coincidence with back-scattered particles registered in one of the MCP detectors and Doppler corrected for the projectile's velocity. The lines in the spectrum not originating from ^{42}Ca are marked by squares (Pb isotopes), a triangle (511 keV) and circles (^{43}Ca). Insets show portions of the spectrum zoomed on the 1600-3000 keV and 850-1300 keV energy ranges, the latter presenting also (in red) the spectrum collected with the ^{197}Au target (multiplied by a factor of 3).*

A set of reduced electromagnetic matrix elements between the low-lying states in ^{42}Ca was extracted using the GOSIA COULEX code. As a result, Q_0 was deduced, yielding the deformation parameters of the ground state and the superdeformed (SD) bands close to their band-heads. The ground state band in ^{42}Ca has been attributed to fluctuations around the spherical shape, while a large static deformation with $\beta = 0.43(2)$ and $\beta = 0.45(2)$, respectively, was deduced for the states 0_2 and 2_2 , members of the SD band. In addition, the triaxiality parameter $\gamma = 13(6)^\circ$ was extracted. All the results confirmed the existence of superdeformation in ^{42}Ca and, in addition, suggested its 3-axial character, observed for the first time in such light nuclei.

Nuclei composed of one valence particle and a doubly magic core are ideal for investigating the interplay between microscopic (focusing on the motion of individual nucleons in a mean field potential created by all constituents) and mesoscopic (focusing on a highly organized complex system, exhibiting collective behaviour) properties of a nuclear system. In such nuclei the coupling between collective core excitations (phonons) and the valence nucleon, can be efficiently studied as it strongly influences the structure already at low excitation energy. This is of primary importance for understanding many nuclear phenomena, such as quenching of spectroscopic factors or damping of giant resonances.

We have performed experimental and theoretical investigations which **demonstrated striking changes in the coupling between the valence proton and excitations of the ^{132}Sn core,** along the yrast line in the exotic nucleus ^{133}Sb [Phys. Lett. B **760**, 2016, 273–278]. The one-valence-proton ^{133}Sb nucleus was produced using cold-neutron induced fission of ^{235}U and ^{241}Pu targets, during the EXILL campaign at the ILL reactor in Grenoble. By using a highly efficient HPGe array, coincidences between γ-rays prompt with the fission event and those delayed up to several tens of microseconds were investigated, allowing us to observe, for the first time, high-spin excited states above the 16.6 μs isomer. Also, nuclear state lifetimes were assessed by fast-timing technique with $LaBr_3$ (Ce) scintillators. In the cascade of gamma rays connecting yrast states, we observed a transition which showed a difference of almost two orders of magnitude in B(M1) strength with respect to the neighbouring transitions, indicating a drastic change in the nuclear structure along the yrast sequence in ^{133}Sb.

To understand the experimental result, a microscopic model named "Hybrid Configuration Mixing Model" (HCM) was developed, which takes into account couplings between core excitations (both collective and non-collective) of the doubly magic nucleus ^{132}Sn and the valence proton, using the Skyrme effective interaction in a consistent manner. The model accounts very well for the energies of the observed states in ^{133}Sb and provides an explanation for the large difference in the M1 strength revealed for the yrast transitions (Fig. 2). This drastic change is related to the passage from structures originating from the coupling between proton and non-collective core excitations, to states arising from the proton-phonon coupling.

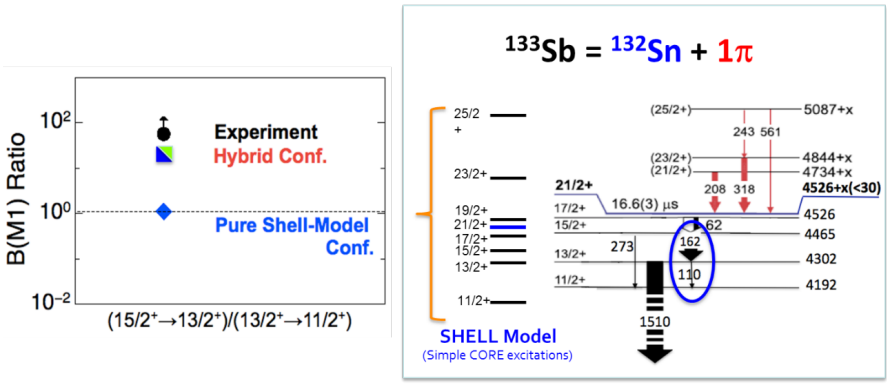

Fig. 2 *The large difference between consecutive magnetic dipole $15/2^+ \rightarrow 13/2^+$ and $13/2^+ \rightarrow 11/2^+$ transition probabilities in ^{133}Sb, derived from lifetime measurements is a clear signature of the fast change in the nature of ^{133}Sb yrast excitations. As shown on the left, the experimental result cannot be described in the framework of the "pure shell model" configurations and points to the hybrid nature of excitations, where couplings between the valence proton and excitations of the ^{132}Sn core, of both genuine phonon type and of less collective character, coexist.*

The Pygmy Dipole Resonance (PDR) is considered as a kind of collective excitation mode of an atomic nucleus involving loosely bound neutrons – the so called neutron skin. Studies in which different probes, such as high energy photons or alpha particles were used to excite the PDR, revealed that the isospin nature of the PDR is mixed. It's low energy component seems to be predominantly associated with isoscalar vibration (in phase oscillation of protons and neutrons), while at higher energy the PDR overlaps with the tail of the isovector giant dipole resonance (GDR), which is an oscillation of protons against neutrons.

Our group has recently studied the PDR using, for the first time, inelastic scattering of heavy ions. A beam of ^{17}O of 20 MeV/u bombarded a 140Ce target at the Legnaro National Laboratories, Italy. The scattered ions were detected by two ΔE-E silicon telescopes of the TRACE array. The γ rays emitted by the excited nuclei were measured by the AGATA Demonstrator (HPGe) and HECTOR+ (large volume $LaBr_3$) detector systems.

Fig. 3 shows the obtained differential excitation cross sections for the sum of states in the energy region 4.0-6.2 MeV (black dots) where predominantly isoscalar PDR states are expected. In order to describe the excitation mechanism, DWBA calculations were performed. As one may observe in Fig. 3, the calculation taking into account only the Coulomb interaction (dotted purple line) reproduces only about 10% of the measured yield, suggesting that nuclear interaction is predominantly responsible for exciting this isoscalar mode. An innovative approach was used to derive the nuclear form factor suitable for considering PDR, because the standard collective model, which is traditionally employed to describe GDR excitations, failed in this case (dashed green line). Microscopic RQRPA calculations of neutron and proton transition densities, specific for the PDR states, were double-folded with the projectile densities. The resulting form factor applied in the DWBA calculations (blue solid line) allowed us to reproduce the experimental data remarkably well.

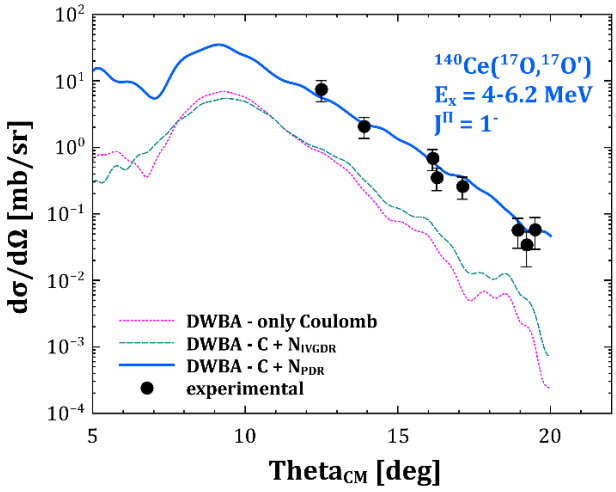

Fig. 3 *Experimental differential cross sections for PDR transitions in ^{140}Ce below 6.2 MeV measured in the (^{17}O, ^{17}O'γ) reaction at different scattering angles. The dotted purple line represents the calculated Coulomb cross section with the DWBA while the dashed green line is the cross section using the standard collective form factor. The solid blue line represents the cross section obtained using the microscopically calculated form factor.*

Comparison of the experimental data with the results of calculations allowed us for the first time to determine in ^{140}Ce the fraction of the Isoscalar Energy-Weighted Sum Rule (ISEWSR) exhausted by the PDR states, to be 2.03%. This value corresponds to the amount of excitation energy transferred to the pygmy vibration mode in this nucleus.

The same method was also applied to other magic nuclei, namely ^{90}Zr, ^{124}Sn and ^{208}Pb, where the ISEWSR fractions were found to be 4%, 7.8% and 9%, respectively. This rather non-smooth dependence on the nucleus mass (including the result for ^{140}Ce) is likely to arise from the specific shell structure of the examined nuclei, therefore, further systematic PDR studies are clearly needed over different regions of the nuclear chart.

The PISA experiment, performed at the KFA Juelich with significant participation and contribution of the staff from our Department, delivered **the most extensive data base of double differential cross-section (dσ/dΩdE) for products of proton – target collision in the GeV energy range**. Both

light or heavy targets (C, Al, Ni, Ag, Au) were irradiated with protons at energies from 0.175 to 2.5 GeV. The reaction products were registered at eight angles with respect to the beam direction. Isotopic identification of particles was performed for masses below A = 12.

Careful analysis of the data collected and their critical interpretation using available theoretical models have demonstrated significant discrepancies between model predictions and experimental data. Disagreement is most pronounced over the higher energy range of the ejectiles, which are emitted during initial phases of the collision, i.e., before thermalisation of the system. Study of this phase of the reaction is especially important since it provides insight into mechanisms of hadronic interactions in excited nuclear matter.

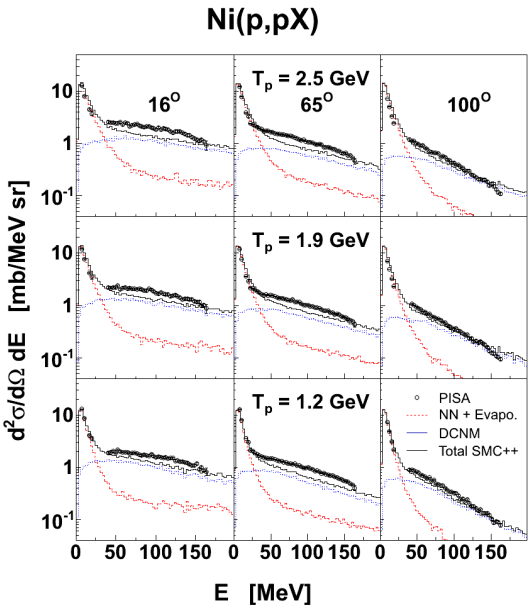

Fig. 4 *Double differential cross-sections for protons emitted at 16°, 65° and 100° after p-Ni collision at 2.5, 1.9 and 1.2 GeV simulated with the SMC++ model and compared with relevant experimental data from the PISA experiment. For details see text.*

It was concluded that the commonly accepted assumption about the cascade of binary nucleon-nucleon collisions occurring shortly after projectile impact on target nucleus is insufficient to reproduce the observed energy and angular yield distributions of reaction products. A process which permits for much faster energy transfer from the projectile to the target and more efficient energy dissipation among the target constituents has been postulated and called Dynamic Clustering in Nuclear Matter (DCNM). It relies on the creation of momentary clusters of nucleons in the excited nuclear medium due to the fluctuations of nuclear density. Dynamic Clusters are also responsible for emission of higher energy composite particles produced abundantly in spallation reactions.

This new Dynamic Clustering mechanism has been implemented into new microscopic model of proton-target reaction at intermediate energies called **Spallation Model with Cascade++ (SMC++)**. As a result, **significant improvement in the description of experimental data was obtained over the whole energy range, both for protons and neutrons and also for other composite light charged particles** [Phys. Rev. C **91**, 2015, 011602]. Fig. 4 shows an example of the SMC++ calculation, which is confronted against experimental data of the PISA experiment obtained for p-Ni reactions at 1.2, 1.9 and 2.5 GeV. Besides the conventional contribution of binary NN collisions and evaporation (responsible for the low energy part of the spectra) shown by red lines, the component from the DCNM mechanism is shown by blue lines. Agreement with data is then much better than obtained applying other models of spallation processes.

Triggered by the progress in the theoretical description of few nucleon system dynamics, a set of precise experiments covering large phase space areas were performed over the last decade at KVI and Forschungszentrum Juelich, with active involvement of physicists of our Division. Over the investigated energy range **the analysed data showed unexpectedly large effects of Coulomb interaction affecting the breakup reaction cross section, even at large relative proton emission angles**.

As an illustration of this effect the differential cross section data measured with the Germanium Wall detector at Juelich are compared with relevant theoretical predictions in Fig. 5.

An extensive statistical analysis of a great number of measurements, constituting a major part of the world's data base in this field, was performed by a Polish-Dutch collaboration, unambiguously proving the importance of the three-nucleon force – an elusive interaction which cannot be reduced to a simple pairwise nucleon-nucleon interaction.

It has also been recognized that in order to clarify the still remaining ambiguities, new data with well controlled systematic uncertainties and collected over continuous sets of energies are necessary. They would allow us to investigate the influence of all dynamical ingredients, also including relativistic effects at

conditions of their greatest prominence, apart from Coulomb effects and the three-nucleon force discussed above. In order to continue this research the BINA detector setup has been installed and is ready for data taking at the Cyclotron Center Bronowice. Considering that the contribution of three-nucleon force to system dynamics is enhanced in systems built of four nucleons, we have recently began to analyse deuteron-deuteron data and are planning experiments involving four nucleons in the spin oriented initial state.

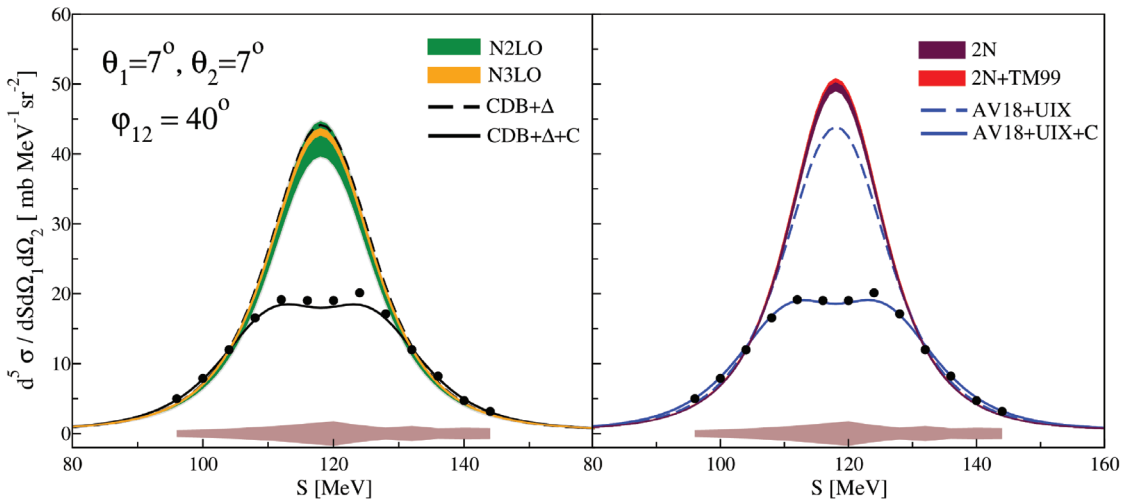

Fig. 5 *Differential cross section for emission of two protons as a function of their relative energy. Points are experimental data, lines are theoretical model predictions.*

Analysis of charge splitting of collective flow of electrically charged π^+ and π^- mesons and of π^+/π^- ratios delivered new information on the evolution of the distance in position space, d_E, of the formation zone of π mesons from the nuclear remnant not participating in the collision. This quantity is defined in Fig. 6 (insert). The same Figure 6 shows this distance as a function of pion-normalised rapidity, y/y_{beam} (main plot, points with error bars). A model analysis of this information was performed based on the production of final state pions from unstable strongly decaying particles (hadronic resonances). Compared to the information obtained from EM interactions, this **analysis excluded the hypothesis of immediate pion production** (dashed curve). On the contrary, **it confirmed the existence of an intermediate state of hot and dense matter in nucleus-nucleus collisions at CERN SPS energies** (the different solid curves correspond to different assumed scenarios for resonance composition and kinematical spectra). A first estimate of the time of pion emission at midrapidity (y = 0) has thus been obtained from EM effects, corresponding to 5.3P∋2.2 fm/c while an approximate estimate obtained from existing HBT data gives $t_f \approx 6$ fm/c. Studies along these lines will be continued by a newly formed scientific group of IFJ PAN physicists, established in the reported period – this group was admitted as a full member to the international NA61/SHINE collaboration.

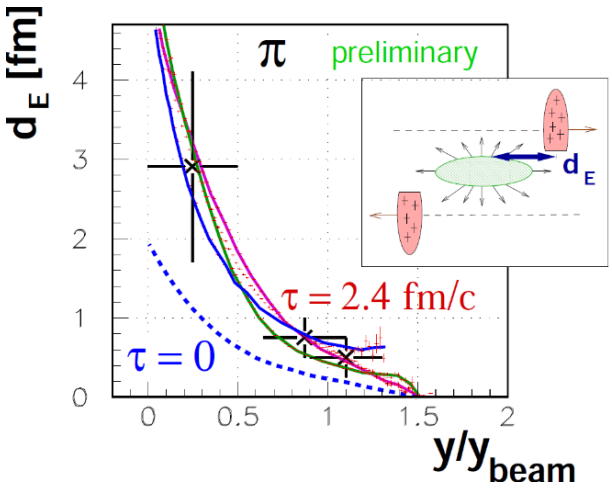

Fig. 6 *Dependence of the distance d_E obtained from EM effects in directed flow in Au+Au and Pb+Pb collisions at c.m.s. energies of $\sqrt{s}NN$=7.7 and 17 GeV, respectively. The different curves correspond to the model analysis described in the text. For more information on this study, see Acta Phys. Pol. Supp. 9 (2016) 303. References to experimental data sets used and addressed in the text can be found therein.*

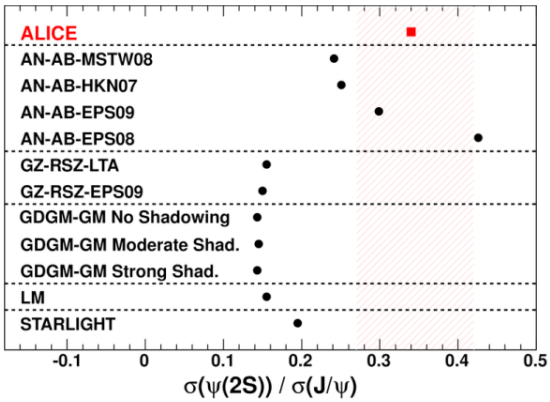

Fig. 7 *Ratio of Ψ(2S) do J/Ψ coherent cross-section in Pb+Pb collisions.*

The ALICE experiment measured for the first time the cross-section for J/Ψ and Ψ(2S) production in ultraperipheral Pb+Pb collisions at √SNN = 2.76 TeV. While the coherent cross-section for J/Ψ production in ultraperipheral Pb+Pb collisions was earlier published by the ALICE experiment, no published data on coherent Ψ(2S) production off nuclear targets exist in the literature. The numerical value obtained by ALICE is 0.83 +/− 0.19 (stat. + sys.) in the rapidity interval −0.9<y<0.9. Fig. 7 shows **the ratio of Ψ(2S) to J/Ψ cross-section, which,** being free of systematic uncertainties, **can be used as a sensitive probe of the development of the collision**. Most of the existing models fail to describe correctly the obtained results, which suggests that nuclear effects may be different in Ψ(2S) than in J/Ψ production.

A particularly useful tool for model discrimination and investigation of the nuclear system properties are studies of *event-by-event fluctuations and correlations* in particle production during ultrarelativistic nucleus-nucleus collisions. In particular, **the analysis of "long-range" correlations**, extending over a wide range in rapidity, **brings information on the early dynamical stage of the reaction**. To extract the appropriate experimental information, we developed the method of analysis, a background estimation procedure, a correction technique of detector effects and an estimation of systematic effects. The forward-backward correlation factor, the intensive quantity ω and the strongly intensive quantity Σ were studied in Pb+Pb collisions at $\sqrt{S_{NN}}$ = 2.76. TeV. A schematic view of forward-backward correlation is shown in Fig. 8. In Fig. 9, the correlation factor and the strongly intensive quantity are plotted against the width of the pseudorapidity interval and compared with HIJING Monte-Carlo results.

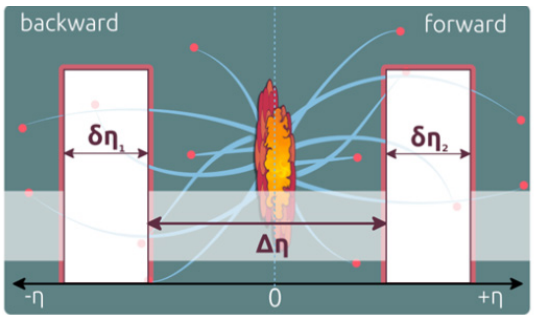

Fig. 8 *Schematic illustration of correlation and fluctuation studies in heavy ion collisions at the LHC. The produced charged particles can be measured in pseudorapidity bins of respective widths $\Delta\eta_1$ and $\Delta\eta_2$. The long range correlation is defined by a large distance in pseudorapidity Δη (such as, e.g., Δη>1).*

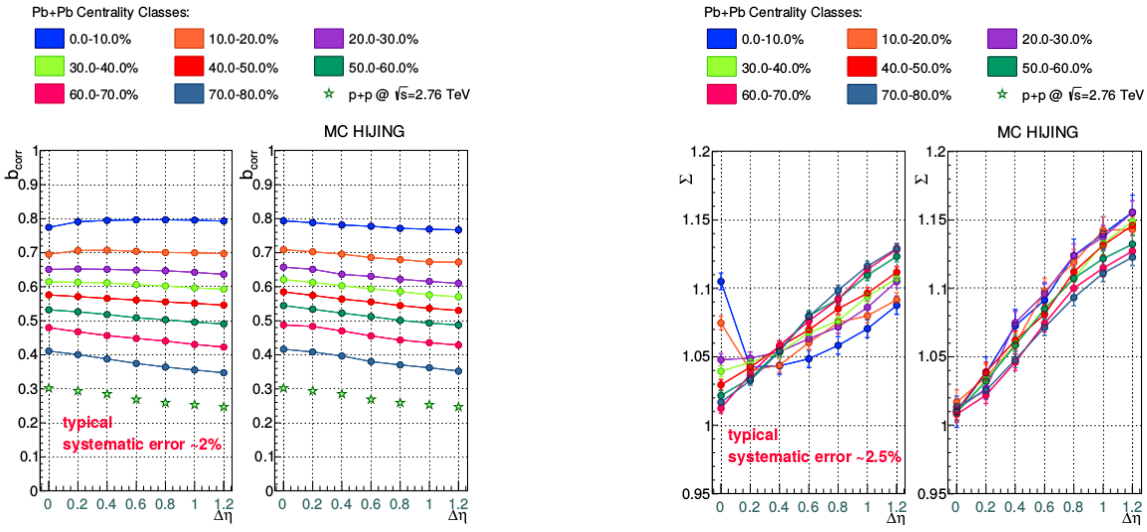

Fig. 9 *Correlation coefficient bcorr and strongly intensive quantity Σ as a function of the pseudorapidity interval Δη.*

The phenomenon of symmetry breaking observed at nuclear shape transitions was investigated [Phys. Rev. C **91**, 034301 (2015)]. It was shown that **a hot rotating nucleus with increasing angular momentum can change its most probable shape from spherical to oblate-triaxial-prolate** – which is called the Jacobi transition – **and next, from prolate to octupolly deformed** – which is the Poincare transition**.** The revised formula of macroscopic energy was employed to obtain the fission barriers, and, further, to make large-scale calculations for spins 0-130 ħbar. Energy minimisation was performed in 12-16th deformation parameters space, and projections of axial-nonaxial quadrupole (Fig. 10, left) and quadrupole-octupole (Fig. 10, right) energy maps for each spin were applied to solve the Schrödinger equation to describe the collective vibration of the nucleus. The static deformation (read as the energy minima in Fig. 10) was compared to dynamical shape parameters and its dispersion was estimated. The method allows one to predict the spin range where shape transition occurs. Also, a further study of the best nuclear mass region to investigate this manner of symmetry breaking is in progress. Experimental probes of the Jacobi transition are, for example, Giant Dipole Resonances, but for the Poincare transition it could be the mass asymmetry of the fission fragments. Our method allows one find the best mass region and the best spin range for measuring the Poincare transition.

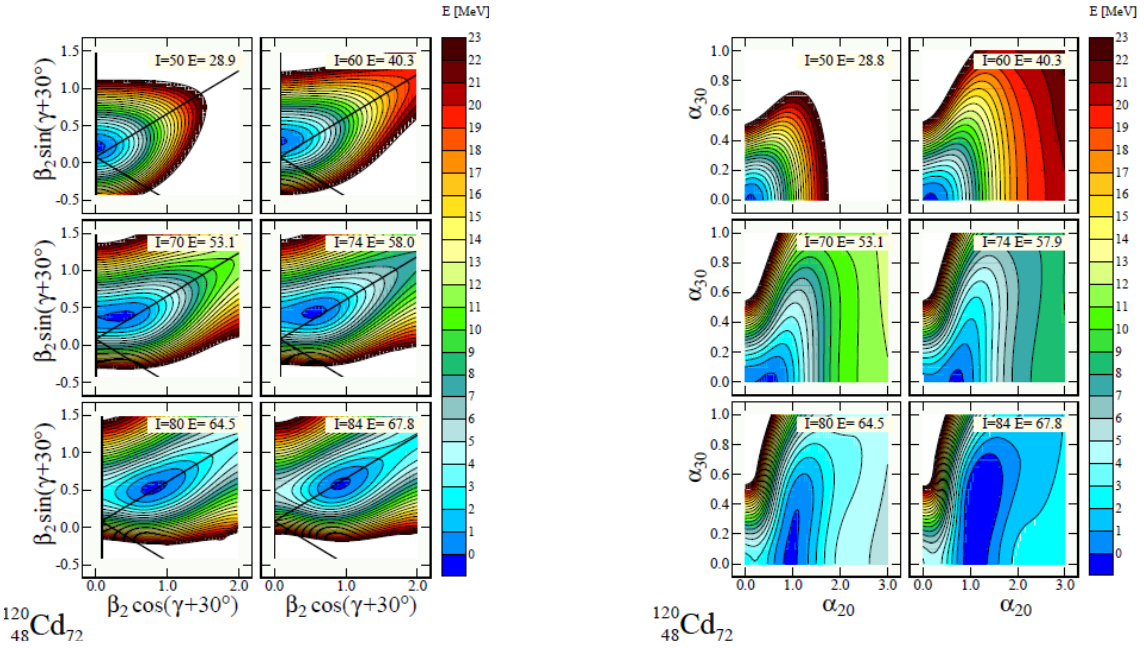

Fig. 10 *Total energy surfaces at increasing spin in ^{120}Cd, (left) using the 'traditional' shape-coordinate representation with quadrupole deformation parameters ((β,γ)) of Bohr. The vertical, up-sloping straight lines correspond to γ = 60° (representing oblate shapes, with the spin of 'non-collective' origin aligned with the symmetry axis) whereas the 'path to fission' (γ = 0° axis) has 30° inclination with respect to the O_x axis. (right) Example of Poincare-type shape evolution with spin using the two-dimensional projections (α_{20}, α_{30}). The minimization over axial-deformation coordinates $\alpha_{\lambda 0}$ with ≤12; the insets contain the actual spin and the energy minimum in MeV using normalization to zero at I = 0ħ.*

Antiprotonic helium atoms p^-He^+ are created when antiprotons are decelerated in helium targets and then replace one electron in helium targets. About 3% of antiprotons are captured in highly-excited metastable states (n,l) with lifetimes of the order of microseconds. This phenomenon enabled high-precision laser spectroscopy of these atoms, which was employed by the ASACUSA Collaboration at CERN. One of the results is the determination of the antiproton-to-electron mass ratio with the best accuracy to date. Such measurements require an estimation of the shift and broadening of the spectral lines due to interaction with the neighbouring He atoms in dense-gas, fluid, superfluid and solid helium targets. **The shift and broadening of the resonance lines in the spectrum of antiprotonic helium atoms p^-He^+ implanted in solid helium were estimated** using the available experimental pair-correlation functions $g(r;T,\rho)$ for crystalline ^{4}He at a few temperatures T and densities ρ, as shown in Fig. 11

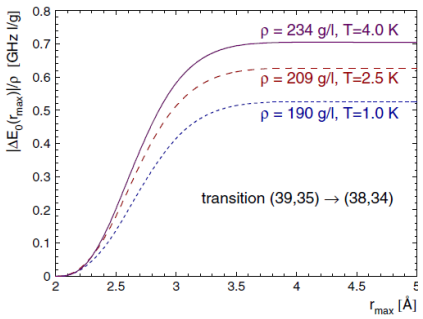

Fig. 11 *The absolute value* $|\Delta E_0|/\rho$ *of the reduced resonance-line shift in solid* ^{4}*He as a function of* r_{max}.

[Phys. Rev. A **90**, 054501 (2014)]. The interaction of the antiprotonic helium atom with the neighbouring ^{4}He atoms was described using a pairwise radial potential $V_{nl}(r)$ of the $\bar{p}\,\mathrm{He}^+$ interaction with a single ^{4}He atom, which was obtained in the semiclassical approach. A plot (Fig. 11) of the calculated normalized line shift $\Delta E_0/\rho$ for the transition $(n = 39, l = 35) \rightarrow (n = 38, l = 34)$, as a function of the upper limit r_{max} of integration over the radial variable r shows significant dependence of the line shift on the target temperature and density. Laser-spectroscopy measurements of the $\bar{p}\,\mathrm{He}^+$ atom in fluid and superfluid ^{4}He were already performed. An experiment with solid helium is planned at CERN.

Double charm production was predicted by us to be one of the most promising channels for studies of double-parton scattering (DPS) effects at the LHC [Phys. Lett. B, **758**, 458-464, (2016)]. Starting from LHC energies the cross section for standard single $c\bar{c}$ pair production via single-parton scattering (SPS) and for DPS double mechanism become comparable (see left panel in Fig. 12). This means that at the LHC charmed mesons are beginning to emerge in pairs as often as single ones – or even more often. With increasing energy of proton-proton collisions the multiple-parton interaction undoubtedly starts to play a dominant role in the phenomenology of charm particle production. Our finding was further supported by experimental observations reported by the LHCb Collaboration. This is the first time that multiple-parton scattering has been recognized as the leading production mechanism of charm particles at LHC energies.

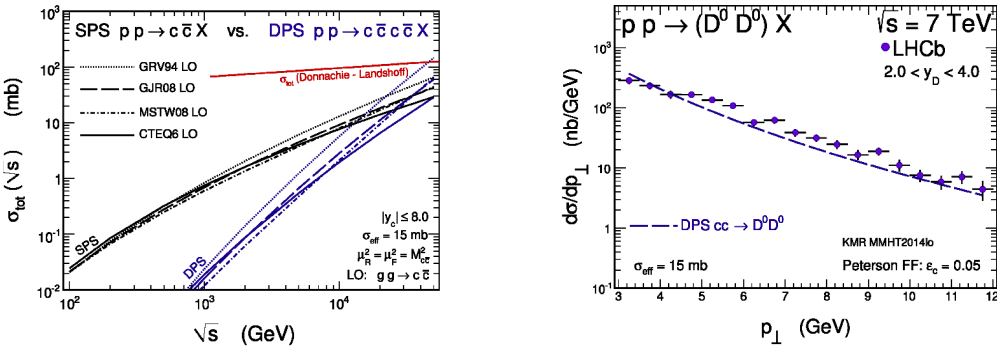

Fig. 12 *Total cross section for charm production in single-parton and double-parton scattering as a function of centre-of-mass proton-proton collision energy (left panel). Transverse momentum distribution of one D meson from the DD-pair, compared with LHCb data (right panel).*

We have next carefully examined the phenomenology of meson-meson pair production in the k_t-factorization approach and achieved a relatively good description of the LHCb experimental data for both the total yield and the dimeson correlation observables (see right panel in Fig. 12). In the theoretical analyses, both single- and double-parton scattering mechanisms were taken into account. The contribution of the single-parton scattering (SPS) mechanism $gg \rightarrow c\bar{c}\,c\bar{c}$, discussed in detail in the collinear and k_t-factorization approaches, was found to be rather small and definitely not able to describe the relatively large cross sections measured by the LHCb. This leads to a rather definite conclusion that the observed double production of charmed mesons cannot be explained without the phenomenon of double-parton scattering. It also demonstrates that double charm production is probably the best-known area to study effects of multiple-parton interactions at the LHC. In future accelerators, such as the already designed Future Circular Collider, the LHC's successor, this phenomenon will certainly play a dominant role in the production of charm particles. DPS effects in the charm sector seem also to be very important in theoretical studies of prompt fluxes of high energy neutrinos, generated from

charmed meson decays, which are produced in the interactions of ultra-highly energetic cosmic rays with Earth's atmosphere.

In classical Maxwell theory, photons do not interact. In contrast, in quantum theory they can interact via quantal fluctuations. So far only inelastic processes, i.e., production of hadrons or jets via photon-photon fusion could be measured e.g., in e^+e^- collisions or in ultraperipheral collisions (UPC) of heavy-ions. It has been realized only recently that ultraperipheral heavy-ion collisions can also be a good region where photon-photon elastic scattering could be tested experimentally.

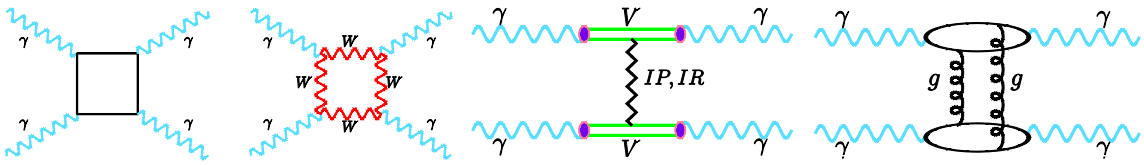

Fig. 13 *Light-by-light scattering mechanisms with lepton and quark loops (first diagram) and for the intermediate W-boson loop (second diagram). The third diagram represents the VDM-Regge mechanism and the last diagram illustrates the two-gluon exchange.*

In Fig. 13 we show several mechanisms considered by us recently in photon-photon scattering. These elementary processes were embedded into nucleus-nucleus ultraperipheral ultrarelativistic Heavy Ion collisions (Fig. 14). **We have made corresponding calculations and made first predictions of integrated and differential cross sections for this photon-photon elastic scattering process** [Phys. Rev. C vol. **93**, 044907 (2016)].

Very recently, the ATLAS Collaboration presented first evidence of light-by-light scattering in quasi-real photon interactions from ultraperipheral lead-lead collisions at $\sqrt{S_{NN}}$ = 5.02 TeV. The data set, recorded in 2015, yields cross section of 480 mb for this process. The measured fiducial cross section which includes limitation on photon transverse momentum, photon pseudorapidity, diphoton invariant mass, diphoton transverse momentum and diphoton acoplanarity, has been estimated at 70 ± 20 (stat.) ± 17 (syst.) nb, which is compatible with the value of 49 ± 10 nb predicted by us for the ATLAS cuts.

Diamond is considered to be a very promising material for particle detectors as several parameters, such as carrier mobility, fast response, very low noise, etc. are superior to those of semiconductors. In addition, its high radiation hardness makes the diamond a promising material for radiation detection and particle counting.

Within our research and development activities we wished to prove the usefulness of single-crystal diamond detectors produced by Chemical Vapour Deposition (sc-CVD) for accelerated proton beam diagnostics using the single proton counting approach.

We have measured the in-beam response of a 50 μm thick sc-CVD diamond detector with 60 MeV protons delivered by the AIC-144 cyclotron. Rapid signals from the detector provide intrinsically good time resolving power, however wideband, ultra-low noise electronics with high amplification needs to be applied.

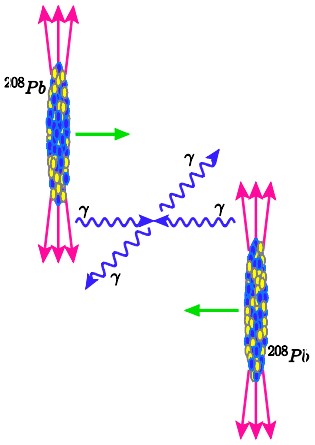

Fig. 14 *A schematic picture of light-by-light scattering in UPC.*

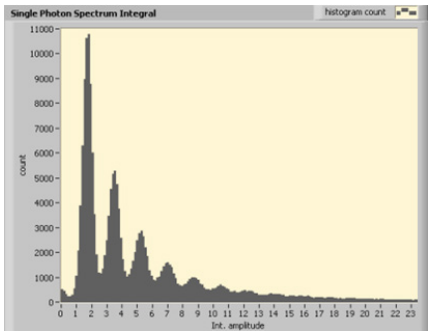

Fig. 15 shows the ability of this diamond detector to separate different numbers of 60 MeV protons (from the AIC-144 cyclotron) simultaneously impinging on

Fig. 15 *Signal amplitude spectrum of different numbers of 60 MeV protons simultaneously impinging on a diamond detector The highest peak corresponds to the detection of single protons*

its surface. The results of measurements of distances between beam micropulses (38.1 ns) or of typical beam current density (1567±37 p/ms/mm^2) are in good agreement with the system specifications.

It is thus demonstrated that **an individual particle counting technique with the sc-CVD diamond detector makes it possible to measure intensities of proton (and also heavier ion) beams with extremely high sensitivity** (at single particle level) and dynamic range >10^6, and may be applied in harsh radiation environments.

Within the last few years investigations of symmetry energy at high densities with the use of heavy ion collisions has become one of our main projects. Analysis of the neutron-proton flow from Au+Au collisions at 400 MeV/nucleon yielded a moderately soft to linear density dependence of the symmetry energy (slope parameter L = 72 ± 13 MeV). These data have been obtained within the ASY-EOS experiment at GSI where midrapidity light charged particles were measured using the KRATTA triple telescope system.

Another experiment, carried out at RIKEN in May 2016 within the SPiRIT collaboration, was focused on the influence of the symmetry energy on pion production in the $^{108, 112, 124, 132}$Sn + ^{124}Sn reactions at 300 MeV/nucleon.

The trigger/veto signals for this experiment were generated using the KATANA triggering system constructed at IFJ PAN within the NCN projects. The main ingredients of the system are depicted in Fig. 16.

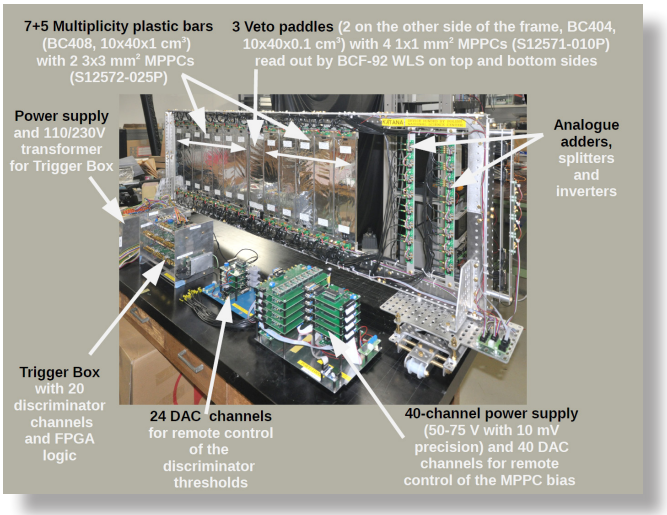

Fig. 16 *The KATANA triggering system.*

The KATANA detector played a significant role in the detection system, protecting the SPiRIT TPC against the risk of damage by excessive ionization produced by heavy ion beams. Fast response, high veto and triggering efficiency, insensitivity to magnetic fields, stability, portability and the possibility of remote control are the main attributes of this array.

IFMIF-DONES (International Fusion Materials Irradiation Facility – DEMO-Oriented Neutron Source) is a powerful neutron irradiation facility for studies and qualification of materials. It is planned as part of the European roadmap to fusion-generated electricity. Its main goal will be to study properties of materials under severe irradiation in neutron fields similar to those present in the first wall of a fusion reactor. It is a key facility to prepare for the construction of the DEMO Power Plant envisaged to follow ITER. Poland is one of the countries which have declared interest in hosting the IFMIF-DONES facility. The ELAMAT (European Laboratory for Material Science) consortium was founded in 2014 by the Rzeszów University of Technology and the Institute of Nuclear Physics of the Polish Academy of Sciences (IFJ PAN) as a bottom-up initiative of the science community to prepare a proposal to site IFMIF in the Podkarpackie region of Poland (http://elamat.portal.prz.edu.pl/en/). One of the decisions of the Consortium was to establish the Scientific Council of ELAMAT with the aim to study possible extensions of the objectives of the IFMIF-DONES facility beyond its envisaged programme (http://elamatscience.ifj.edu.pl/). At the workshop "Town Meeting on IFMIF/ELAMAT Complementary Scientific Programme", which took place on April 2016, it was decided to prepare **a collection of complementary science cases for the future IFMIF-DONES facility in the form of a White Book** [Report IFJ PAN No. 2094/PL].

The editors and contributors of the White Book are prominent scientists from all over Europe, representing applications of interest to medicine, nuclear physics, radioactive ion beams, basic physics and to industrial applications of neutrons. The possible scientific opportunities, discussed in this White Book, require certain modifications of the IFMIF-DONES facility layout (see Fig. 17). The intention of the

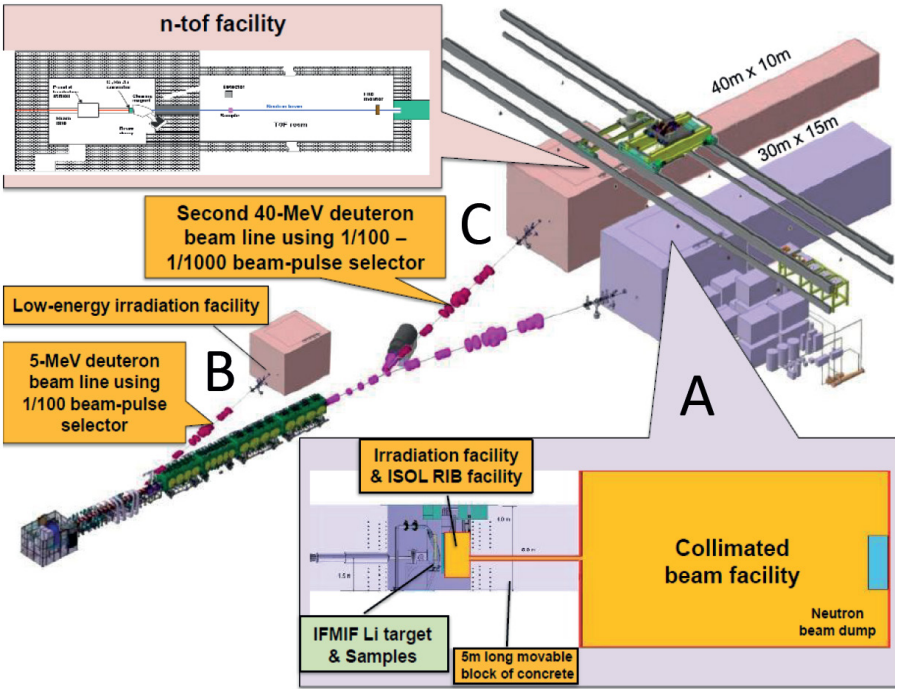

Fig. 17 *A schematic drawing of the IFMIF-DONES facility showing the baseline IFMIF accelerator with the irradiation cell (in blue and yellow) and additional parts of the facility dedicated to research topics described in the White Book (in yellow and mauve). The proposed installations consist of an irradiation facility for materials, backed by a setup for producing radioactive ion beams with an additional setup for a collimated beam facility, for a neutron time-of-flight facility, and a low-energy irradiation facility. The last two installations require two additional beam lines (in red) and beam-pulse selectors to deviate 0.1-1% of the primary deuteron beam to the dedicated setups.*

authors was to demonstrate that many important topics and urgent questions of today's science in several research fields could be addressed and investigated at the IFMIF-DONES without compromising its main role of a materials irradiation facility for the fusion programme. It is hoped that elements of the complementary science programme will be incorporated into the original design of the proposed facility.

III. DIVISION OF CONDENSED MATTER PHYSICS

Materials science is an interdisciplinary field which deals with systematic studies of physical and chemical properties of materials using complementary techniques. Over centuries, knowledge about chemical elements and compounds has been gathered by craftsmen, alchemists and material researchers. But only by applying quantum mechanics were scientists finally able to explain the macroscopic features of such materials and to correlate them with the microscopic structures of metals, dielectrics and magnetic elements of the Mendeleyev Table, while describing these properties through a theoretical formalism. This new era began with the inventions of semiconductors, superconductors and novel magnetic materials of complex behaviour. The parallel introduction and development of extensive computer simulations and mathematical modelling, significantly aided in resolving experimental observations. Another sign of the new era in materials science was the synthesis of first synthetic polymer materials. Other soft materials, such as a plethora of newly synthesised liquid crystals, amphiphiles, colloids and molecular glass-formers, often feature properties which surpass those of materials of natural origin. Newly synthesised soft materials became important in molecular biology and biomedicine. Solid-state physics became the tool to manufacture devices which have deeply affected our civilisation, such as the transistor, the laser, integrated solid-state electronics or solar panels, which are now broadly applied in modern telecommunication, computer technology or energy production. Unique technologies of material preparation have been developed such as methods of manufacturing nanostructures of molecular thickness, ultrathin coating or forming thin multi-layer films, specifically doped to precisely control their conductivity and magnetic properties. In condensed matter physics new fields have emerged, such as low-dimension systems, amorphous materials, quasi-crystals, or granular matter, studied at temperatures ranging from the lowest achievable to those observed in plasma. The discoveries and inventions of material scientists and engineers have made everyday life easier, healthier and more exciting. They have changed our culture, leading to the emergence of new ideas and further extending our knowledge and range of endeavours.

At the **Division of Condensed Matter Physics** most of the research is carried out in our own laboratories, on IFJ PAN premises. Since the last reporting period, the structure of the Division has changed. It now consists of five departments: **Department of Structural Research, Department of Computational Materials Science, Department of Magnetic Research, Department of Soft Matter Research** (since July 2014) and **Department of Physics and Material Engineering** (since October 2016). At the beginning of 2015 the Department of Magnetic Resonance Spectroscopy became incorporated into the Department of Magnetic Research. Our studies of the characteristic features of various classes of materials focus on searches for new physical phenomena and on understanding and describing the mechanisms of such phenomena. Along this line of research, we also develop complex material structures of desired properties to make them useful in various applications. Our pioneering studies on

phase transitions and on fast dynamics in molecular crystals using NMR and neutron scattering spectroscopy began already at the time at which the Institute of Nuclear Physics was founded, through close cooperation with foreign partners, first with the Joint Institute of Nuclear Research in Dubna (Russia, formerly USSR), and then with the Institute for Nuclear Energy in Kjeller (Norway). The tradition of close collaboration with leading laboratories abroad has been continued. Our laboratories now have extensive collaborations with several research institutions in Poland and abroad. This allows their unique instrumentation to be shared with our facilities in joint experiments and studies. Neutron diffraction and scattering experiments are performed at the Laue-Langevin Institute in Grenoble (within a Belgian-French-Polish-Swedish consortium which we coordinate), at the Joint Institute of Nuclear Research in Dubna, the FRMII in Munich, PSI in Villigen and at the Helmholtz-Zentrum in Berlin, where we use their beam time. We apply several complementary techniques (x-ray diffraction, magnetometry, dielectric relaxation and infrared spectroscopies, inelastic x-ray scattering, positron annihilation, polarizing microscopy and calorimetry) which became our tools in studies of properties of thermodynamic phases with various degrees of long range order over different levels of structural organization. In our studies we deal with several classes of condensed matter systems – soft materials, novel magnetic systems and superconductors, or low-dimensional structures. We also study compounds which find applications in environmental protection and energy storage (several classes may be represented in our samples). Of our main interest in these systems are phase transitions and features of newly discovered phases in relation to their structure. We often work in small groups which gather experimentalists and theoreticians together in joint projects. To extend our knowledge of mutual interactions the molecules of our samples at different external conditions, wherever possible we trace relaxation processes which evolve over large time scales by analysing changes of characteristic frequencies of internal molecular bonds.

Soft matter, a term coined by Pierre-Gilles de Gennes, covers a broad range of organic materials, including polymers, liquid crystals, amphiphiles, gels and also colloids - combinations of disperse phase and dispersion media, both in all possible states of matter. In such systems, on the one hand there is a lack of three-dimensional long-range order typical of crystalline solids, and on the other they are much more viscous and/or viscoelastic than ordinary liquids. Despite exhibiting various types of structural organization, soft materials share some common features, such as weak interactions between molecules and rich solid-like and/or liquid-like polymorphism. In general, not much energy is required to transform one phase to another. Metastable phases, disordered and those exhibiting partial long range order of molecules, such as e.g. in orientation – (ODIC) and conformation- disordered (CONDIS) crystals, have a tendency to glass formation, in a manner similar to that observed in isotropic liquid phases. Soft materials are highly complex not only in their structure but also in their dynamics. Searches for theoretical descriptions of phenomena observed in soft matter are not easy. While their dynamical/relaxation features are rather of multiscale character, it is often possible to find scaling relationships which appear to be universal over larger classes of materials. We developed a special formula which allows one to present complex dielectric relaxation related to molecular dynamics in liquid-like phases (isotropic liquid, cholesteric, nematic, smectic A) and solid-like phases (smectic B, conformationally disorder crystal, plastic crystal – ODIC, ferroelectric and paraelectric states) by a common master-curve [J. Appl. Phys. **118** (2015) 064101]. This suggests a universal origin of the mechanism of these dynamics, defined by long-range and local correlations of the detected rotational motions. We are now working on understanding how do details of molecular structure, interactions and dynamics affect their complex interplay, resulting in a particular sequence of thermodynamic phases of the substance under study. To this end, it is necessary to use complementary methods in order to establish factors responsible for the competing effects of phase stabilization and phase transition. Automation in performing experiments and in the analysis of data is extremely helpful in accelerating the rate of scientific discoveries. We developed special software to transform sequences of microscopic images to light intensity vs. temperature plots, to show anomalies of even very weak phase transitions which were otherwise untraceable in microscopic textures studied by the naked eye only [https://github.com/Natalia-Osiecka/TOApy]. We study soft materials (in bulk or enclosed in cavities) of relatively flexible molecules, often interconnected by hydrogen bonds. In soft matter a strong response may result from weak external perturbations, which offers application opportunities. It has recently been discovered that soft material may be a component of a magnetic system. New features of soft materials appear if the dimensions of samples under study are reduced to nanoscale layers or if they are encapsulated in a nanopore matrices of different geometry.

New advanced molecule-based magnetic materials are currently an important topic of research in many laboratories throughout the world. We are interested in these novel metal-organic magnets, and especially in coordination networks designed from discrete molecular building blocks containing 3d-4d(5d) or 3d-4f electron metal centres. Such structures are obtained by complex synthesis processes, showing many interesting features against conventional magnets – such as low weight, optical transparency and so-called molecular "softness" of the crystal network which makes them susceptible to modifications. Molecular magnets are potentially switchable systems, the properties of which may be controlled by external stimuli, such as temperature, light, pressure and electric or magnetic fields. Some of our samples appear to show magnetic sponge behaviour due to a reversible change of the ordering temperature T_c and of coercive field H_c upon hydration/dehydration processes, while those with micropore architecture present similar properties upon sorption/desorption of various guest molecules. Due to the localized character of the magnetic moments interacting through chemical bonds, molecular magnets provide us with fertile ground for testing theoretical spin models. Apart from gaining better understanding of some aspects of magnetism and structure-property relations, our investigations are aimed at inventing functional and multifunctional materials which may be used in modern miniaturised technology, informatics, electronics or medicine. Up to date we have found a number of compounds showing such potentially applicable features due to spin-crossover phenomena, room-temperature magnetism, photomagnetism, luminescence and non-linear optical behaviour. The main subjects of our investigations are studies of the properties of cyano-bridged systems, including three-dimensional bulk structures as well as molecular layers, chains or magnetic clusters. Here the main tasks are to gain information on the magnitude of magnetic moments and on phase transition to the collective state, on the type of magnetic order, to estimate the magnetic coupling energy, and to analyse their critical behaviour and relaxation properties. We also study changes induced by irradiation with light, external pressure or chemical modification. Our investigations in the area of new technologies concern the magnetocaloric effect (MCE) in high-spin molecular clusters as potential magnetic coolers in the low and ultra-low temperature ranges. An important part of our activity is modelling of the characteristic features of such materials taking into account crystal field effects, single-ion anisotropy and the non-trivial topology of the investigated systems.

Our theoretical studies are focused on properties of novel **superconducting materials**. We study the effect of magnetic field on multiple phase transitions and new high temperature superconducting phases in iron-based materials. We study, using *ab initio* methods, the influence of low-energy phonon anharmonicity on the superconductivity in MV_2Al_{20} caged materials. We have also investigated dynamical properties of the lattice in strongly correlated transition-metal oxides, 4f-electron rare-earths and 5f-electron uranium compounds.

Studies of features of **low dimensional systems** are currently a topic of high interest in contemporary condensed matter physics both from the fundamental research point of view and in view of the potential applicability of artificially fabricated structures. Low dimensionality effects may also arise naturally in solids of a special crystal structure (as for example via long relaxation time in 0D molecular nanomagnets) or manifest themselves in materials confined in nanopores or nanocages – detected as changes of their electric and magnetic parameters. In the case of substances placed in a confined space, dielectric relaxation spectroscopy and nuclear magnetic resonance provide means of investigating the details of their molecular dynamics. Studies of deuterated molecules confined in nanoscale cages of zeolites show features of molecular dynamics characteristic of the gas phase (diffusion), of liquid-like layers (surface mediated diffusion) and of immobilized molecules in the temperature range down to 10 K [J. Phys. Chem. A **118** (2014) 5371]. Also the problem of wave propagation in cavities of different sizes and shapes is interesting from the fundamental research point of view [Phys. Status Solidi B **252** (2015) 1595], but also due to many application opportunities in areas of seismic phenomena, ultrasonic defectoscopy, or blood transport in arteries, or micro and nanopores of molecular systems. We are currently also working on the synthesis and a comprehensive study of molecular and hybrid thin layers of a well-defined functional magnetic material required for nanoelectronics or nanosensors. Especially attractive here are thin films of Prussian blue analogues built of anionic hexacyanometallates $[M(CN)_6]$ and 3d metal ions, which show a range of photomagnetic and magnetooptical effects. We have devised methods to develop molecular films based on hexa- and octacyano-metallates and, in a parallel project, hybrid thin silica-based films, containing metal ions or magnetic molecules. We have

successfully achieved the first step to this end, i.e. homogeneous deposition of the well-recognized Mn_{12} – acetate molecules inside the channels of SBA-15 amorphous silica [RSC Advances **6** (2016) 49179]. We have also performed *ab initio* studies on low-dimensional magnetic systems: iron platinum nanoparticles – candidates for future magnetic recording media, and on a novel phase of iron-oxide ultrathin films [Phys. Rev. Lett. **115** (2015) 186102], which exhibit ferromagnetic order at room temperature.

SELECTED RESEARCH HIGHLIGHTS OF THE DIVISION OF CONDENSED MATTER PHYSICS

Systematic investigations of the complexity of phase polymorphism and molecular dynamics in four hexanol isomers (dimethylbutanols of globular molecules $C_6H_{11}O$) exhibiting ODIC phase have been performed using various complementary experimental methods and DFT calculations. For 2,3-dimethylbutan-2-ol (2,3-DM-2-B) and 3,3-dimethylbutan-2-ol (3,3-DM-2-B) our research is now completed by studies of stochastic molecular dynamics with the technique of elastic scattering of neutrons of various momentum transfer. For 2,3-DM-2-B the mean square displacement of the hydrogen nuclei from the equilibrium positions occurred to be of about 0.2 Å^2, remaining at this value up to the melting point, confirming that the only solid phase is the ordered crystal (Fig.1, left). In contrast, for 3,3-DM-2-B the corresponding mean-square displacement is close to 1 Å^2, decaying on cooling (Fig.1 right). The "elastic window scan" measurements in 3,3-DM-2-B allowed us to determine the temperature of vitrification of the low temperature rotational crystal phase at around 200 K and freezing of the fast rotational degrees of freedom at around 120 K. Interestingly, **in the 3,3-DM-2-B isomer, ODIC rotational crystal phases were identified while in 2,3-DM-2-B isomer only an ordered crystalline solid phase was detected.**

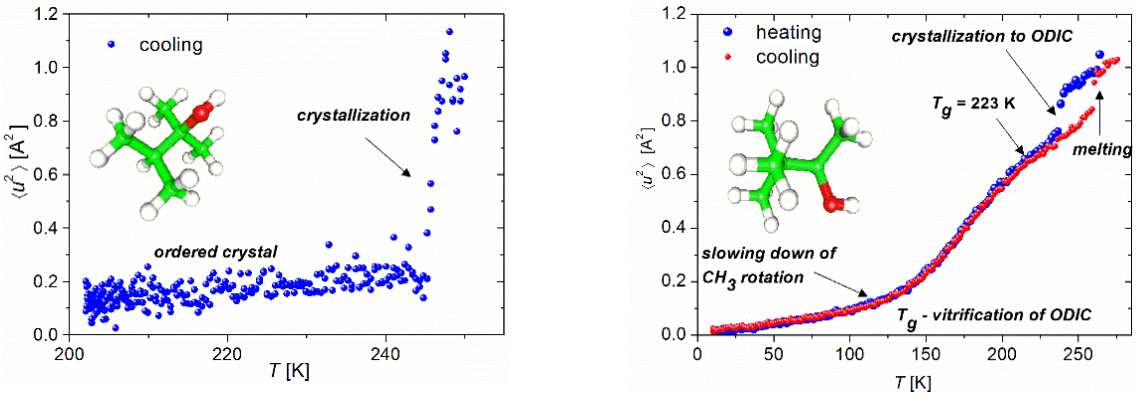

Fig. 1 *Elastic window scans for 2,3-DM-2l and 3,3-DM-2B obtained during temperature changes (in cooperation with the Joint Institute of Nuclear Research in Dubna).*

The unobserved so far glass transition of highly ordered smectic SmB_{Cr} phase was studied in 4-n butyloxybenzylidene-4'-n'-octylaniline (BBOA) liquid crystal, revealing an interesting sequence of phases (nematic, smectic A, smectic B hexatic and smectic B crystal (SmB_{Cr})) between isotropic liquid and ordered crystal. Particularly complex molecular dynamics was found using Broadband Dielectric Spectroscopy (BDS) for the quenched SmB_{Cr} phase on approaching glass transition (see Fig.2): At high temperatures typical Vogel–Fulcher–Tammann (VFT) non-Arrhenius type of temperature dependence of the structural relaxation time $\tau(T)$ was found while at low temperatures $\tau(T)$ deviation from VFT to Arrhenius type dependence was stated, typically identified in confined liquids. In this context we concluded that **cooperative motions in nanometre-sized domains of the quenched SmB_{Cr} are restricted by the surrounding crystalline phase**. The kinetics of the isothermal crystallization of metastable SmB_{Cr} phase observed on heating was described in terms of the classic Avrami approach and by an analytical method, recently proposed by Avramov. The values of the kinetics parameters, obtained by both methods, coincide [J. Phys. Chem. B **120** (2016) 12160].

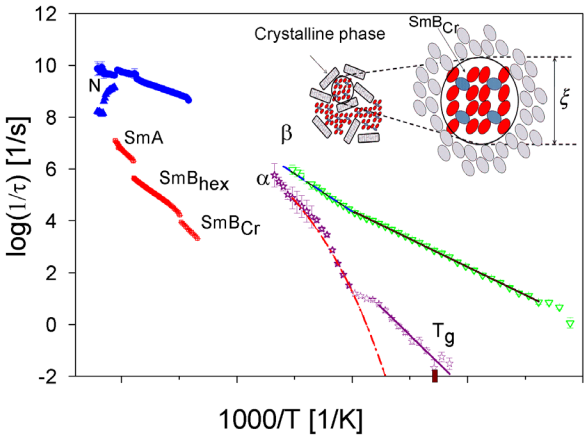

Fig. 2 *Activation diagram for various relaxation processes observed in BBOA upon heating of the quenched sample (empty symbols) and on slow cooling (solid symbols). The scheme illustrates the idea of a cooperatively rearranging region, where ξ denotes the length scale of cooperativity.*

In numerical analyses of the BDS and ^{1}H Nuclear Magnetic Resonance relaxometry results, agreement was found between microscopic and macroscopic points of view on complex dynamics of the 4ABO5* liquid crystal 4′-butyl-4-(S)-(2-methylbutoxy)azoxybenzene with chiral molecules [J. Phys. Chem. B **120** (2016) 5083]. Arrhenius-type flip-flops related to rotations around the long molecular axis were detected at the temperature range of isotropic and cholesteric liquid phases and the disordered crystal phase, while in cholesteric and crystal phases additional collective motions of Vogel-Fulcher-Tammann type were identified and described by the Havriliak-Negami model. We found from NMR data that internal and overall reorientations, molecular translational diffusion, and collective motions contribute to relaxation in both liquid phases, whereas in the crystal phase relaxation is mainly determined by internal motions and molecular reorientations.

Pressure ac/dc magnetic measurements of a molecular ferromagnet $[Co^{II}(pyrazole)_4]_2[Nb^{IV}(CN)_8]\cdot 4H_2O\}_n$, of unique structure with one type of Co-NC-Nb linkage **have shown its remarkable behaviour**: magnetic phase transition at ambient pressure occurs at $T_c = 5.4$ K, shifting to $T_c = 3.4$ K at about 4 kbar and returning to 5 K at about 12 kbar (Fig. 3). The spin values of magnetic ions are ½ for cobalt (with $g_{Co} \approx 4.33$) and ½ for niobium (with $g_{Nb} \approx 2.0$). We have verified that the magnetic order changes from ferro- to ferrimagnetic, with the niobium moment directed antiparallel to the cobalt moments at high pressures. A detailed phase diagram (Fig. 4) was established on the basis of pressure changes of coercivity (almost 16 times larger in 13 kbar than at ambient conditions), saturation magnetization, θ Weiss constant and the critical exponent. The ratio of the magnetocaloric effect at ambient conditions to that at 12.9 kbar strongly depends on the applied magnetic field.

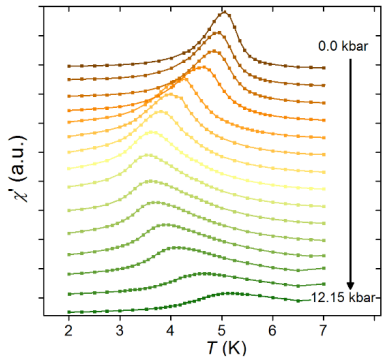

Fig. 3 *AC magnetic susceptibility at different values of applied pressure for* $[Co(pyrazole)_4]_2[Nb(CN)_8]\cdot 4H_2O\}_n$.

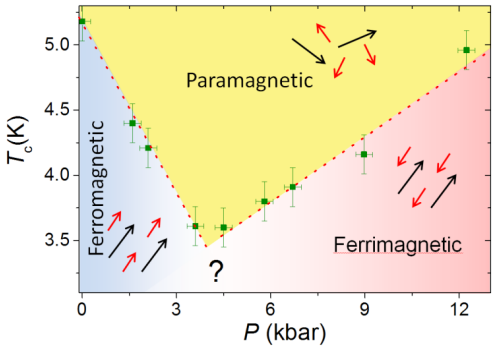

Fig. 4 *Phase diagram for a molecular magnet* $[Co(pyrazole)_4]_2[Nb(CN)_8]\cdot 4H_2O\}_n$ *under external pressure.*

To fully understand this intricate magnetic behaviour, high pressure single crystal X-ray diffraction analysis was performed in collaboration with the Adam Mickiewicz University research group. Mechanical stress-induced modification of the structure (changes observed in the Co-CN-Nb bond angles and lengths) correlates with the magnetic results. With regard to two competing contributions, of ferro- and antiferromagnetic character involved in the total coupling of Co^{II} $(t_{2g})^5(e_g)^2$ electrons with the Nb^{IV} 4d electron, the enhanced overlap of the orbitals caused by pressure results in strengthening of the antiferromagnetic interaction. In this manner, **the critical temperature first decreases with pressure in order to increase at the ferrimagnetic phase**. The compound is a rare example of a system where applied pressure changes the nature of magnetic coupling.

Simulation of the magnetic properties of lanthanide helicates revealed a change of sign of the exchange coupling in the homonuclear dimer along the heavy lanthanide series of isostructural dinuclear lanthanide $[Ln_2L_3](NO_3)_3$ molecules with Ln^{+3} = Tb (**1**), Dy (**2**), Ho (**3**), Er (**4**), Tm (**5**), and Yb (**6**). They represent an important class of supramolecular compounds, due to their rich applications inherently associated with 4f-block luminescence properties. The temperature-dependent and field-dependent magnetic properties of **1**–**6** compounds were modelled using a Hamiltonian consisting of a crystal field (CF) term, a super-exchange term and a Zeeman term. Application of the generalized van Vleck formalism enabled an estimation to be made of the CF parameters for Ln^{+3} ions within the quasi-symmetrical approximation and the determination of the superexchange coupling constants between the constituent Ln^{+3} ions in a dimer unit.

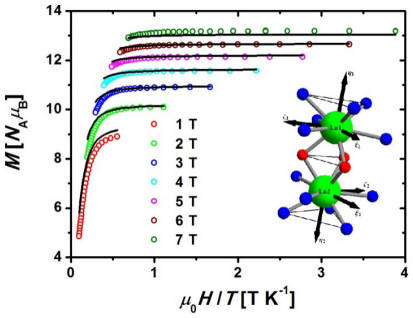

Fig. 5 *Magnetization vs. reduced magnetic field in sample* **1** *at indicated applied field values. Experimental points form separate branches indicating the presence of magnetic anisotropy. Inset: the di-nuclear lanthanide complex with local frames used in the calculations. Colour code: blue – N, red – O, green – Ln.*

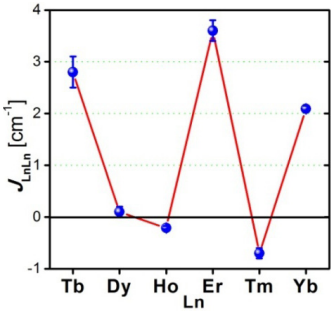

Fig. 6 *Changes in the exchange coupling constant between* Ln^{+3} *ions in the homonuclear dimer along the heavy lanthanide series.*

Optimization calculations were performed for temperature dependences of magnetic susceptibility and field dependences of magnetization. Figure 5 shows magnetization vs. reduced magnetic field H/T for the terbium analogue **1**. The exchange coupling mediated through phenolate bridges was found to change sign almost in an alternating fashion along the heavy lanthanide series, see Fig. 6. Ferromagnetic interactions were obtained in **1**, **2**, **4** and **6**, while antiferromagnetic interactions were revealed in **3** and **5**. Only the erbium analogue **4** demonstrated field-induced Single Molecule Magnet behaviour [Dalton Transaction **44** (2015) 16833].

Heteronuclear 3d-4f complexes are of great interest due to their unique structures and functional properties as magnetic, catalytic, optical and electronic materials. We investigated the magnetic properties of the novel hexanuclear cluster Cu^{II}_4–Gd^{III}_2 ($[Cu_4Gd_2(H_2L)_4(NO_3)_4(H_2O)_3](NO_3)2{\cdot}5.5H_2O$). **Despite the complicated structure, the Gd-Cu and Cu-Cu exchange couplings in the Cu^{II}_4–Gd^{III}_2 cluster could be unravelled.** The cationic moiety was regarded as two [Cu2Gd] units linked by a nitrate group which bridges two copper ions (Fig. 7). The Gd and Cu ions are exchange-coupled. Besides, the bridging unit NO_3 enables transmission of electronic effects between two adjacent Cu ions. The unit does not possess any symmetry elements, so the lengths and angles of the oxygen bridges are all different. In order to avoid an

over-parametric model, only two exchange coupling constants J_{GdCu} and J_{CuCu} were assumed. Quantitative analysis was performed on the basis of a Hamiltonian consisting of superexchange coupling and Zeeman terms. Intermolecular zJ' coupling was introduced within the framework of molecular field theory.

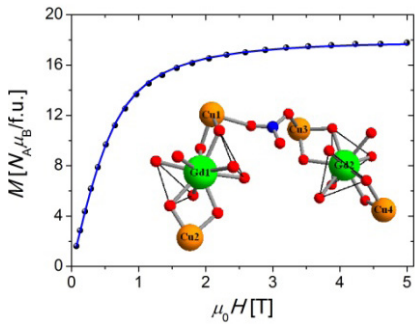

Fig. 7 *Isothermal magnetization of the compound at T=2 K and scheme of the hexamer unit. Solid line represents the best fitted curve.*

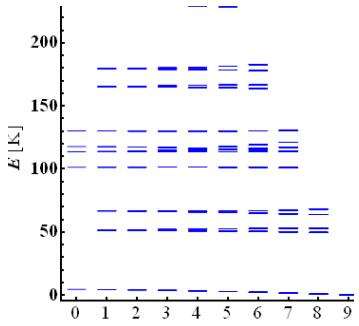

Fig. 8 *Calculated energy diagram for the hexamer unit.*

Temperature-dependent susceptibility and isothermal magnetization were used in a simultaneous fit to find the optimum values of J_{GdCu} = 9.9 cm^{-1}, J_{CuCu} = 5.9 cm^{-1}. The isotropic character of exchange interactions assumed in the model implied that the total spin S is a good quantum number. The obtained energy diagram is shown in Fig. 8. As all the exchange interactions are ferromagnetic, the ground state of the cluster has total spin S = 9 [Inorganic Chemistry Communications **54** (2015) 81].

Nanoalloys are bi- or multi-component metallic nanoparticles with complex structures and properties which depend on their size, structure, and composition. The size of nanoalloys (1–100 nm) places them between small molecules and bulk crystals. By adjusting the size, geometry and chemical composition, nanoalloys can be optimised for various applications in catalysis, nanomedicine, optics, data recording and energy storage. The structure, dynamics and stability of Fe–Pt nanoparticles were investigated using DFT-based techniques: total energy calculations and molecular dynamics. The investigated systems included multi-shell and disordered nanoparticles of iron and platinum. The study concerned icosahedral particles with the magic number of atoms (55): iron-terminated $Fe_{43}Pt_{12}$, platinum-terminated $Fe_{12}Pt_{43}$, and disordered $Fe_{27}Pt_{28}$. Additionally, the Fe_6Pt_7 cluster was investigated to probe the behaviour of extremely small Fe–Pt particles. **Molecular dynamics simulations,** performed for a few temperatures between T = 150–1000 K, **revealed high structural instability of the Fe-terminated nanoparticles and a strong stabilising effect of Pt-termination in the shell-type icosahedral particles.** Platinum termination prevented disordering of the particle even at T = 1000 K indicating very high melting temperatures of these Fe–Pt icosahedral structures. The analysis of evolution of the radial distribution function showed a significant tendency of Pt atoms to move to the outside layer of the particles – even in platinum-deficient cases (Fig.9). Further analysis of the trajectories of the Fe-Pt indicated the presence of two phase transitions in the 100-2000 K temperature range [Phys. Chem. Chem. Phys. **17** (2015) 28096].

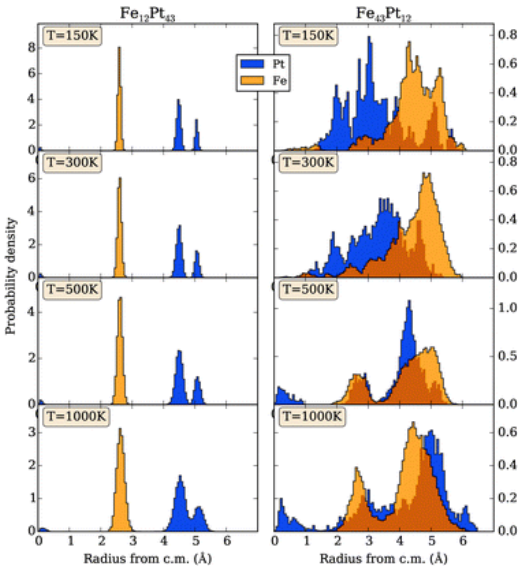

Fig. 9 *Radial distribution of atomic positions from the mass centre of the icosahedral-shell system. The results for all temperatures are compared side-by-side for the two investigated systems Pt-terminated (left) and Fe-terminated (right).*

In the standard BCS theory of superconductivity, the formation of Cooper pairs, with total momentum equal to zero, is discussed. However, in some materials where orbital effects are negligible and the upper critical magnetic field is given by the paramagnetic (Pauli) effect, a phase in which Cooper pairs with non-zero total momentum are present, can also be stable. This phase named the Fulde-Ferrell-Larkin-Ovchinnikov (FFLO) state could be expected e.g. in iron-based superconductors. In our studies of this possibility by using different multi-band models of these materials, it was shown theoretically that the FFLO phase can be stable in iron-based materials. Using a three-band model we found, among other results, the temperature versus magnetic field phase diagram (Fig. 10a) with the FFLO phase above the BCS phase, at low temperatures and high magnetic fields. Moreover, in every band this phase disappears at different magnetic fields, which is a consequence of different dispersion relations in each band. **Unconventional superconductivity in iron-based superconductors is manifested by a multiple phase transition which is observed experimentally as multiple discontinuities in the temperature dependence of specific heat** (Fig. 10b). This could be taken as a proof of the possibility that the FFLO phase exists [J. Phys.: Condens. Matter **27** (2015) 482001].

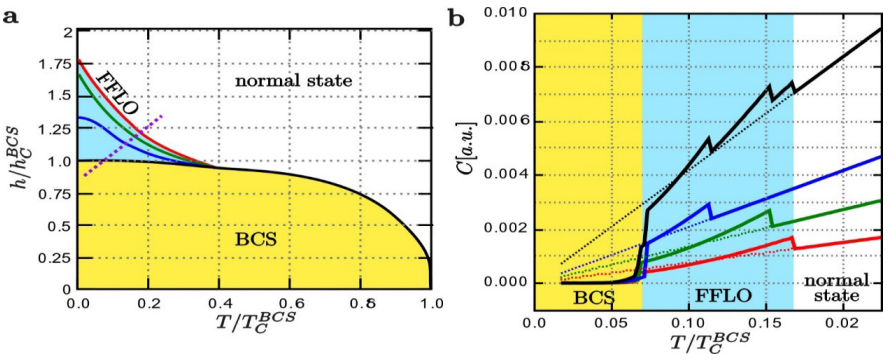

Fig. 10 *(a) Temperature versus magnetic-field phase diagram. (b) Specific heat C in each band as a function of temperature along the dotted line marked in panel (a). The full black line represents the total specific heat over the three bands; red, green, and blue lines show bands 1, 2, and, 3, respectively.*

Iron oxides occur in nature in many forms, often significantly different from each other in terms of structural and physical properties. Wustite (FeO) has challenged experimental and theoretical condensed matter physics for over sixty years. In particular, the extent of its non-stoichiometry and its defect structure have been the subject of extensive experimental studies and are still a matter of discussion. We investigated the role of strong electron correlations on Fe atoms and the high concentration of cation vacancies in modifying the electronic and dielectric properties of wustite. We demonstrated that both substantially affect the electronic properties of this compound and have an opposite effect on its band structure. While the local electron interactions in the Fe 3d states are responsible for opening the insulating gap, the Fe vacancies reduce its magnitude [Phys. Rev. B **91** (2015) 195111]. A new variety of iron oxide, recently prepared, modelled and tested by scientists cooperating within the KNOW collaboration, revealed features previously unobserved in any other material. The new form of iron oxide (FeO) is a metallic crystal with unique electrical and magnetic properties. Our calculations carried out for a single monolayer have established the types of vibrations performed by atoms in the crystal lattice at different energies. The theoretical results were verified using the European Synchrotron Radiation Facility in samples with multiple monolayers of iron oxide on a platinum substrate prepared by a special procedure. Experiments confirmed that vibrations of atoms in the crystal lattice agree perfectly with the theoretical model (Fig.11). Of particular interest was the analysis of vibrations dependent on the number of layers of FeO on the platinum substrate. **In the case of one or two layers the movement of atoms is of two-dimensional nature. If the number of layers is six or more, atoms vibrate as in a typical three-dimensional crystal.** In the materials studied to date the nature of the vibration was closely associated with the dimensionality of the system. Meanwhile, a new variant of iron oxide with three, four and five layers of atoms was proved to vibrate in an intermediate manner, corresponding to a fractional numbers of dimensions [Phys. Rev. Lett. **115** (2015) 186102].

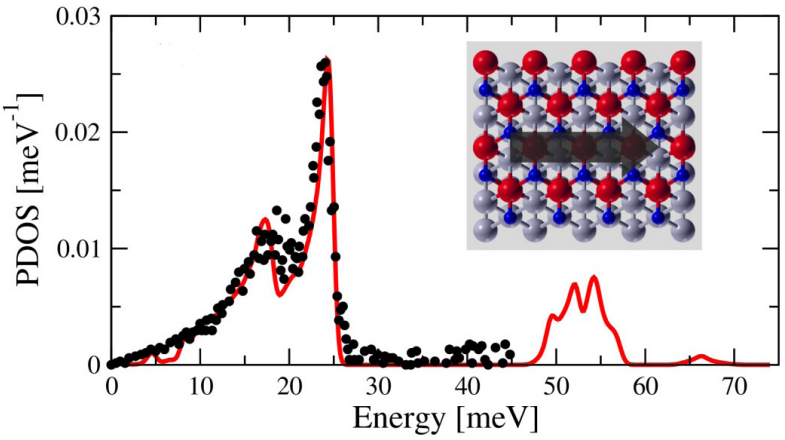

Fig. 11 *Comparison of the calculated (red line) and measured (black dots) phonon density of states in a thin film of a new form of iron oxide. Inset shows the top view of the FeO/Pt(111) thin film and the direction of measurement.*

Interesting physical behaviour, observed in cage-type structures, frequently originates from the so-called "rattling" effect associated with a localized, anharmonic, low frequency, and high amplitude vibration mode, at a specific crystallographic site, such as at the centre of an oversized atomic cage. To analyse the superconductivity mechanism in intermetallic cage compounds ScV_2Al_{20}, LuV_2Al_{20}, and YV_2Al_{20} (with critical temperatures T_c = 1.00, 0.57, and 0.60 K, respectively) we have (in *cooperation with the AGH University of Science and Technology*) undertaken density functional theory (DFT) calculations of the electronic structure and phonons, as indicated by measurements (at the *Gdansk University of Technology*) of electrical resistivity, magnetic susceptibility, and heat capacity. We confirmed the major influence of the cage-filling atom occupying the central position in the cubic cell on the overall electron and phonon properties of these materials. Essential differences between the phonon density of the state spectra were observed in some vibrational spectra of metal(8a) atoms that are almost dispersionless low-frequency phonon modes and to a lesser extent by the lowest Al(16c) optic modes. Electronic and phonon structure calculations confirmed the weak-coupling regime of the electron-phonon interaction and showed the importance of rattling-like metal atom modes in driving them into the superconducting state (Fig.12). In particular, we may conclude that **in caged materials in the low-frequency mode, anharmonicity is clearly correlated with the magnitude of superconductivity** (with the T_c value enhanced in the most anharmonic ScV_2Al_{20}). LaV_2Al_{20} stands out as the only non-superconducting system [Phys. Rev. B **93** (2016) 134507].

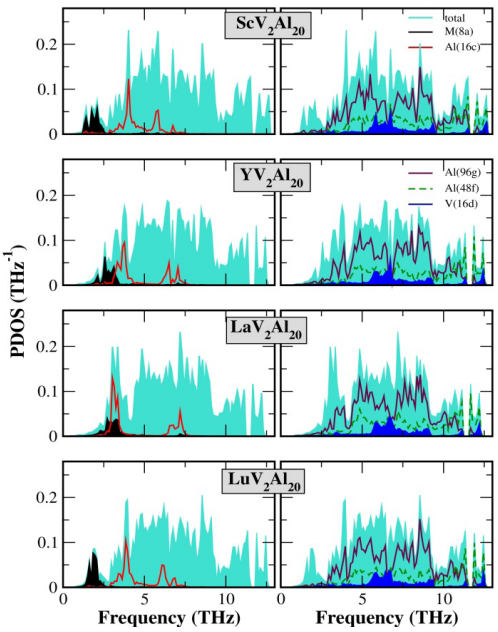

Fig. 12 *Total and partial phonon density of states calculated for* MV_2Al_{20} *(M = Sc, Y, La, Lu).*

The magnetocaloric effect (MCE) of a high-spin cluster with a Ni_9W_6 core has been determined by employing relaxation calorimetry in an applied magnetic field. MCE can be used for cooling in the process of adiabatic demagnetization. There is an on-going quest for highly efficient MCE coolers. It has been recently noticed that molecular nanomagnets are prospective systems for applications at the lowest temperature range. We have performed a study of the unique cluster compound $\{Ni[Ni(L)(H_2O)]_8[W(CN)_8]_6\}\cdot 17H_2O$ ($L\text{–}C_{20}H_{24}N_2O_4$) based on cyanido-bridged Ni_9W_6 cores, with spins of the metal ions $S_{Ni} = 1$ and $S_W = ½$ (Fig. 13). The ferromagnetic coupling through cyanido linkages leads to a ground state of $S = 12$. The entropy content associated with this spin value amounts to $R\ln(2S+1) \approx 26.76\ J\ K^{-1}mol^{-1}$. The clusters were found to display axial and rhombic anisotropy. The temperature dependence of MCE given by the magnetic entropy change ΔS_M and/or the adiabatic temperature change ΔT_{ad}, due to applied field change $\mu_0\Delta H$ ranging from 1 to 9 T, shows that the maximum value of ΔS_M at $\mu_0\Delta H = 5$ T is 18.38 $J\cdot K^{-1}\cdot mol^{-1}$ at 4.3 K. The corresponding maximum value of $\Delta T_{ad} = 4.6$ K is attained at 2.2 K, see Fig. 13. The exponent n characterizing the dependence of ΔS_M on the change of magnetic field H according to $\Delta S_M \propto H^n$ was determined for the first time over a broad temperature range (see inset in Fig. 14). **Our study revealed that the Ni9W6 compound may be treated as a possible candidate for cryogenic magnetic cooling** [J. Magn. Magn. Mater. **414** (2016) 25].

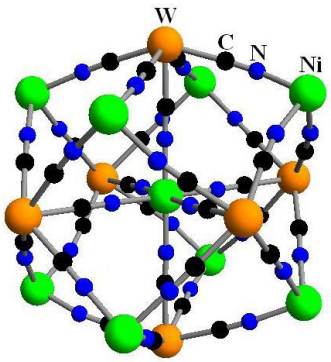

Fig. 13 *Schematic view of the cyanido-bridged core of the $Ni(II)_9W(V)_6$ molecular cluster with spin S = 12.*

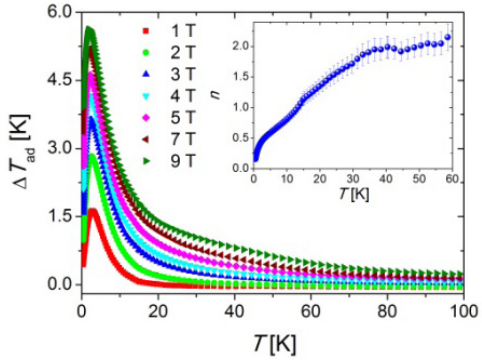

Fig. 14 *Temperature dependence of the adiabatic temperature change ΔT_{ad} at different field strengths. Inset: Temperature dependence of the exponent n quantifying the field dependence of the isothermal entropy change ΔS_M.*

A related study concerned **MCE in the Mn12 molecular cluster immobilized in SBA-15 mesoporous silica**. The Mn12 molecules ($[Mn_{12}O_{12}(CH_3COO)_{16}(H_2O)_4]\ 2CH_3COOH\cdot 4H_2O$) of total spin S = 10 were linked to the silica channel walls by means of COOH groups. The efficiency of synthesis of the SBA-Mn12 sample (see Fig.15) was examined by means of X-ray diffraction, infrared spectroscopy, nitrogen sorption and TEM techniques. The behaviour of SBA-Mn12 was compared to the performance of free molecules in polycrystalline Mn12. The change in entropy, ΔS, was determined from isothermal demagnetization curves. Relaxation of the magnetic moments was also explored by means of AC and DC magnetic measurements. As a result of incorporation into silica, magnetic relaxation slightly slowed down, while the distribution of the relaxation times increased by a factor of two (not shown). Fig. 16 presents the magnetic entropy change for both systems. The maximum $|\Delta S|$ at field variation 50 kOe in SBA-Mn12 is equal to 13.8 $J\ K^{-1}\ mol^{-1}$ at T = 2.8 K, which is much less than 25.3 $J\ K^{-1}\ mol^{-1}$ observed for Mn12 at 3.2 K, yet still a significant value. Narrow $|\Delta S|$ peaks are due to the small sweeping rate of the applied field. Interestingly, the temperature of $|\Delta S^{max}|$ for SBA-Mn12 is not dependent on the field strength, yet it increases with increasing field for free Mn12. In the superparamagnetic region at T > 3.6 K, the data for both samples are similar. **The altered relaxation and significant differences in MCE for free and immobilized Mn12 molecules point to the successful and homogenous incorporation of Mn12 into the silica channels.** The present work is the first step to obtain well-defined technologically important layers functionalized with high-spin entities [RSC Advances **6** (2016) 49179].

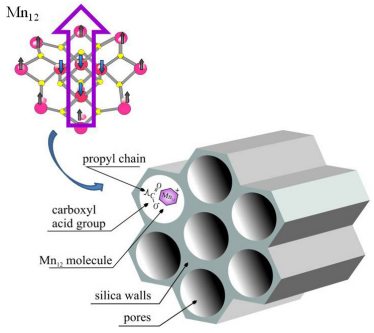

Fig. 15 *Schematic presentation of the functionalization of SBA-15 silica of 4.8 nm pore diameter with Mn12 magnetic molecules (only the molecule core is shown).*

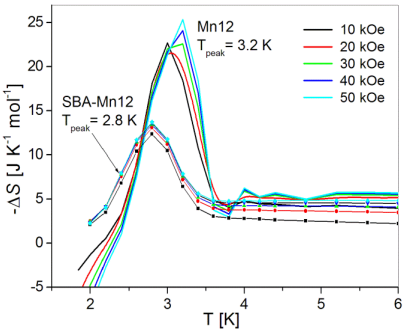

Fig. 16 *Comparison of magnetic entropy changes at different magnetic fields for SBA-Mn12 and for Mn12 samples.*

To gain knowledge about the influence of constrained geometry on the dynamics of encapsulated 4CFPB, molecules of 1.67 nm length and 0.46 nm width (as obtained from quantum-chemical calculations), were placed in 6 nm and 8 nm porous matrixes. This small difference in confined space for molecules proved to be of great importance to molecular dynamics, as well as to temperatures of phase transitions. Molecular arrangement parallel to the pore walls was first found (see inset on Fig. 17), with the width of immobile molecular layer along the walls growing on heating [Liquid Cryst. **14** (2014) 1073]. Dielectric relaxation times characterizing molecular flip-flop motions inside the pores turned out to be shorter than those in the bulk material, and much shorter than those observed in earlier experiments performed under pressures up to 200 MPa. In addition, motions not observed in bulk were found. Moreover, in pores the nematic 4CFPB transforms into isotropic liquid at a temperatures lower those in bulk and much lower than those found in pressure experiments. Based on a typical linear pressure dependence of the clearing point, **the pressure experienced by 4CFPB molecules reorienting in pores was estimated to be negative,** which is shown in Fig. 17: in pores with a diameter of 8 nm the pressure value of –4.9 MPa, while in pores with a diameter of 6 nm, that of –11.2 MPa, were estimated. Due to ordering of the molecules along walls, the remainder of the liquid is less dense than the liquid under normal conditions. Such a metastable liquid can exist only inside a porous matrix.

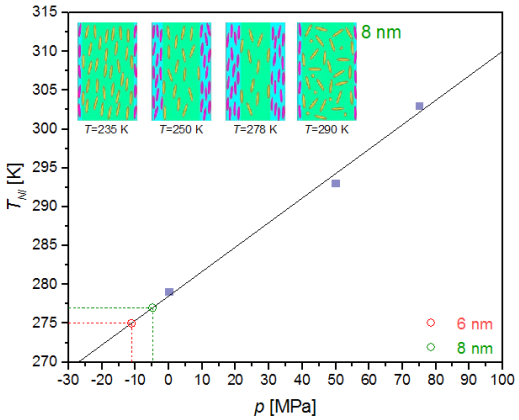

Fig. 17 *Pressure dependence of the clearing point in 4CFPB used to determine conditions in nanopores. Inset shows the molecular arrangement during heating in 8 nm nanopores.*

A unified description of the surface dynamics on inner surfaces of cylindrical cavities in elastic media has been established over the whole range of transverse contraction to longitudinal extension ratio (Poisson's ratio). Curvature of the surface is at the origin of new dynamical properties, unlike that in flat surface dynamics. The dispersion relations of the true surface waves (TSW), i.e. the excitations characterized by infinite life times have been calculated (Fig. 18), exhibiting cut-off wave vectors, except such of flexural mode. We have obtained cut-off wave vectors of TSWs as functions of the Poisson ratio and

azimuthal index *n* (equal to one-half of the number of nodes on the circumference of the cavity). The inflection points, also called Airy phases, have been found and shown to exist for $n < 6$ only. The corresponding wave vectors for n = 0 and n = 1 significantly increase with negative Poisson ratio. Apart from the above secular waves the cylindrical geometry gives rise to a number of excitations that radiate their energy into the bulk in a fairly slow way. Such excitations are called surface leaky waves. The dispersion relation for the leaky waves and their special linear combination of incoming and outgoing waves, i.e. the so-called *total conversion mode* and *no conversion mode* has been obtained for given elastic parameters of the material up to $n = 3$. The response to an external periodical perturbation (Local Density Of States) has been obtained in fully-symmetrical mode for selected values of the Poisson ratio [Phys. Status Solidi B **252** (2015) 1595].

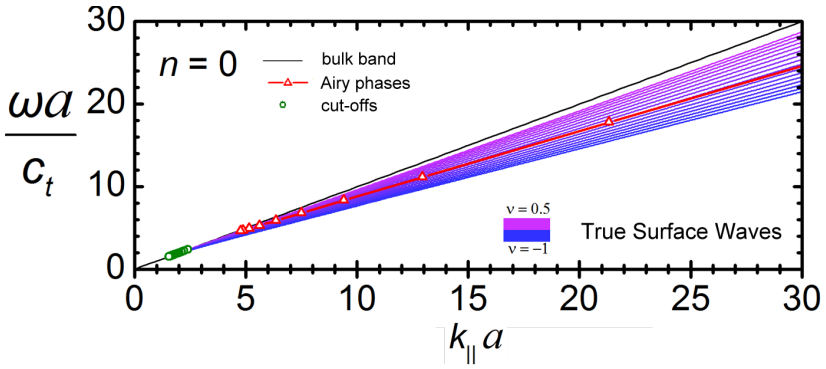

Fig. 18 *Dispersion relations for fully-symmetric (n = 0) true surface waves on the inner surface of a cylindrical borehole in an elastic medium, over the allowable range of Poisson's ratio. Cut-off wave vectors and Airy phases are indicated.*

Deuteron spectra were measured in D_2O confined in NaX, NaY and DY zeolites with the aim to study the molecular mobility of confined water as a function of the Si/Al ratio, loading and temperature. At low loading, a component related to water deuterons jumping about the twofold symmetry axis dominated the recorded spectra, while at high loading these became doublets of rigid water deuterons. A set of the quadrupole coupling constant values $C_Q(D)$ for localized water deuterons was derived from analysing these doublets. Comparison of the results with DFT calculations allows the assignment of deuterons to locations at oxygen atoms in the zeolite framework and of water clusters inside cages (Fig.19). The $C_Q(D)$ depends on the OD distance according to the relation $C_Q(D) = (-2.732d_{OD} + 2.938)$ [MHz]. Catalytic activity is higher for positions with smaller $C_Q(D)$ [J. Phys. Chem. C **119** (2015) 19548]. Studies of spin-lattice relaxation rates allowed us to find that **translational diffusion of water molecules is related to the strength of the electrostatic interaction of water oxygen atoms with sodium cations, while water molecule reorientations seem to depend on the strength of hydrogen bonding to the framework oxygen atoms and on the strength of hydrogen bonds between water molecules, at outer and inner positions in water clusters, respectively.** Hysteresis of spin-lattice relaxation rates R_1 and R_2, observed for sample with 280 water molecules per unit cell of DY (Fig.20) in heating/cooling cycles most likely reflects the formation/decomposition of water clusters at different temperatures, usually termed as a fragile-to-strong structure transition [J. Phys. Chem. A, **118** (2014) 5371].

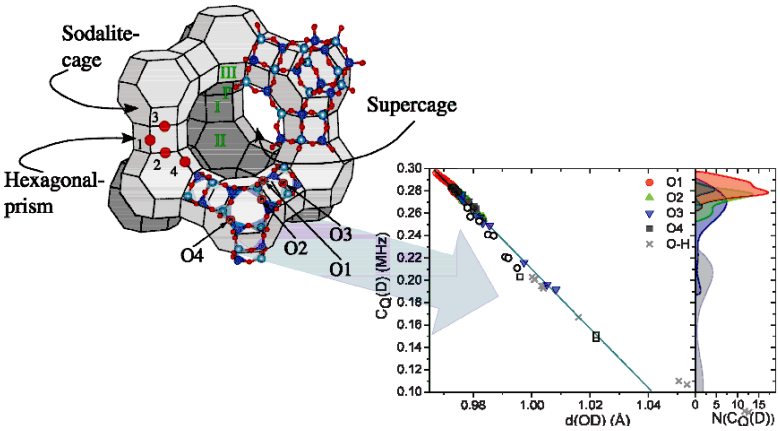

Fig. 19 *Dependence of the deuteron quadrupole coupling constant $C_Q(D)$ on O–D bond length, as given by DFT calculations. The abundance $N(C_Q(D))$ (projection) of deuterons at respective labelled oxygen positions in the structure of DY zeolite is also shown.*

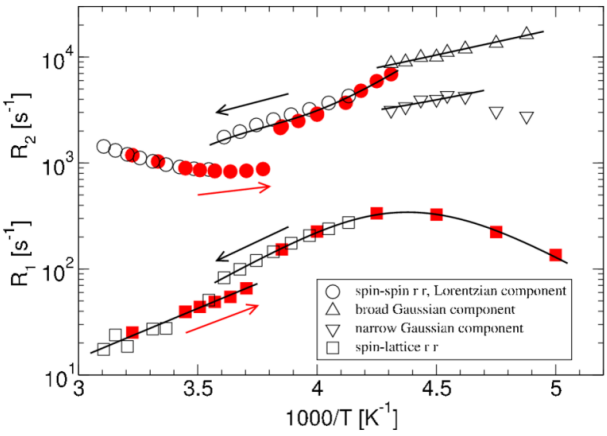

Fig. 20 *Temperature dependence of deuteron relaxation rates R_1 and R_2 for the DY zeolite with 280 D_2O molecules per unit cell loading. Filled and open symbols represent results obtained on cooling and heating, respectively.*

Well-defined films of Prussian blue analogues of the general formula $Ni^{II}_{1.5}[Fe^{III}(CN)_6]_x[Cr^{III}(CN)_6]_{1-x}$ ($x = n_{Fe}/(n_{Fe}+n_{Cr})$, were successfully produced using the multisequential adsorption technique. In that technique a solid support is repeatedly immersed in an aqueous solution containing cations and then in a solution containing anions (Fig. 21). The ratio of the Fe:Cr content was controlled by the deposition sequence. Thin films of average thickness of 200-300 nm were synthesized.

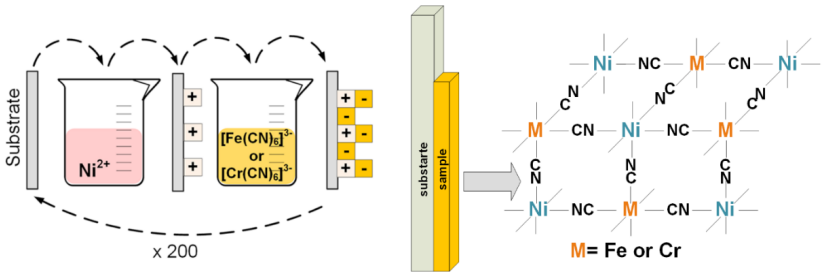

Fig. 21 *Scheme of "layer by layer" film deposition and structure of PBA thin film.*

The microstructure and magnetic properties of the obtained films strongly depend on the x value. Temperature dependences of the real component of AC magnetic susceptibility χ' show that the critical temperature T_c of the magnetic transition to the ordered state increases with decreasing value of x (Fig. 22 a). T_c is equal to 21 K, 33 K, 48 K, 62 K and 75 K at x = 1, 0.8, 0.55, 0.23 and 0 (as determined by Energy Diffraction X-ray spectroscopy), respectively. The shape of the χ'(T) curves correlates with the magnetic hysteresis loops M(H): the minimum value of the coercive field H_c, i.e. the smallest anisotropy, is observed for x = 0 while it increases with increase of the Fe content, reaching 1.77 kOe at x = 1 (Fig. 22 b). Both dependences, T_c vs. x and H_c vs. x, are approximately linear. **The systematic change of T_c and of H_c with the Fe/Cr content points to the high precision and efficiency of the "layer by layer" deposition method in varying the magnetic properties of thin films of Prussian blue analogues.**

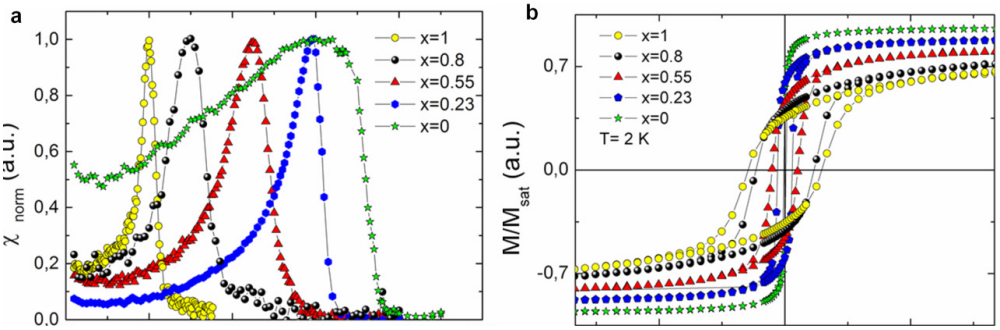

Fig. 22 *Temperature dependence of the real component of AC magnetic susceptibility(a) and hysteresis loops at T=2 K obtained for thin films oriented parallel to the DC field (b).*

In cooperation with the Department of Applied Chemistry of Chiba University (Japan) a new experimental technique, i.e., the positron probe micro-analyzer (PPMA) was applied to studies of the defect induced by ball indentation or sliding on the surface of well-annealed copper. A focused positron beam of energy 24.5 keV and 70 μm spot diameter was used to scan the deformed region over its surface. In the case of indentation by ball, the measured defect distribution correlates well with the stress distribution of the Hertz contact and the von Mises yield criterion. **For a wear track produced by a pin on disc dry sliding, an asymmetric defect distribution near the wear track is observed** (Fig.23). This indicates the presence of a tangential force which additionally deforms the sample. PPMA was also used to study defect profiles in the subsurface region of machined metals: Cu, Fe and Ti. The extent of the profile depended on the metal and on cutting speed. PPMA allowed us also to trace the evolution of the profile after annealing in different temperatures [Tribol. Lett., **56** (2014) 101, Tribol. Lett., **60** (2015) 16].

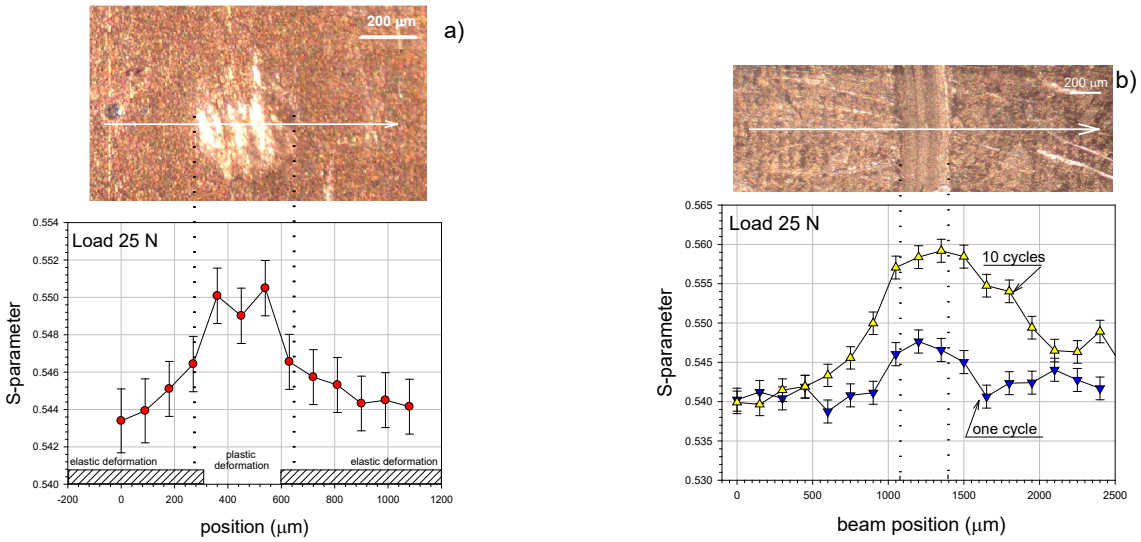

Fig. 23 *a) SEM image of ball indentation with a load of 25 N on the surface of well-annealed copper (top). The arrow indicates the direction of the positron beam scan across the indentation. The lower graph shows values of the S-parameter, i.e., the annihilation line shape parameter sensitive to the presence of defects at different points at the vicinity of the indentation. b) SEM image of the wear track induced by the ball sliding over the surface of well-annealed copper with a normal load of 25 N (top). The lower graph shows values of the S-parameter at different points in the vicinity of the track after 1 and 10 sliding cycles.*

Hydrogen storage is a key technology for advancement in applications of hydrogen and fuel cell technologies to portable/stationary power and transportation. The issue of hydrogen storage is still unresolved [Applied Surface Science **388** (2016) 723, Phys. Status Solidi A, **1** (2016) 7]. Some of the best candidate hydrogen storage materials are intermetallic compounds. Since RMn_2 (R-rare earth) readily absorbs and desorbs hydrogen at relatively low temperatures and pressures, we found it important and interesting to determine its physicochemical properties above room temperatures, especially those close to real conditions of its possible applications in hydrogen storage and recovery. Our *in-situ* neutron diffraction experiments of a partially saturated $HoMn_2D_x$ sample were performed at deuterium pressures between 0.5 to 30 bar with the E6 ion diffractometer at the *Helmholtz Zentrum Berlin* using Sievert's apparatus. After introducing deuterium into the reactor, deuterium absorption was demonstrated (Fig. 24a). A strong effect of deuterium pressure on the crystallographic and magnetic structures and on thermodynamics properties was found over the temperature range 300 K-550 K – as seen in the appearance and fading of the magnetic structure lines at 300 K (Fig. 24b). Comparison of deuterated and non-deuterated materials allowed us to determine the positions of deuterium atoms in the crystallographic structure above magnetic ordering temperature, which would have been impossible in a 'classical ex-situ' experiment due to desorption of the escaping deuterium. By analysing the structural and magnetic lines we showed that **deuterium atoms can form ordered superstructures with antiferromagnetic ordering varying from long-range to short-range along with the varying concentration of deuterium, *x*.**

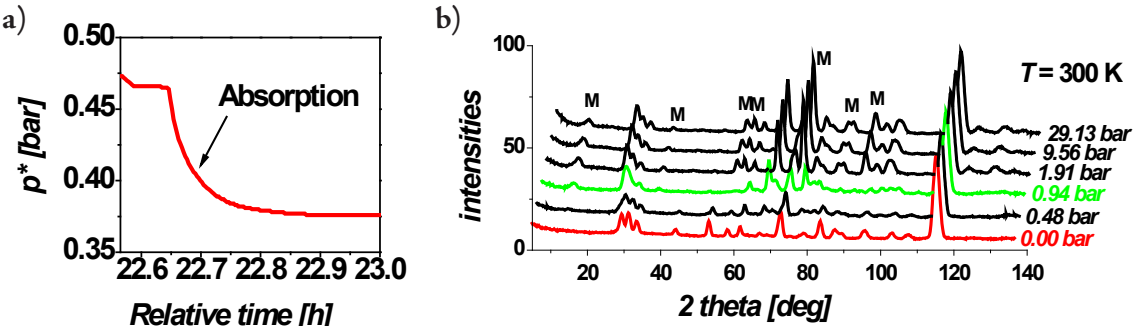

Fig. 24 *a) Changes of deuterium pressure measured above the sample $HoMn_2D_x$ as a function of relative time; b) 'In-situ' neutron diffraction patterns at different deuterium pressure, using Sieverts-type apparatus. M – reflections of magnetic structure.*

A high-pressure phase diagram of manganese borohydride $Mn(BH_4)_2$ was determined by density functional calculations and simulated annealing global structure optimization. The calculations were combined with high-pressure diamond anvil cell powder X-ray diffraction and Raman spectroscopy. Apart from the α-$Mn(BH_4)_2$ crystal phase, two polymorphs were discovered (Fig. 25). The first polymorph, δ-$Mn(BH_4)_2$, is formed around 1 GPa and is isostructural to the magnesium analogue δ-$Mg(BH_4)_2$. This polymorph is stable upon decompression to ambient conditions and can also be obtained by compression of α-$Mn(BH_4)_2$ in a large-volume steel press as well as by high energy ball milling. At ambient conditions it exhibits the space group $I4_1/acd$ with cell parameters a = 7.8524, c = 12.145 Å, and V = 748.91 Å^3. According to respective calculations, it can also be described by an equally stable P-4n2 superstructure.

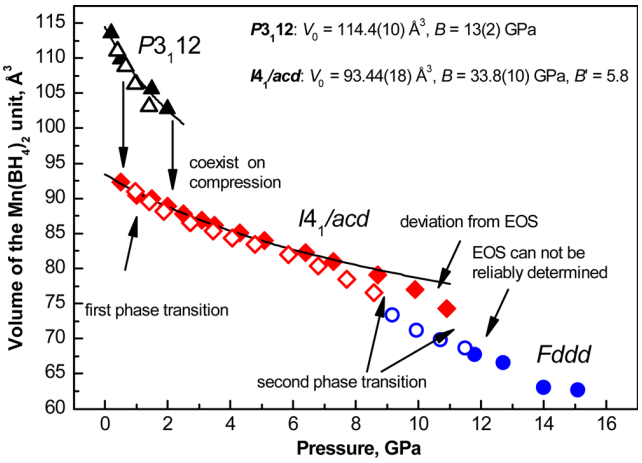

Fig. 25 *Phase diagram for Mn(BH4)2 determined by ab initio calculations and verified by the high pressure X-ray diffraction experiments.*

The δ-$Mn(BH_4)_2$ polymorph undergoes a phase transition to δ'-$Mn(BH_4)_2$ over the pressure range 8.6–11.8 GPa. The δ'-phase is not isostructural to the second high-pressure phase of $Mg(BH_4)_2$, and its structure was determined as a $\sqrt{2}a \times c$ supercell, compared to the δ-phase, and refined to the space group *Fddd* with a = 9.205, b = 9.321, c = 12.638 Å, and V = 1084 Å^3 at 11.8 GPa. Thus, **equations of state were determined for α- and δ-$Mn(BH_4)_2$** [Chem. Mater. **28** (2016) 274].

Means of chemical synthesis allow one to control the shape and composition of nanostructures. Zero-dimensional nanomaterials, with unusual shapes and sizes between 2 to 50 nm, can be fabricated for materials science studies in chemistry and for applications in catalysis, medicine or biology. Currently, one of the most promising catalysts for ethanol oxidation in direct ethanol fuel cells are ternary PtRh/SnO_2 nanoparticles, shown schematically in Fig. 26a. As disruption of the ethanol molecule occurs at the interface between PtRh and SnO_2 particles, their physical contact is of crucial importance for good catalytic activity. By scanning transmission electron microscopy using a wide-angle annular

dark field detector (STEM HAADF) we showed that the synthesis of 12 nm large supports decorated by 2 nm nanoparticles was successful (Fig. 26b). By energy-dispersive X-ray spectroscopy (EDS) mappings we confirmed that SnO2 nanocatalysts, coated by metallic PtRh nanoparticles had been produced (Fig.26c). To enhance the catalytic activity of the ternary catalysts, we decided to increase the Pt surface. To this end, we synthesized novel three-dimensional (3d) Pt frame/Ni core catalysts, Fig. 26d-g, and then removed Ni, obtaining hollow Pt frames, Fig. 26h,i. Our PtNi nanoparticles have initially a dodecahedron shape with Pt at the edges and Ni in the core as confirmed by STEM and EDS, Fig. 26d-g. **When etching away the Ni core, the remaining Pt frame offers a much larger active surface compared to spherical PtNi nanoparticles**, Fig. 26h.

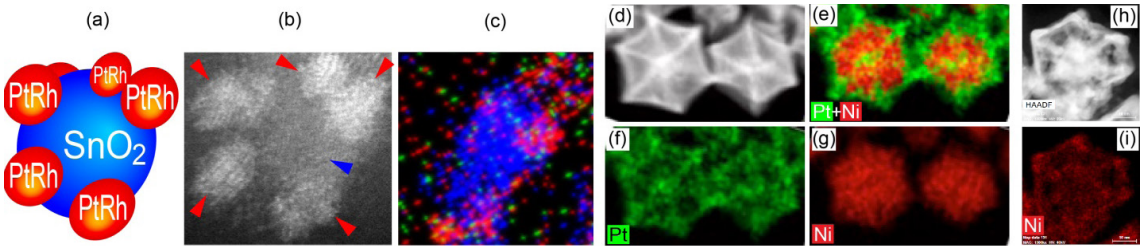

Fig. 26 *(a) Schematic representation of the SnO_2 support decorated by PtRh NPs. (b) STEM HAADF image of the PtRh/SnO_2 nanocatalyst (red arrows points to PtRh, blue arrow to SnO_2) with the corresponding EDS map showing the distribution of Pt-red and Sn-blue (c). (d) PtNi 3d nanoparticles with the corresponding EDS maps showing a Pt frame, in green (e,f) surrounding a Ni core, in red (e,g). STEM HAADF image of the hollow PtNi frames after etching (h) with the corresponding EDS map showing the Ni distribution (i), confirming that the Ni core is porous.*

A green method of synthesis using an extract of camomile was applied to synthesize silver nanoparticles in order to optimise their antibacterial properties by synergy of the therapeutic effects of camomile and of Ag. STEM studies revealed that the camomile extract (CE) consists of porous globular nanometer-sized structures (Fig. 27a-c), which offer perfect support for Ag nanoparticles. The Ag nanoparticles synthesized with the camomile extract (Ag/CE) of 7 nm average sizes, were uniformly distributed on a CE support (Fig. 27d,e). EDS chemical analysis showed that camomile terpenoids adsorbed on the surface of Ag/CE (Fig. 27e), act as capping agents, which prevent agglomeration and help in reducing Ag^+. Fourier Transform Infrared (FTIR) and UV-Vis spectroscopy measurements confirmed these findings: compared to pure CE, in the spectra of Ag/CE the 1109 cm^{-1} band (FTIR) and the peaks at 280 and 320 nm (UV/Vis) corresponding to –C–O groups of terpenoids, are not present. **Antibacterial tests using four strains of bacteria showed five-fold improvement of Ag/CE nanoparticle efficiency compared to that of CE and Ag nanoparticles, totally reducing all bacteria within 2 hours.**

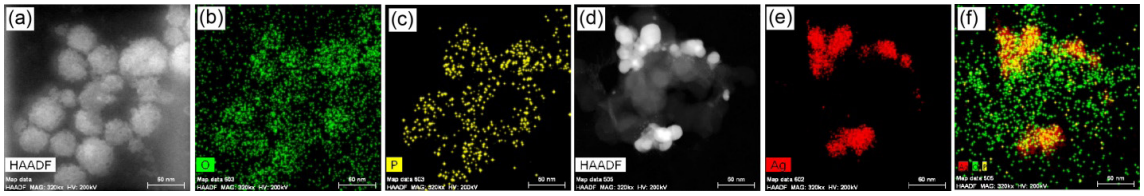

Fig. 27 *STEM HAADF image of a pure camomile extract used for the synthesis of Ag particles (a) with the corresponding EDX maps of O (b) and P (c) distribution. STEM HAADF image (d) of Ag particles synthesized with the camomile extract with the corresponding EDX maps of Ag (e) and Ag+O+P (f) [Bioprocess. Biosyst. Eng.* **39** *(2016) 1213].*

IV. DIVISION OF THEORETICAL PHYSICS

Theoretical Physics guides experiment and contributes to the treasury of the knowledge of mankind. The research at the Division of Theoretical Physics covers a broad range of fundamental issues concerning the structure and dynamics of the Universe studied over all scales available – ranging from the smallest to the largest dimensions. This broad scale of research topics which are dealt with by our Division, has been grouped as follows:

HARD PROCESSES AND PARTON DENSITIES IN COLLIDER EXPERIMENTS

The KrkNLO project is a system of computer calculations in the area of high energy physics in which a description of the parton shower is joined together with a hard matrix element (i.e. with a calculation which describes the central part of the collision of particles) with next-to-leading accuracy. This method is simpler and more accurate than any other available approach. To date only two such methods have been developed: the MC@NLO and the POWHEG. This new solution has been implemented in two independent parton shower calculations used at LHC, SHERPA and HERWIG. The KrkNLO method has been thoroughly tested and compared with results of other methods. The proposed simplification of the method of joining NLO corrections with the parton shower will be crucial in the next stages of improving the precision of Monte Carlo calculations, where similar calculations at a higher, next-to-next-to leading order approximation, will be implemented.

A new framework was developed for the description of jets at high energy processes in colliders. This framework is called ITMD (Improved Transverse Momentum Dependent) factorization. It allows for the evaluation of cross sections where final states are produced in the so-far unexplored, forward region of the detector. ITMD factorization has already been applied to the production of forward-forward dijets in p-Pb collisions. It predicts strong suppression of the cross section, compared to p-p collisions. This can be tested directly by experiment, potentially providing further evidence of saturation. The ITMD factorization also allows one to address Ultra Peripheral Collisions of Heavy Ions. The project has led to advancing the method of evaluating matrix elements for processes with an arbitrary number of final-state partons. In particular, the so called BCFW recursion has been shown to hold also for the case of partons having non-vanishing transverse momenta. The project also aims at gaining better understanding of Double Parton Scattering (DPS). The dominant contribution to cross sections at the LHC arises from cases with a single hard interaction. However, it has been shown that multiple scattering also introduces a significant contribution.

The Herwiri2 MC event generator has been improved. In this improvement, called KKMC-hh, the new exact $O(\alpha^2 L)$ resummed EW generator KKMC 4.22, featuring CEEX multiple photon resummation and EW corrections, is combined with the Herwig parton shower environment. This new MC features exact $O(\alpha)$ pure weak corrections from the DIZET EW library and both CEEX and the EEX YFS-style resummation of large multiple photon effects. It provides a reliable path to 0.05% precision for EW effects in hadron-hadron colliders.

Initial conditions for QCD evolution equations describing double parton distribution functions in the pure gluon case have been constructed. The momentum sum rule and a specific form of the known single gluon distribution function have been implemented. Evolution of the double parton distribution with a hard scale has been investigated. W^+W^- and Z^0Z^0 electroweak boson production in double parton scattering using QCD evolution equations for double parton distributions has been studied.

Research on tau lepton physics, an important element of the phenomenology of the Higgs boson parity determination, was being continued. Innovative methods of Machine Learning were used, in collaboration with members of the Google-New York team. This resulted in a publication describing this novel method of optimizing the Higgs boson CP measurement in H−>ττ decays at the LHC by exploiting machine learning techniques.

Over the years 2014-2016 substantial progress has been achieved in the development of tools to describe final state interactions in the phenomenology of hard scattering processes at accelerator experiments. This is an important domain, as the precision of measurements of lepton directions at LHC experiments is an order of magnitude higher than that of any other measurable quantity in such experiments. Earlier publications and programs concerning the tau lepton decay generator TAUOLA and of photonic effects in decays, PHOTOS, have increased their citation index during the last 3 years by over one hundred each. In both cases this index now exceeds 700. This progress was partly achieved through new publications – for instance on the tau-lepton decay, on properties of final states in Drell-Yan processes, and through computer algorithms. Newer publications were cited less frequently, not only as being more recent, but also because earlier publications on Monte Carlo generators were quoted instead. Thus, the discussed projects continue to be important tools in lepton and heavy boson physics at most high energy accelerator experiments.

A new parametric representation of the hadronic current for the tau-lepton decay to three pions, derived from the chiral lagrangian with explicit inclusion of resonances, was proposed. In addition to the generally considered vector and axial-vector resonances, also the scalar and, for the first time, the lowest tensor $f_2(1270)$ resonances have been included. The sigma-$f_0(980)$ splitting was taken into account. At low energies all form-factors reproduce chiral behaviour. By imposing high-energy conditions and demanding QCD-prescribed behaviour by the form-factors at short-distances, a set of equations to calculate the vertex constant values were obtained.

Principles of the mini-jet model with soft gluon resummation were applied to estimate the total and inelastic hadronic cross section over the high energy region. It was demonstrated that the model fails to simultaneously describe the total and elastic cross sections. To correct the model, a phenomenological parametric description of the single diffractive contribution was added and the combined distribution compared against LHC data.

HEAVY MESON DECAYS AND LIGHT MESON INTERACTIONS

Studies of CP violation and of final state interactions in D^0-meson decays into a kaon and two charged pions measured at BaBar have been undertaken in collaboration with the LPNHE Laboratory in Paris. The heavy-meson decay amplitudes are constructed in the QCD factorization framework. Unitarity plays an important role in constraining the number of free parameters required in the description of experimental data obtained in D-meson factories.

Multichannel two-meson interactions below 2 GeV have been studied. A full set of $\pi\pi$ partial wave amplitudes has been constructed and tested by comparison with experimental data and the crossing symmetry constraint. A scalar-isoscalar π-π form factor has been calculated and compared to experimental data and with theoretical constraints. The spectrum of light mesons decaying into various two meson channels has been investigated using newly derived theoretical amplitudes. The contribution of multichannel two-meson scattering to the final Y-meson family decays has been calculated and compared with the available data and with various theoretical predictions. Amplitudes for $\pi\eta$ photoproduction on the nucleon processes have been calculated for application in the Jefferson Laboratory (GlueX detector).

PHYSICS OF HEAVY-ION COLLISIONS AND QUARK-GLUON PLASMA

Longitudinal correlations at initial stages of ultra-relativistic nuclear collisions have been examined against recent experimental data. A model framework involving event-by-event fluctuations of the initial conditions, followed by 3D viscous hydrodynamic evolution and statistical hadronization, has been used. Thermal shifts and fluctuations at finite temperature below the deconfinement crossover from hadronic matter to quark-gluon plasma were used to search for missing states of given quantum

numbers in the hadronic spectrum. The heavy quark entropy shift and baryon charge and strangeness susceptibilities were elaborated in the context of hadronic completeness and thermodynamic equivalence and in view of the lattice QCD trace anomaly. Predictions of the wounded quark model for particle production and properties of the final state formed in ultra-relativistic A+A, p+A and p+p collisions have been explored and compared with predictions of the wounded quark model.

Ultrarelativistic collisions of ^{12}C ions with heavy targets were investigated. Alpha clustering in the ground state has been confirmed. Fireball eccentricities in the Glauber Monte Carlo model were examined.

One-dimensional non-boost-invariant evolution of quark-gluon plasma was analysed within the frameworks of viscous and anisotropic hydrodynamics. Predictions obtained using several formulations of second-order viscous hydrodynamics were compared with the results of a recent approach to anisotropic hydrodynamics. It has been found that the results of anisotropic hydrodynamics and viscous hydrodynamics agree over the central hot part of the system. Gradient expansion for anisotropic hydrodynamics has been computed and compared with the corresponding expansion of the underlying kinetic-theory model with a collision term treated in the relaxation time approximation. A generalized relaxation-time-approximation form of the collision term in the Boltzmann kinetic equation has been elaborated, allowing for the use of different relaxation times in elastic and inelastic collisions. Non-equilibrium transport phenomena with inclusion of confinement effects has been studied using plasma containing confined gluons resulting from Gribov-type quantization.

Dissociation of heavy quarkonia at high temperatures has been analysed in order to explore quark-gluon plasma dynamics in heavy-ion collisions at LHC energies. Results obtained at CMS and ALICE in Pb-Pb collisions at 2.76 TeV could be reproduced using an internal-energy based model coupled to hydrodynamic evolution. The predicted results concerning creation of deconfined quark-gluon plasma agreed with those obtained via analysis of collective flow coefficients, providing further evidence that the behaviour of quark-gluon plasma created in relativistic heavy ion collisions is that of a nearly perfect fluid.

SINGLE ATOMS AND MULTIPARTICLE SYSTEMS

A platform for complete start-to-end simulations of experiments at large scale photon facilities, such as optical laser laboratories, synchrotrons or free electron lasers, has been implemented. Realistic effects, such as radiation from the source, through the beam transport optics to the sample or to the target under investigation, its interaction with the sample, scattering from the sample, and registration in a photon detector, including a realistic model of the detector response to the resulting radiation, have been accounted for.

Such analyses are of a vital importance for experiments with more complex physical systems, such as e.g. biomolecules, complex materials or ultra-short lived states of highly excited matter. They will help to simulate experiments and instruments within real-life scenarios, to identify promising and unattainable regions of parameter space and ultimately to make better use of valuable beam time.

Results of single-shot resonant magnetic scattering experiments of Co/Pt multilayer systems using 100 fs ultraintense pulses from an extreme ultraviolet free-electron laser have been analysed. X-ray-induced breakdown of the resonant magnetic scattering channel within the pulse duration has been observed, together with significant reduction of the speckle contrast of the high-fluence scattering pattern. Simulations of non-equilibrium evolution of the Co/Pt multilayer system within the XUV pulse duration have been performed.

THEORY OF COMPLEX SYSTEMS

Hierarchy patterns appear to be the most characteristic attribute of complex systems at various levels of their organization. The term "complex systems" refers to a new scientific paradigm according to which full comprehension of such systems demands a holistic approach, at all underlying scales. In this context the most meaningful are scale-free-laws and their geometrical counterparts – fractals – objects the appearance of which is similar at any level of their magnification. Therefore, multiscaling points to the general direction at which the most basic properties of complexity may be handled quantitatively. The presence of self-similar, or more generally self-affine, forms and patterns of activity in systems

generally considered as being complex, appears to suggest the existence of a single underlying and universal law which governs the principles of Nature's organization. Moreover, traces of self-similarity, ubiquitous in Nature, indicate that its architecture may be based on a programme which - in proportion to the perceived complexity - is comparatively simple. Identification of any such law is considered to be the ultimate aim of the science of complexity.

By its very nature the concept of complexity pervades all science, thus implying cross-disciplinary studies which are conducted in our Theory Division. The related issues currently under study involve in particular the dynamics of financial markets, social phenomena such as global scientific collaboration networks, solar magnetic activity, geological processes related to mountain formation, quantitative linguistics as well as some selected topics related to the manner in which the human brain operates. From an empirical point of view, such systems are typically represented by huge ensembles of data. In order to best describe their multiscaling characteristics, these data are analysed using advanced procedures of multifractal analysis and their cross-correlation variants. As a supplementary element of methodology the issue of multiscaling is studied in appropriate representations of complex networks and is quantified in terms of the corresponding network characteristics.

MATHEMATICAL PHYSICS

Understanding elementary particles, the concept of mass, and the emergent space-time have been the subjects of studies. The broad conceptual, philosophical, and phenomenological background concerning the problem of mass and the relevant Clifford algebra of non-relativistic phase space have been studied in substantial detail. A generalization of the concept of the fermion mass, with the concept of the quark mass being inherently different from that of a lepton, was formulated in terms of Clifford algebra.

An algebraic approach was elaborated to describe the shape transition of two-fermion systems, confined in a three-dimensional axially symmetric parabolic potential, in an external magnetic field. Explicit algebraic expressions were derived in terms of parameters of this system and of the magnetic field strength, in order to trace such transitions in the classical limit.

SELECTED RESEARCH HIGHLIGHTS OF THE DIVISION OF THEORETICAL PHYSICS

THE KRKNLO MATCHING METHOD IN QCD CALCULATIONS

High precision predictions in Quantum Chromodynamics (QCD) calculated at fixed-order expansion in the strong α_S coupling can be performed only for processes with a limited number of final state particles. Such theoretical results are generally insufficient to perform realistic modelling of processes measured at the Large Hadron Collider (LHC).Therefore, a complementary approach, named *NLO+PS matching*, is often applied. This approach combines results obtained at fixed, next-to-leading order in QCD, with partial resummation of logarithmically enhanced terms, performed by means of a parton shower (PS). One successful approach of that type was developed at IFJ PAN and is known as the KrkNLO matching technique [S. Jadach, W. Płaczek, S. Sapeta, A. Siódmok and M. Skrzypek, JHEP **1510** (2015) 052]. The aim of this method was to simplify to the extent possible the NLO+PS matching procedure. The latter is achieved by using a new factorization scheme (the MC scheme) for parton distributions in a hadron and by reweighing PS events with simple positive weights. As was shown, such a procedure preserves complete NLO accuracy while offering fully exclusive predictions for multi-particle final states. The KrkNLO technique has been implemented in the Drell-Yan process and recently applied to Higgs production in gluon fusion [S. Jadach, W. Płaczek, S. Sapeta, A. Siodmok and M. Skrzypek, Eur. Phys. J. C76, **649** (2016)], where predictions for the LHC were also obtained. Moreover, a completely defined set of MC parton distribution functions has been studied. Results for integrated cross sections, as well as for differential distributions at low and moderate values of transverse momentum, were found to be consistent both with pure NLO and with other matching techniques. Unlike other methods, they are also closer to the complete next-to-next-to-leading order (NNLO)

predictions than pure NLO and other matched calculations, as shown in Figure 1, where predictions by the KrkNLO method and by the NNLO calculation for the transverse momentum distribution of the Z boson produced in the LHC experiment are compared.

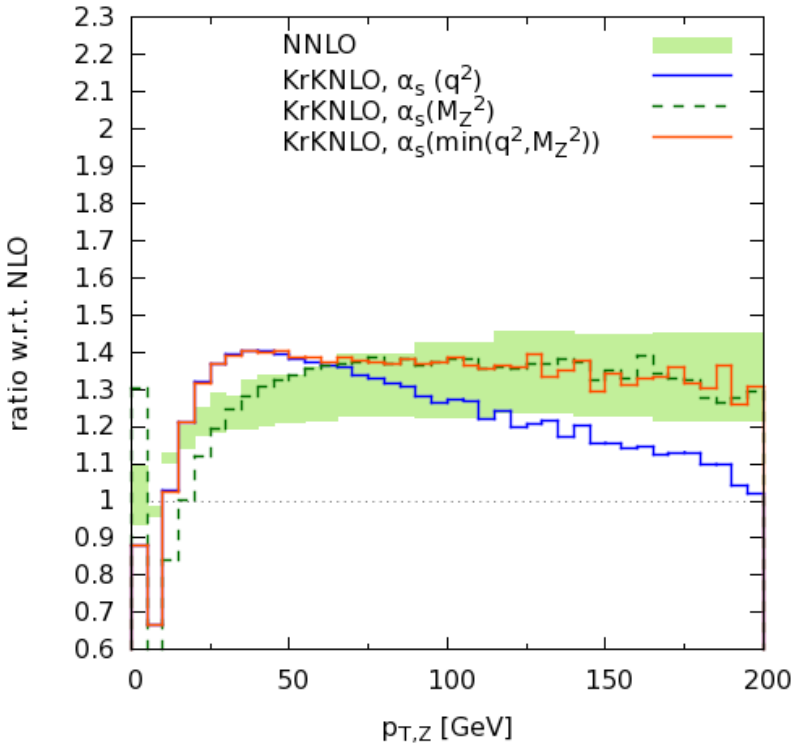

Fig. 1 *Comparison of predictions of the transverse momentum distribution of the Z boson produced in the LHC experiment, by the KrkNLO method and by the NNLO calculation.*

IMPROVED TRANSVERSE MOMENTUM DISTRIBUTION FACTORIZATION

At the Large Hadron Collider (LHC), protons are collided with protons and with lead nuclei, and lead nuclei are collided with each other. Collisions occur at a maximum energy of almost 14 TeV, enabling us to explore the dynamics of QCD at an unprecedented level. Factorization theorems of QCD allow for decomposition of cross sections in terms of parton density functions (characterizing the hadrons) and hard matrix elements (defining the observable). In particular, High Energy Factorization has been formulated in order to take into account effects which dominate at high energies in proton-proton collisions. Recently, an important contribution to establishing factorization for proton-lead collisions has been made in collaboration with researchers from Penn State University (USA), Ecole Polytechnique (France), and Universidade de Santiago de Compostela (Spain) [P. Kotko, K. Kutak, C. Marquet, E. Petreska, S. Sapeta and A. van Hameren, JHEP **1509** (2015) 106]. The new factorization, called Improved Transverse Momentum Factorization, allows one to take into account the complex nonlinear dynamics of gluonic fields, and to express the cross section in terms of a parton density function defined through a gauge link, and matrix elements, allowing "low-*x*" off-shell initial state gluons to be accounted for. The newly obtained factorization is valid in the so-called "forward-forward" and "forward-central" kinematics. Dijet configurations produced in such kinematic regions probe one of the initial-state hadrons in the dense "low-*x*" regime, while the other is probed in the dilute "large-x" regime. The framework has already been used to provide predictions for the cross section of dijet production in proton-lead collisions at the LHC. The results concerning the absolute cross section for azimuthal angular distribution of the produced jets show significant deviations from results based on the High Energy Factorization scheme [A. vanHameren, P. Kotko, K. Kutak, C. Marquet, E. Petreska and S. Sapeta JHEP **1612** (2016) 034].

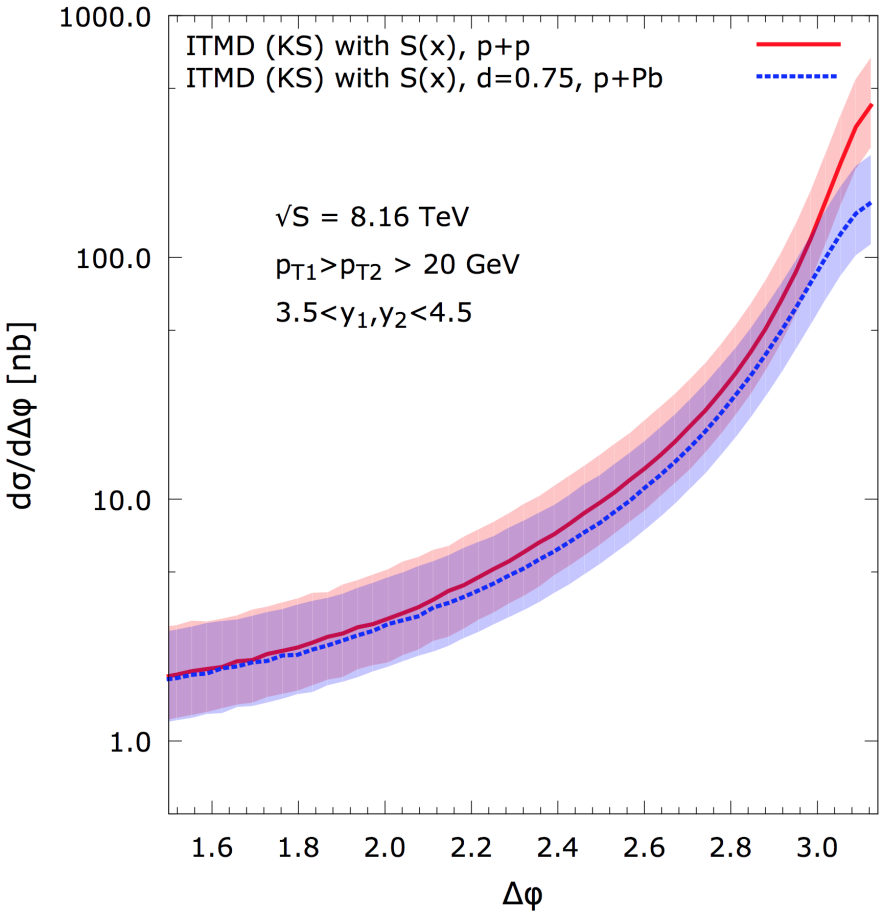

Fig. 2 *Predictions of absolute cross section for azimuthal angular distributions of dijets produced in proton-proton and proton-lead collisions at the LHC, calculated using the Improved Transverse Momentum Factorization (ITMD) scheme.*

FINAL STATE INTERACTIONS FOR HIGH ENERGY ACCELERATOR PROCESSES

The reputation of the TAUOLA and PHOTOS, Monte Carlo programs for tau-lepton decay and radiative corrections in decays of particles and resonances has already been well established. They were quoted for example in the breakthrough publication of ATLAS collaboration on the new particle (Higgs boson) discovery at LHC. It is believed that the discovered particle is indeed the Higgs, but as it is the first, and possibly the only particle of the new type, lacking any responsibility for matter or interactions, it has to be thoroughly verified and confirmed.

A completely new approach to constrain the parity of the Higgs boson was proposed by analysing multi-dimensional distributions in Higgs to tau-tau decays with the use of Machine Learning algorithms [R. Jozefowicz, E. Richter-Was and Z. Was, Phys. Rev D **94** (2016) 093001], developed with the help of TAUOLA. The published result was obtained in collaboration with a Google software team member. Once applied in the experiments, it will improve the sensitivity of Higgs boson parity measurements for the tau decay channel by a factor of up to two. This measurement is of fundamental importance to our understanding of the basic properties of the Higgs sector which is responsible for the fundamental properties, such as masses, of all other particles. Up to 24 such distributions need to be combined to achieve the required improvement of sensitivity. This shows the usefulness of modern computing techniques, of mutual interest to science and to software companies.

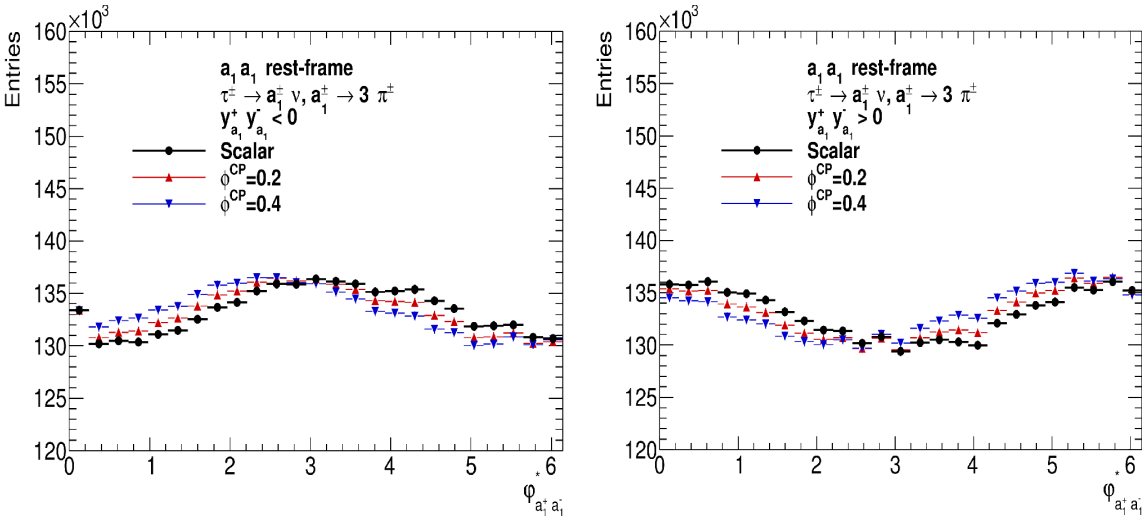

Fig. 3 *Examples of results obtained with the use of Machine Learning algorithms [R.Jozefowicz, E.Richter-Was and Z.Was, Phys. Rev D94 (2016) 093001](see text). Distributions of the acoplanarity angles of oriented half-decay planes in the rest frame of the visible decay products for the cascade Higgs decay to a tau-pair and consecutive tau decay to 3 pions and a neutrino are shown. Events are grouped by the sign of energy differences (left/right) of the decay products. Shown are distributions for three values of Higgs parity mixing angle 0.0 (scalar), 0.2 and 0.4.*

BOTTOMONIA SUPPRESSION REVEALS PERFECT FLUIDITY OF QUARK-GLUON PLASMA

One of the ultimate goals of ultra-relativistic heavy-ion collision studies at the Large Hadron Collider (LHC) at CERN is to extract the thermodynamic and transport properties of the new state of matter called quark-gluon plasma (QGP). From the theory point of view, over the last decade significant progress was achieved in restricting the QGP equation of state and the values of viscosities, nevertheless several issues are still open. In particular we still have limited knowledge of the key processes taking place at the very initial stages of these reactions, such as thermalization and hydrodynamization of the QGP, and their possible impact on the extraction of QGP properties.

The most abundant light hadronic states which attract most of the practitioner's attention, are unfortunately a limited source of information on QGP dynamics since, due to the Debye screening phenomena, they disassociate already around the pseudo-critical temperature for parton-hadron transition. On the other hand, heavy quarkonia, such as bottomonia, may survive up to temperatures of the order of 600 MeV and show a sequential dissociation pattern, with lighter states "melting" before heavier states and excited states melting prior to their respective ground states. As a result their suppression, if studied systematically, may serve as a thermometer for the QGP. At the same time it is commonly believed that elementary proton-proton collisions do not attain creation of a thermal QGP medium, thus melting of heavy quarkonia should not be observed in this case.

Following these ideas it was shown [B. Krouppa, R. Ryblewski, and M. Strickland Phys. Rev. C **92** (2015), 06190] that the R_{AA} suppression factor of Υ and χ_b states measured by CMS and ALICE in the LHC Pb-Pb collisions at 2.76 TeV may be described very well by the internal-energy-based pNRQCD model coupled to an anisotropic hydrodynamics evolution code. In this case the R_{AA} factor measures the thermal suppression of heavy quarkonia in heavy-ion collisions due to the creation of QGP with respect to properly scaled proton-proton interactions.

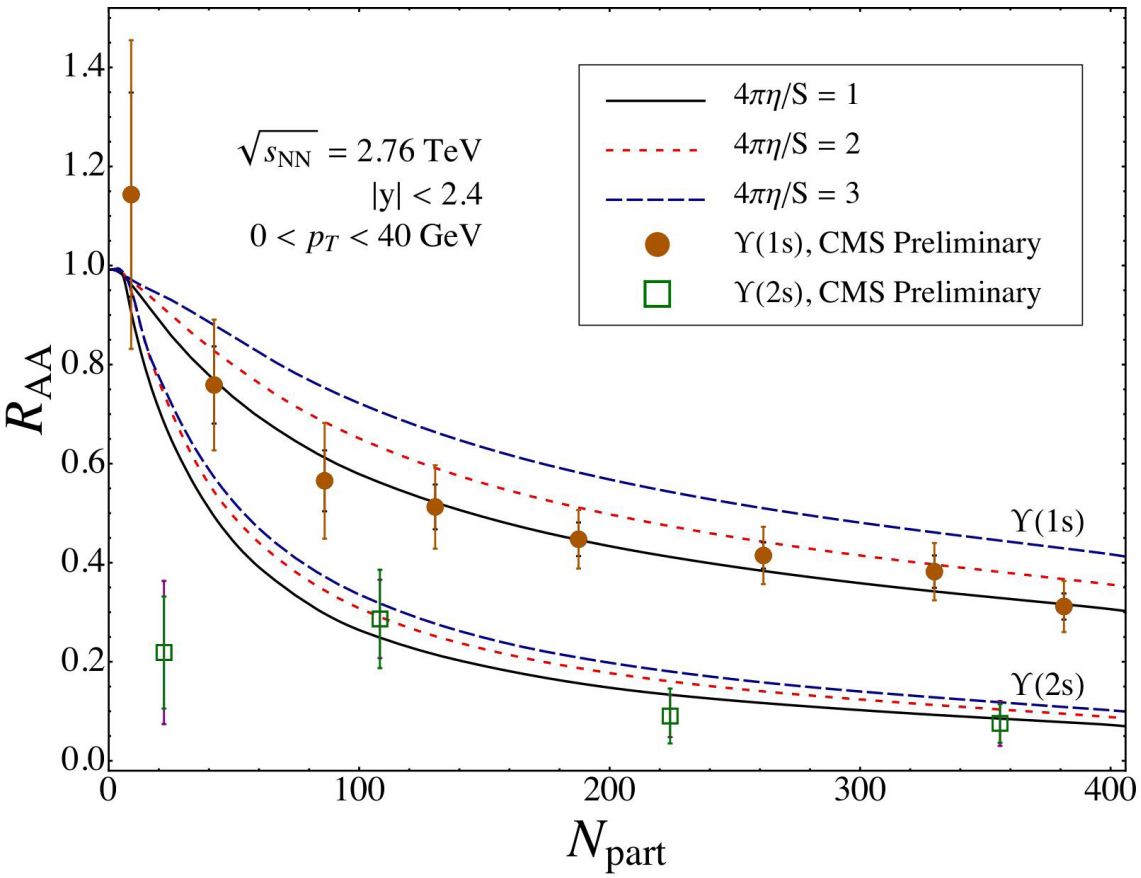

Fig. 4 *The R_{AA} suppression factor of Υ(1s) and Υ(2s) bottomonium states (lines) as a function of the number of participants in 2.76 TeV Pb-Pb collisions at the LHC, compared with CMS experimental data (symbols). The results of modelling show best agreement with the data if low viscosity ($\eta/s=1/(4\pi)$) is assumed in the quark-gluon plasma phase.*

The obtained results (Fig. 4) confirm the creation of a deconfined QGP with the shear viscosity to entropy density ratio η/s of roughly between 1 and 2 times the lower bound of $1/(4\pi)$ found by gauge/gravity duality studies. These values are consistent with those obtained via analysis of the collective flow coefficients for light hadrons, thereby they provide further evidence that the QGP created in relativistic heavy ion collisions behaves as an almost perfect fluid.

DESCRIPTION OF PHOTOLUMINESCENCE EFFECTS VIA STRETCHED EXPONENTIALS

The relaxation processes and photoluminescence effects are commonly described by the Kohlrausch-Williams-Watts function (named also the KWW function or the stretched exponential) $\exp\,[-(t/\tau 0)^{\alpha}]$, $t > 0$. Its inverse Laplace transform is uniquely given by the so-called one-sided Lévy stable distributions $\Phi_{\alpha}(u)$, $u > 0$. The symbol τ_0 denotes the effective time constant. Here, the word "stable" means that the Lévy distribution is invariant with respect to the Laplace convolution, namely that the convolution of two Lévy distributions leads to another Lévy distribution. The KWW functions and Lévy stable distributions are widely observed in amorphous and disordered systems, e.g. in polymers, glass, nano-crystals, and porous materials. For example, the data measured in the photoluminescence effect, which occurs in nano-crystals of silica, are fitted by the KWW function. Then, by using numerical calculations, a Lévy stable distribution related to these KWW functions has been found. Knowledge of the one-sided Lévy stable density provides us with information about the localization of relaxing centres and for this reason, it is important to know its analytic version. The analytic form of the Lévy density is used to correct the numerical fitting of data measured during the photoluminescence experiment; see Fig. 5 [G. Dattoli, K. Gorska, A. Horzela, and K.A. Penson, Phys. Lett. A 378, **2201** (2014)]. This form

is also used to find the differential equation which governs the behaviour of relaxing centres. Starting with the very natural evolution condition telling us that the stretched exponential at interval of time $t_2 - t_0$ is the composition of stretched exponentials at $t_2 - t_1$ and $t_1 - t_0$ for $t_0 \le t_1 \le t_2$, an integral form of the evolution equation was obtained [K. Górska, A. Horzela, K.A. Penson, G. Dattoli, G.H.E. Duchamp, Frac. Calc. Appl. Anal., **20(1)**, 260(2017)]. Next, taking infinitesimally small time intervals, this equation may be rewritten in differential form with a fractional space derivative. Thus, one arrives at the anomalous diffusion equation the solution of which is given via the Green function with the kernel being the one-sided Lévy stable distribution. It was noted that these approaches can be generalized to 3- and more dimensional cases where the one-sided Lévy stable distribution is replaced by the so-called Holtsmark distribution.

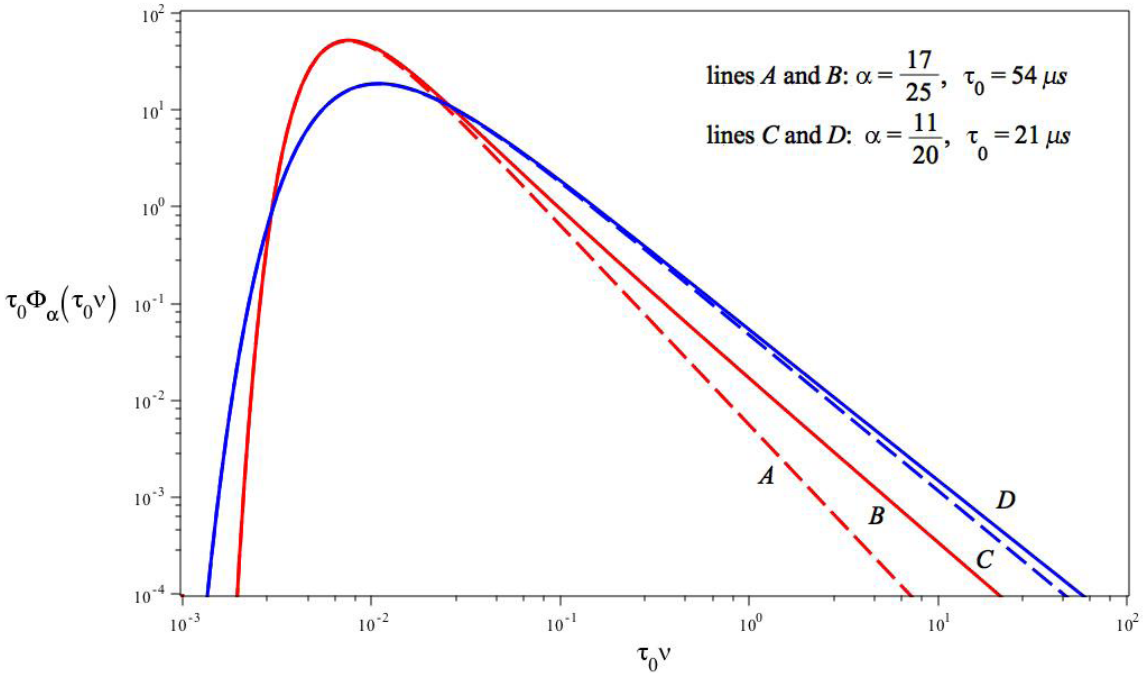

Fig. 5 *Comparison between the exact and explicit forms of the one-sided Lévy stable distribution* $\Phi_\alpha(\tau_0\nu)$ *(solid line) with a numerical fit of experimental data (dashed line).* ν *is the frequency and* $\tau 0$ *is the effective time constant.*

MULTIFRACTAL EFFECTS IN SUNSPOT NUMBER VARIABILITY AND IN NARRATIVE TEXTS

Multifractal analysis provides crucial information on dynamic phenomena, as they occur at varying degrees of complexity. The results of such analyses are useful in a number of ways, but most importantly, they may allow us to eliminate the influence of current, long-term trends. Tests carried out using multifractals disclose properties encoded in the data, revealing relationships at different scales. The basic related graphic tools are known as multifractal spectra or spectra of singularity. If the data reflect the structure of a simple fractal, the multifractal graphs are reduced to a point. If the structure of a multifractal is homogenous, then the graph takes an ideally symmetrical form resembling an inverted parabola. In many graphs representing actual data, there is no ideal symmetry, however. In such cases, left-sided asymmetry is the most frequent. Yet, there are phenomena which reveal signs of right-sided asymmetry. The famous sunspots on the surface of the Earth's star result from the dynamics of strong magnetic fields. The sunspot numbers, an important indicator of the state of activity of the Sun, appear to belong to this category of phenomena [S. Drożdż, P. Oświęcimka; Physical Review E **91**, 030902(R) (2015)]. The results of multifractal analysis in sunspot variability thus point to the hypothesis that the Sun may function not by a single but by a dual-dynamo mechanism which is responsible for the generation of its magnetic fields (Fig. 6).

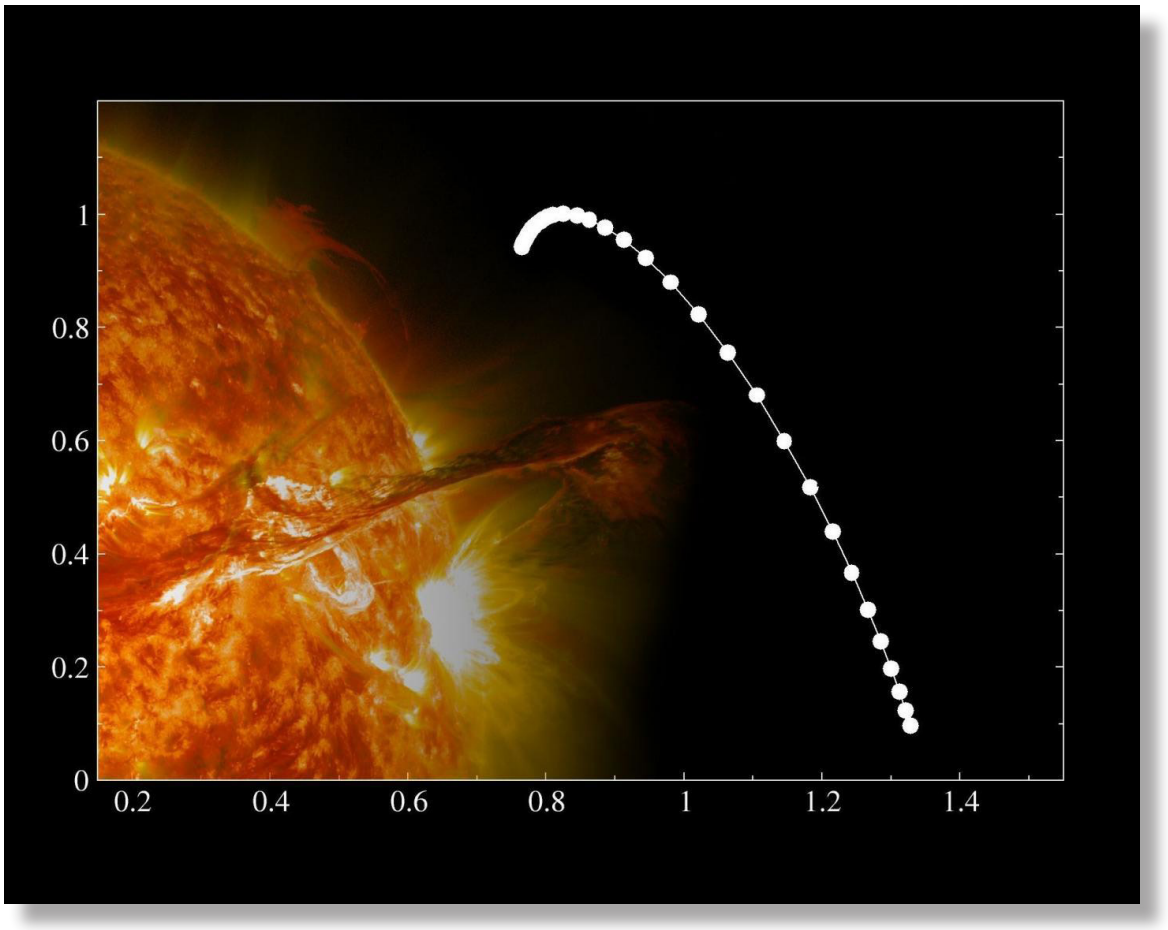

Fig. 6 *Graphs on multifractal analysis of the variability of sunspots show a clear right-sided asymmetry. The horizontal axis represents the degree of singularity and the vertical axis shows the spectrum of singularity.*

Natural languages developed remarkable hierarchical, scale-free patterns in the organization of their syntax. Quantifying the related principles of formation of narrative texts thus appears to be extremely helpful in improving our understanding of their complexity. An innovative quantitative study of the multiscale characteristics in the sentence length variability (SLV) in a large corpus of world-famous literary texts has shown [S. Drożdż, P. Oświęcimka, A. Kulig, J. Kwapień, K. Bazarnik, I. Grabska-Gradzińska, J. Rybicki, M. Stanuszek; Information Sciences, vol. **331**, p32, (2016)] that it involves self-similar, cascade-like alternation of sentences of various lengths. In particular the power spectra $S(f)$ characterizing SLV universally develop a convincing scaling with the average exponent $\beta \approx 1/2$, close to what has been identified before in musical compositions or in the brain waves. The majority of the studied texts simply obey such fractal attributes, but especially spectacular in this respect are hypertext-like, "stream of consciousness" novels. In addition, they appear to develop patterns characteristic of multifractals. Particularly spectacular is *Finnegans Wake* by James Joyce. Scaling of $S(f)$ implies the existence of long-range correlations in texts and appearance of multifractality, signals even a nonlinear component in corelations. A distinct role of the recurrence times of full stops in inducing long-range correlations in texts is documented, but to a much lesser degree in the recurrence times of the most frequent words. In this latter case, nonlinear correlations, thus multifractality, disappear even completely in all the texts considered so far. At the same time, treated as one extra word, the full stops appear to obey the Zipfian rank-frequency distribution. Our above discovery has been reported worldwide by many newspapers and journals, such as The Guardian and Die Welt.

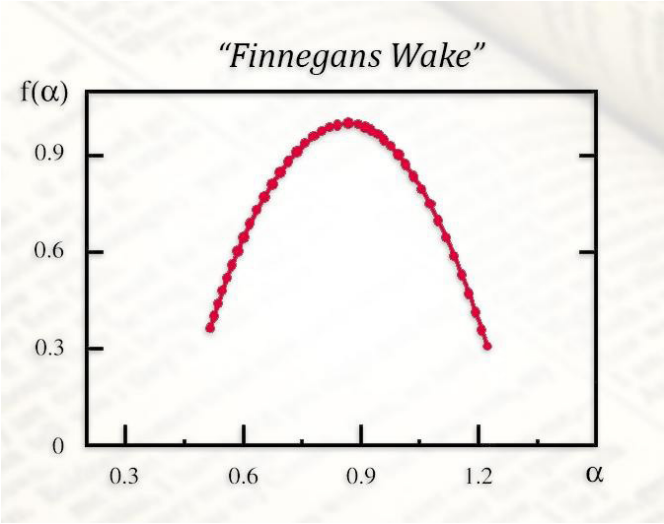

Fig. 7 *Multifractal spectrum of Finnegans Wake by James Joyce: The shape of the graph is indistinguishable from the results for purely mathematical multifractals. The horizontal axis marks the degree of singularity, and the vertical axis shows the spectrum of singularity.*

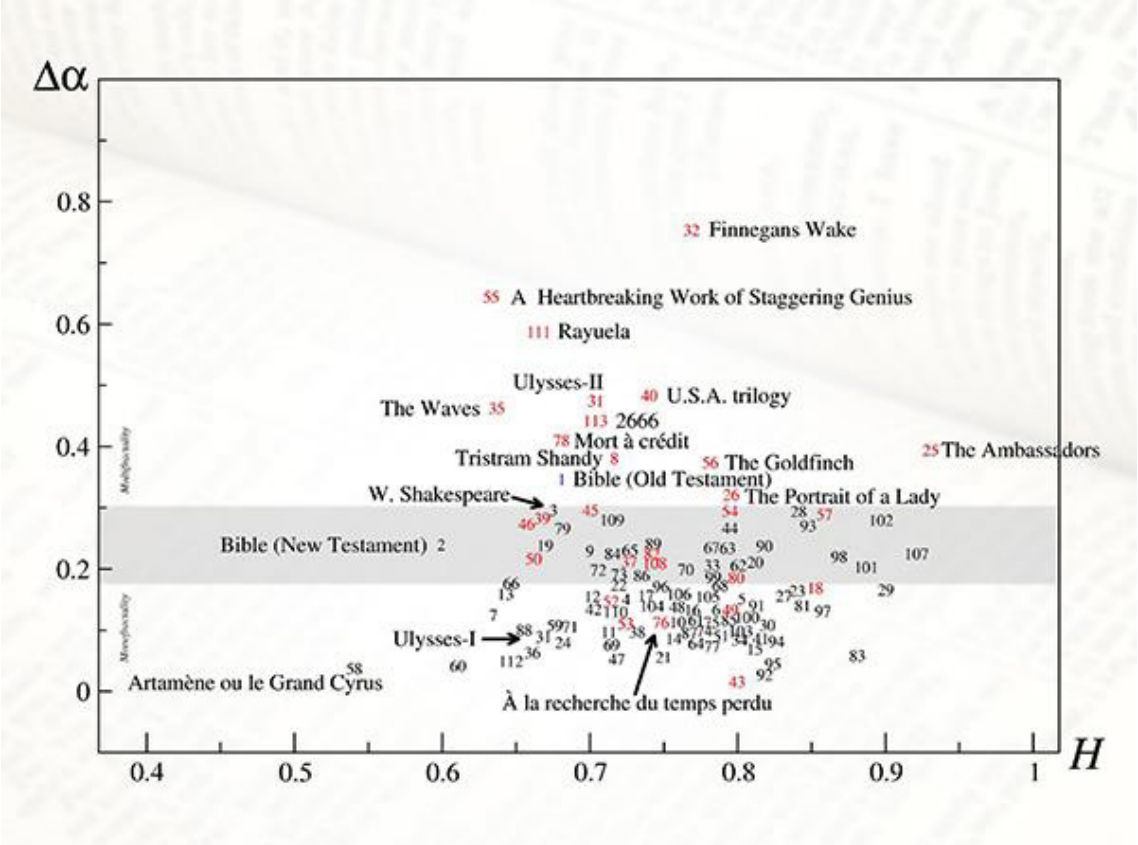

Fig. 8 *Multifractality vs persistence in sentence length variability: The numbers correspond to a given literary work in the pool. Red colour indicates works belonging to the "stream of consciousness" genre. On the vertical axis there is the width of the multifractal spectrum - for those closer to unity, there is a better multifractal organisation. The horizontal axis is the degree of persistence H in the length of the sentences. A higher value of H means a greater probability of a long sentence immediately following a long one, and a short one following another short one. H = 0.5 means the lack of such a tendency.*

ELEMENTARY PARTICLES AND PHASE-SPACE SYMMETRIES

The Standard Model (SM) of elementary particles contains various elements that are put in "by hand". Understanding their origin requires that one goes beyond that model. A new fundamental approach to this question was suggested several years ago. It was proposed that – just like the quantum concept of spin being related to the rotational symmetry of the 3D position space – that the internal quantum numbers and the pattern of the lepton-quark generation are related, via the Dirac-Clifford linearization idea, to appropriate symmetries of 6D nonrelativistic phase space. It was also shown that this approach naturally explains a substantial part of the SM U(1) x SU(2) x SU(3) symmetry structure and leads to the observed pattern of a single generation of SM fermions. In addition it bears a striking resemblance to the Harari-Shupe rishon model in which eight fundamental fermions are built as three-rishon composites of only two kinds of spin-half subparticles (rishons): T and V of charges +1/3 and 0 respectively. In the recently published book [P. Żenczykowski, „Elementary particles and emergent phase space", World Scientific 2013, ISBN: 978-981-4525-68-8, 232 pages] the idea was sited over a much broader conceptual, philosophical, and phenomenological background. The problems of mass and the relevant Clifford algebra of nonrelativistic phase space are studied there in substantial detail. In particular a generalization of the concept of the fermion mass, with the concept of quark mass being inherently different from that of a lepton, was formulated in the language of Clifford algebra. It was also shown – although Clifford algebras lead to antisymmetric tensors only – that the Clifford algebra of nonrelativistic 6D phase space involves a tensor which is symmetric in 3D spatial indices and which appears to be related to the generalized concept of mass. An idea of how to generalize the phase-space scheme to take care of relativistic covariance, modelled on the original Dirac's extension, was proposed. It was shown in detail how the phase-space approach evades the assignment of subparticle interpretation to the rishons, thus avoiding many shortcomings of the original Harari-Shupe model.

V. DIVISION OF APPLIED PHYSICS AND INTERDISCIPLINARY RESEARCH

The work of our Division is focused on three main areas of science: life and health, energy and environmental hazards, and physical properties of low-dimensional materials. The Division consists of seven Departments which carry out their research using modern and sophisticated equipment and work together in close collaboration.

The **Department of Experimental Physics of Complex Systems** is involved in interdisciplinary studies in the fields of biology, medicine, culture heritage and protection of the environment, using mainly ion, X-ray, and synchrotron radiation microprobes. Vibrational spectroscopy is also applied. Our HVEC KN-3000 Van de Graaff (VdG) accelerator, equipped with a proton microprobe (3 MeV proton beam, 7 μm in diameter) plays a key role in these studies. It should be noted that this microprobe instrument is the only such facility in Poland. Extensive elemental analysis is performed using PIXE, STIM, and RBS beam techniques, and by XAS and XES methods, using pulsed neutron beams at LNF (Dubna, Russia) or synchrotron radiation at collaborating institutions abroad, such as, TRIESTE (Italy), PSI (Switzerland), ANKA (Karlsruhe, Germany), SOLEIL (France), DIAMOND (UK), and HASYLAB (DESY, Hamburg, Germany). Our other microprobe, an X-ray one, further extends the experimental capability of this Department. Research is carried out using computer microtomography including phase contrast tomography, XRF and Total Reflection XRF, microcrystalography, and targeted irradiation of mammalian cells and tissues. Studies of biomarkers associated with alterations in the DNA repair processes, and the corresponding radiation hazard as well as a retrospective biological dosimetry have been implemented in our Department for rapid evaluation of radiation exposure. The classic cytogenetic, molecular cytogenetic – fluorescence in situ hybridization (FISH), and the alkaline version of single cell gel electrophoresis (SCGE) methods are applied for diagnostic and research purposes. We are presently developing and optimizing the Premature Chromosome Condensation (PCC) technique.

In order to further extend the research capability of the Department, new equipment was purchased within a project co-funded by the Małopolska Regional Operational Programme Measure 5.1 Krakow Metropolitan Area, as an important hub of the European Research Area for 2007-2013, project No. MRPO.05.01.00-12-013/15. This equipment has now been installed in the laboratory of spectroscopic imaging for radiobiology, therapy, and for complex systems research.

Since 2016 a part of the Department of Experimental Physics of Complex Systems became the **Department of Biophysical Microstructures**, which carries out biomedical studies at the nanometre scale using atomic force microscopy (AFM) integrated with a fluorescence microscope. This research is focused on biomechanical alterations

of single living cells and of tissue samples, including neoplastic tissues in which cancer progression is studied. The AFM technique has found many applications in several research areas, such as biophysics or medical sciences.

The **Department of Materials Science** applies nuclear and non-nuclear methods to study condensed matter. Research in that Department covers a broad spectrum of topics related to thin films, coatings and the structure of intermetallic compounds and alloys. Various methods, such as molecular beam epitaxy, laser ablation, ion beam sputtering, dual ion beam assisted deposition, chemical vapour deposition or chemical synthesis, are used to develop new materials. These materials are fabricated using micro- or nanopatterning with direct laser interference lithography, nanosphere lithography or with nanopore metal oxide templates. In studies of these materials it is possible to apply classic solid state-physics methods (magneto-resistance measurements, SQUID magnetometry, X-ray diffraction), spectroscopy and microscopy (Raman spectroscopy, Auger spectroscopy, atomic/magnetic force microscopy, electron microscopy) and to combine them with nuclear analytical techniques such as RBS, NRA, ERDA and local probe methods, such as Conversion Electron Mössbauer Spectroscopy or the Perturbed Angular Correlation technique.

We are currently developing the computed X- ray micro-tomography technique (phase contrast) to evaluate micro-images of samples composed of materials of similar absorption coefficients.

The **Department of Radiation Transport Physics** is mainly engaged in developing diagnostics for burning plasma experiments essential for designing the ITER project. Research in this Department is generally applicable to all programs concerning fusion energy and for achieving progress towards the implementation of fusion energy production in particular. The Department is a third-party member of the EUROfusion Consortium and takes part in ITER-related projects. The Department is equipped with a 14 MeV pulsed neutron generator with a tritium target and with two plasma sources – a double-module Plasma-Focus device. Since 2014, the Jan A. Czubek Laboratory of Neutron Sources has been established around these sources. The Department of Radiation Transport Physics is strongly involved in calculations of radiation transport in complex systems using Monte-Carlo methods, which are applied in the design and interpretation of neutron and gamma-ray experiments for different applications, for plasma physics, and also for nuclear borehole geophysics.

The **Department of Magnetic Resonance Imaging** is an interdisciplinary laboratory dedicated to biomedical and materials research and to the development of new MRI techniques. Our main MRI research system is the Bruker Biospec 9.4T horizontal magnet equipped with gradient coils capable of generating magnetic field gradients up to 1 T/m, with a number of dedicated ^{1}H, ^{31}P, ^{19}F, ^{13}C RF probe heads, including the CryoProbe™. This system is also equipped with advanced animal monitoring and control systems. The equipment was purchased with partial EU funding and is used predominantly for interdisciplinary biomedical studies *in vitro* or *in vivo* using animal models of civilization diseases. Another 4.7 T MR imaging system equipped with an USP-4 compatible probe head is used for dis-

solution studies of pharmaceuticals in different encapsulations. Apart from biomedical applications of MR, dedicated actively shielded gradient coils and RF micro-probes are also being designed and developed at this Department.

At the **Department of Nuclear Physical Chemistry** measurements of plutonium, americium, uranium, thorium, polonium, ^{90}Sr, ^{63}Ni, ^{7}Be, ^{99}Tc and ^{137}Cs in various environmental samples are performed. The main equipment consists of low background, high resolution (germanium) gamma-ray spectrometers, semiconductor alpha-ray spectrometers and a liquid scintillator spectrometer. From 1990 onwards, the Laboratory has also joined the national monitoring network for radioactive contamination organized by the Polish National Atomic Energy Agency (PAA) and the Central Laboratory for Radiation Protection. Air filters are exposed and measured every week to assess the activity of gamma-emitters in aerosols. The detection limit of this system is below 1 μBq/m^3. Apart from alpha-spectrometry, mass spectrometry has also been introduced as a measurement technique, in collaboration with the Institute of Geological Sciences of the Polish Academy of Sciences. Over the recent years, investigations of radioactive contamination in polar environments of both the Arctic and the Antarctic became a very important topic of environmental studies conducted in this Department.

In the **Department of Physicochemistry of Ecosystems**, research is based on application of chromatographic methods Results of these investigations are applied in medical diagnostics, environmental physics and in hydrogeology. The methods of gas chromatography are also being further extended in order to apply them in systematic air monitoring with respect to concentrations of chlorofluorocarbons (CFCs) and of SF_6.

ENERGY AND CIVILIZATION HAZARDS

To assess the civilization hazards related to energy production, several methods are applied. Methods of experimental physics are applied to thermonuclear plasma diagnostics in the future sources of energy-thermonuclear reactors based on tokamak or stellarator principles. Methods based on neutron transport physics are being developed for applications in geophysical prospecting of hydrocarbons, especially for the Polish shell-gas deposits, a conventional source of energy.

The related civilization hazards are studied in terms of the health impact of natural and man-made radioactivity in the environment (via individual and environmental dosimetry) over a wide range of exposures, or over different migration pathways of radionuclides in the environment. Levels of greenhouse gases are monitored as well as pollution of the environment by toxic trace elements, including carcinogens. Environmental markers (e.g. noble gases, CFCs and SF_6 as hydrological markers) are studied.

The technology of improving the properties of water by magnetic treatment is also being developed. Two working packages of the Strategic Research Project "Technologies supporting the development of safe nuclear power", financed by the National Centre for Research and Development (NCBiR) were carried out by the IFJ PAN, mainly in our Division (N05). This project has been completed in 2014 and ranked very highly by the NCBiR.

We are deeply involved in the EU ITER project. The grant for a conceptual design of the High Resolution Neutron Spectrometer (HRNS) for ITER was awarded in 2014 to a consortium of IFJ PAN and Uppsala University, with IFJ PAN as its leader. The HRNS system is composed of a set of four differently designed neutron spectrometers to achieve the extended dynamic range required by ITER. The Department is also contributing to other ITER-related projects, in which the Early Neutron Source project (EUROfusion WPENS) is worth noting. Progress in fusion research requires the use of a large testing facility where materials and their performance under conditions of irradiation by 14 MeV neutrons at extreme doses and temperatures may be qualified and validated. Construction of a European Neutron Source (ENS) has been proposed at the EU level, based on the collision of high energy deuterons (D+) with lithium (Li (d,xn)) providing sufficient flux and a suitable spectrum to reproduce conditions inside the plasma adjacent to the components of the fusion reactor. Our activity in this project, in collaboration with the Division of Scientific Equipment and Infrastructure Construction (DAI), concerns neutron calculations and design of the test system area (STUMM) where samples will be irradiated.

Natural and man-made radioactivity and the contribution of potentially harmful chemical elements in the environment are studied in our Division. Several of our projects deal with radioactivity in the environment over the polar regions of Spitsbergen and of the Antarctic.

Our Division also conducts research on concentrations of trace gases at ppt levels in the environment, such as those of chlorinated compounds (Chlorofluorocarbons-CFCs) which deplete the ozone layer in the Earth's stratosphere and contribute to the greenhouse effect. Our urban-area monitoring station, unique in Central Europe, complies with gaseous working standards required by the SIO2005 scale of the global AGAGE program. Our laboratory uses certified standards of known concentrations of CFCs and SF6 , which allows us to quantitatively evaluate these concentrations in the environment. The compatibility of these standards was verified against standards used at Bristol University in England and those at the Mace Head measurement station in Ireland. By calibrating our primary laboratory standards against the standards of the Mace Head measurement station, we obtained correction factors to be used in our measurements of CFCs and SF_6. Our measurement station also took part in an intercomparison organised within the InGOS EU project, aimed at achieving common standards in measuring the concentrations of individual compounds in the environment. An extensive database of measurements, which we have performed continuously since 1997, has been gathered in our Division, allowing us to systematically review trends in the concentration of chlorinated compounds in the Krakow area. Since we have observed occasional shifts of our baseline concentrations, uncorrelated with the location of our research facility, we conclude that some high pollution events may have arisen in areas outside Krakow, located mainly to the west of the Krakow agglomeration.

Groundwater is currently the largest source of fresh water on Earth. However, human activity threatens the quality of groundwater, affecting the volume of water suitable for consumption. Although groundwater is less polluted than surface water, it can be easily contaminated, for example by infiltration

of industrial waste, by pesticides and herbicides used in agriculture, or as a result of an accident, e.g. at a chemical, industrial or nuclear power plant. Methods based on environmental tracers are useful in determining the dynamics of natural groundwater flow, such as flow rate, flow direction, or time of residence (groundwater age). By knowing these parameters valuable information is gained with regard to groundwater management and to the resilience of the aquifers to the effects of human activity. In our Division two gas chromatography methods for measuring environmental tracers were developed. The first one is applied in measurements of the presence of anthropogenic gases SF_6, F-11, F-12 and noble gases Ne, Ar and He in young groundwater. The second method is used to evaluate the presence of noble gases Ne, Ar and He in old groundwater of ages up to millions of years. Recently, this system was modified to simultaneously perform measurements of helium, neon and argon from one groundwater sample of any age.

LIFE AND HEALTH RESEARCH

In our life and health research the main areas are medical physics and dosimetry, proton radiotherapy and biomedical applications (effects of radiation on cells *in vitro* and *in vivo*, such as generation of mutations, chromosome aberrations or DNA damage, and also variation of mechanical properties of cell membranes, such as their deformability or rigidity). This research is carried out using a wide range of methods: nuclear spectroscopy, vibrational spectroscopy, magnetic resonance imaging (MRI), atomic force microscopy (AFM), gas chromatography, fluorescence in situ hybridization (FISH), single-cell gel electrophoresis (the Comet assay) and by synchrotron radiation-based techniques.

Basic and applied research in biomedicine and radiobiology is carried out with the use of micro-focused ion, X-ray, and synchrotron radiation beams, together with studies of the distribution of oxidation states of sulphur, transition metals and trace elements in pathological cells and tissues. In addition, research on the mechanical properties of living cells in their native environment is also carried out with the use of atomic force microscopy (AFM). Since the AFM technique is able to distinguish between the mechanical properties of normal and cancerous cells, it may be applied to diagnose changes resulting from neoplastic transformation or other pathological manifestations in cells. The main topics are sample deformability studies, quantification of the interaction forces between single ligand-receptor pairs, design of a new class of biosensors based on the behaviour of cells on protein/polymeric based micro-matrices, and the influence of microenvironmental properties such as stiffness or adhesiveness on the behaviour of single cancer cells. Studies of post-irradiation DNA damage and repair processes and of chromosomal aberrations as a function of environmental, diagnostic, therapeutic, professional or accidental exposures (retrospective biological dosimetry), and of the related health risks, are also being performed.

Nuclear magnetic resonance imaging (MRI) is a powerful technique in biomedical research. We are involved in preclinical investigations of pharmaceutics to avert pathological changes in cardiovascular and neurological systems, using animal models of civilization diseases. Investigations of diastolic and systolic heart function failures in Transgenic Mice, of liver function in the mouse model, of inflammation and brain demyelination processes in the mouse cuprizone model, have been performed, as well as MRI and MRS studies of neurological diseases of the brain in rat models. Studies of new molecular imaging approaches to better detect pathologies have also been undertaken. USP4-compatible MRI studies of the dissolution of controlled releases of various dosage forms of pharmaceutics, as well as applications of novel MRI approaches to characterise the properties of model dosage forms. are also being performed.

In our research on biomaterials suitable for the production of implants, we have used porous titanium oxide templates to study the morphology and uniformity of hydrothermally precipitated hydroxyapatite (HAp) coatings. We have demonstrated that the nanostructured surface of titanium oxide has a beneficial effect on HAp nucleation and coverage, both of which are important aspects of implant quality.

We are continuing the development of radionuclides for medical applications and activation analyses with the use of our AIC-144 cyclotron.

Since specific volatile compounds are present in the air exhaled by patients, they may be exploited for diagnostic purposes. Therefore the concentration of sulphur compounds in exhaled breath is analysed in patients with paradontosis, halitosis, liver failure, lung cancer, or allograft rejection. We

continue to measure amine concentration in breath samples in the early diagnosis of renal failure and in monitoring the process of dialysis. We have also began chromatographic studies of compounds emitted from the skin as means of possible medical diagnostics.

PHYSICAL PROPERTIES OF LOW-DIMENSIONAL MATERIALS

The main part of our research is devoted to the rapidly developing field of magnetic phenomena important for future applications such as Giant Magnetoresistance, perpendicular magnetic anisotropy, or the exchange-bias effect. Our present work involves studies of the use of solid-state dewetting to produce ordered arrays of ferromagnetic FePdCu alloy on self-assembled matrices of SiO_2 nanospheres.

Apart from nanosphere lithography we are currently exploring other patterning methods. We have invented a new method of chemical synthesis of porous anodized metal oxide substrates which are now used as substrates for nanostructuring of FePd alloy and Co/Pd multilayers. We demonstrated that after annealing, in arrays of FePd antidots isotropic magnetic properties were revealed, while CoPd antidots conserved their perpendicular magnetic anisotropy, slightly deteriorated in comparison with a continuous CoPd film, due to advanced surface morphology. We are also studying template-assisted electrodeposition of Co nanowires which show other aspects of magnetic behaviour of ordered arrays of nanostructures.

We have also studied magnetic systems exhibiting an exchange bias effect such as [CoO/Co/Pd] multilayers of Co thickness below the limit for continuous layer formation.

A special method for homogeneously depositing carbon coatings on 3-dimensional elements was developed, resulting in perfect bioactivity and very good mechanical strength of elements of carbon-coated endoprotheses.

Some highlights of research results achieved in our Division over the last three years, are presented below in more detail.

SELECTED RESEARCH HIGHLIGHTS OF THE DIVISION OF APPLIED PHYSICS AND INTERDISCIPLINARY RESEARCH

Tip-enhanced Raman spectroscopy (TERS) enables nanoscale chemical imaging of surfaces with a spatial resolution of below 20 nm to be achieved in ambient conditions [Chem. Phys. Lett., **318** (2000) 131–136]. The technique utilizes localized surface plasmon resonance at the apex of a metallized SPM tip to enhance Raman scattering from a highly confined volume of the sample, placed directly under the tip. The excellent spatial resolution of TERS, together with its high sensitivity (down to single molecules), makes it the method of choice for studying a broad range of samples including DNA.

In our research **TERS was applied to follow conformational changes of DNA** along single 500bp DNA molecules deposited on mica [Macromolecules, **49** (2) (2016) 643–652]. Each molecule was measured at eight points. The DNA conformation was assigned based on the position of O-P-O stretching motions of the DNA backbone. **We have confirmed by TERS that cation-deposited DNA upon drying undergoes a conformational transition from partial B-form to A-form, and have precisely located positions along the DNA where this transition was more probable - at the ends of the molecules.** The results are presented in Figure 1.

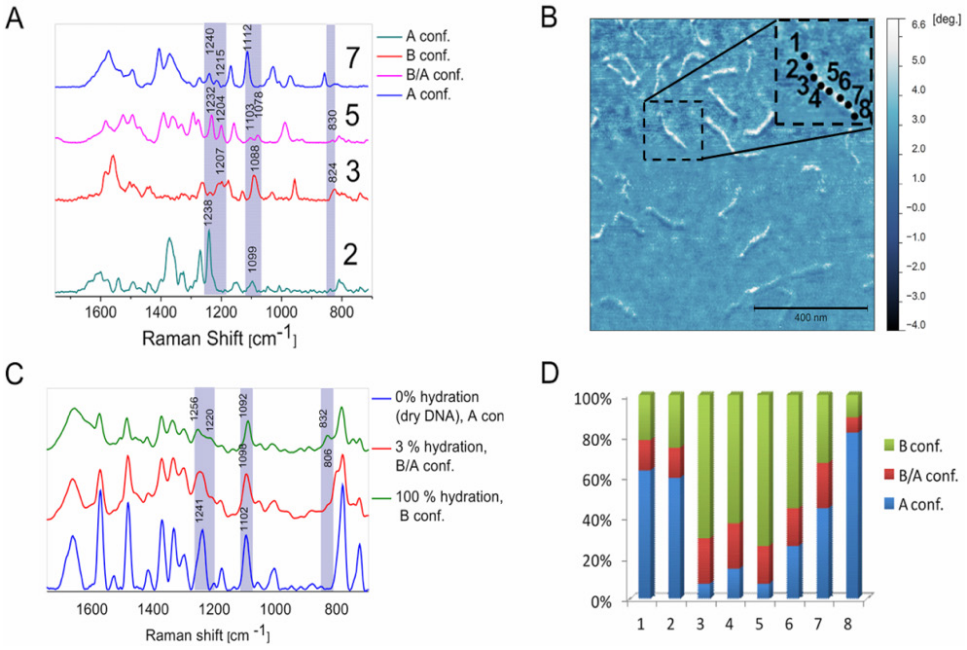

Fig. 1 *A TERS study of 500 bp DNA deposited with Mg^{2+} ions: (A) spectra collected along a 500 bp DNA strand corresponding to tip positions 2, 3, 5, and 7 marked in (B) AFM phase image; (C) single channel Raman spectra of calf thymus DNA in B-conformation (100% hydration), A/B-conformation (3% hydration), and A-conformation (0% hydration, dry DNA), (D) the percentage of A-DNA, B-DNA, and mixture of A-DNA and B-DNA conformations detected at tip positions 1–8. Data were collected along 27 individual 500 bp DNA strands at eight positions along each strand. Adapted from [Macromolecules, 49 (2) (2016) 643–652]*

Additionally, due to the well-defined topology and chemical structure of DNA, this molecule could also become a biological sample standard in the field of nanospectroscopy. This extremely sensitive TERS method was applied to assess chemical changes appearing in DNA upon different surface immobilization protocols [Small, **12** (**35**) (2016) 4821–482].

Both UV and ionizing radiation are well known for their deleterious effect on human cells. Their main target is the DNA molecule which carries all of the important genetic information of the cell. The key issue in achieving more effective radioprotection and radiotherapy is to understand the exact mechanism of the interaction between radiation and biomolecules, and in particular to obtaining the precise structure

of the different forms of damage and their relative ratios. **In this project X-ray spectroscopy was used to study changes in chemical structure around the phosphorus atom of the phosphodiester DNA backbone, caused by exposure to radiation** [Biophys J. **110** (2016) 1304-1311]. In comparison to classically used biochemical methods, the experimental procedure proposed by us does not require any additional chemical substances nor any complex preparation procedures that may affect the biological samples, leading to changes in their structure.

The difference in X-ray absorption spectra between non-irradiated and UVA-irradiated DNA samples was fitted by theoretical models of this difference, representing various possible types of damage (Fig. 2.). **By combining the experimental results with theoretical calculations, it was possible to establish the types and relative ratios of lesions around the phosphorus atoms in DNA.** It was found that strand breaks are the main lesions caused in DNA by UVA and that 3'-phosphate was the dominant form of the termini, indicating that 5' C-O bond cleavage is the most likely location of strand breaks. Cyclobutane pyrimidine dimers (CPDs) were found to be a minor product of the UVA interaction with DNA; nevertheless, their presence confirmed the direct absorption of UV light with wavelengths of about 365 nm. This approach can be readily extended to identify other forms of DNA damage, such as that caused by UVB, UVC, or chemical agents used in cancer chemotherapy.

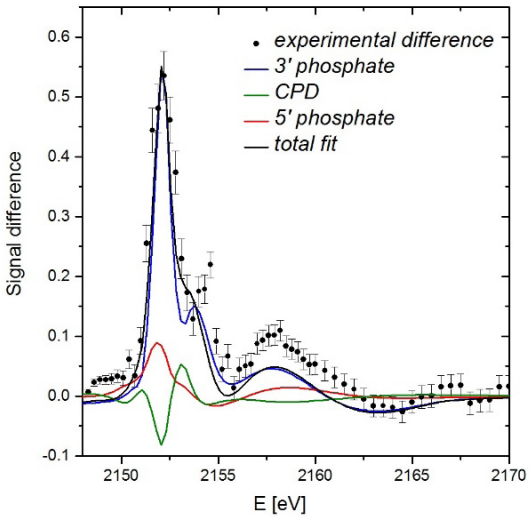

Fig. 2 *Experimentally measured differences in P K-edge X-ray absorption spectra, between UVA-irradiated and non-irradiated DNA samples. Full lines show corresponding best-fitted theoretical spectra calculated for different types of damage [Biophys. J. 110 (2016) 1304-1311].*

A broad, multi–technique study has been made of post–surgical cataract lenses, within a NSC grant (DEC-2012/05/B/ST4/01150). The experimental material was obtained via the phacoemulsification cataract ocular surgery technique, currently applied most frequently to replace the natural eye lens affected by cataract with an intraocular lens implant. The initial phase of **the study was to elaborate an efficient sample preparation protocol, suitable for application of several complementary physical techniques: micro–PIXE, FTIR, Raman, and AFM–IR**. This multi–technique study was performed on a statistically significant set of about 100 samples of post–surgery human lenses with cataract, obtained from the Military Hospital in Cracow and the Military Institute in Warsaw. The study targeted two possible diseases: diabetes and glaucoma.

We first employed the μ–PIXE method (2 MeV protons at the IFJ van de Graaff accelerator) to gather data on changes in trace element concentration. Here, elevated levels of zinc (stronger effect) and iron (weak effect) have been observed in diabetic patients treated with insulin or other pharmaceuticals. However, **the most significant result obtained was the clearly elevated Zn level in glaucoma patients, where the measured concentrations were up to one order of magnitude higher than those in the remaining cases** [J. Trace Elem. Anal. Vol. **4** No. 1 (2016) 1–9] . As these results are the first ever reported, further studies are foreseen.

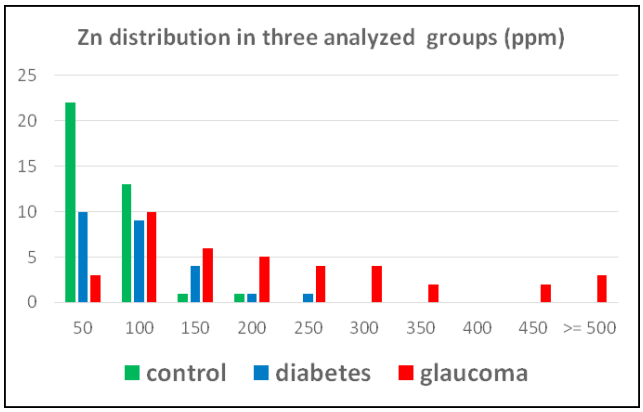

Fig. 3 *Histograms of Zinc concentrations (weight ppm) in the control group and in cataract lenses of patients with diabetes and glaucoma. Median values: ~40 ppm (control), 60 ppm (diabetes), ~150 ppm (glaucoma).*

In parallel, samples were measured using our Almega XR Confocal Raman spectrometer with an excitation laser source of 785 nm. Raman vibrations over the spectral region of 650–1750 cm^{-1} were analysed. The difference spectra revealed an excess of tryptophan, tyrosine, phenylalanine, and β-sheet conformation [Acta Phys. Pol. A, Vol. **129** No. 2 (2016) 244–246]. In the studied lenses two opaque colour phases have been identified: a white- and a yellow one. Both forms are differently arranged, degenerated protein forms. Raman and 2D correlation spectroscopy revealed that the main differences are observed over the amide I, methyl, methylene and O–H vibrational band region. The effect of Asp, Glu and Tyr amino acids in cataract lens transformation was also observed [J. Mol. Structure **1124** (2016), 71–77].

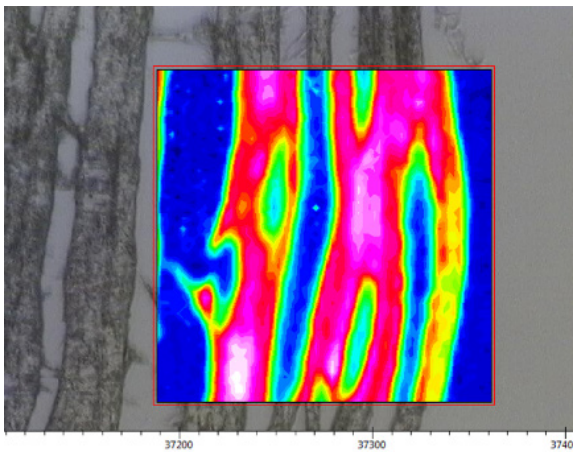

Fig. 4 *Optical image of the studied lens material with overlayed intensity maps revealing the distribution of Amide II molecules (blue: low, to yellow: high).*

The FTIR spectra of lenses are characteristic of natural tissues and are dominated by intense bandwidths derived from amides and lipids. **The analysis performed yielded complex information on the secondary structure of the proteins and on conformational changes of amino acid residues, due to cataract opacification of the human lens** [submitted to Spectrochimica Acta A]. Moreover, analysis at the nanoscale spatial resolution shows that the progress of degradation may not be uniform over the entire lens volume.

Finally, AFM – IR spectroscopy was applied to study the development of cataract at the nanoscale level [submitted to Journal of Pharmaceutical and Biomedical Analysis]. The impact of disease development on the secondary structure of proteins in the eye lens tissue was shown. Domination of β–turn protein secondary structure is observed in the healthy (non-cataract) lens. Lens degradation by cataract is associated with secondary changes in protein, from β–turn/β–sheet parallel over the less changed part of the lens to more stable anti-parallel β–sheet over the more degraded part. Our results of lens spectroscopy were presented and were awarded 1st prize at the 2016 European Association for Vision and Eye Research Conference [Acta Ophthal. Vol. **94**, Issue S256, DOI: 10.1111/j.1755-3768.2016.0628].

Development of various biochemical and biological assays aids in cancer diagnosis, where over the past decades, single-cell biomechanics has been increasingly helpful. Certain diseases are known to alter the biomechanical properties of cells. For instance, the stiffness of single cells changes during cancer development. It has been demonstrated that biomechanics can offer a better description of the mechanisms underlying cancer progression and can also offer means of cancer detection and diagnosis at the level of single cells. An emerging line of research in this area is to correlate cellular biomechanics with biochemical and biophysical properties of single cells. **The main objective of these studies is to determine the link between single cell deformability and properties of the cellular surface in the context of cancer progression.** The morphology and elasticity of melanoma cells were measured by means of atomic force microscopy (AFM) in two groups of cells - those originating from primary tumour sites i.e. from vertical growth phases (VGP, WM115), and those gathered from skin metastases (WM266-4). The surface properties were determined using time-of- flight secondary ion mass spectroscopy (ToF SIMS). Results of photothermal microspectroscopy (PTMS) confirm the presence of surface changes observed in mass spectrometry (Figure 5.).

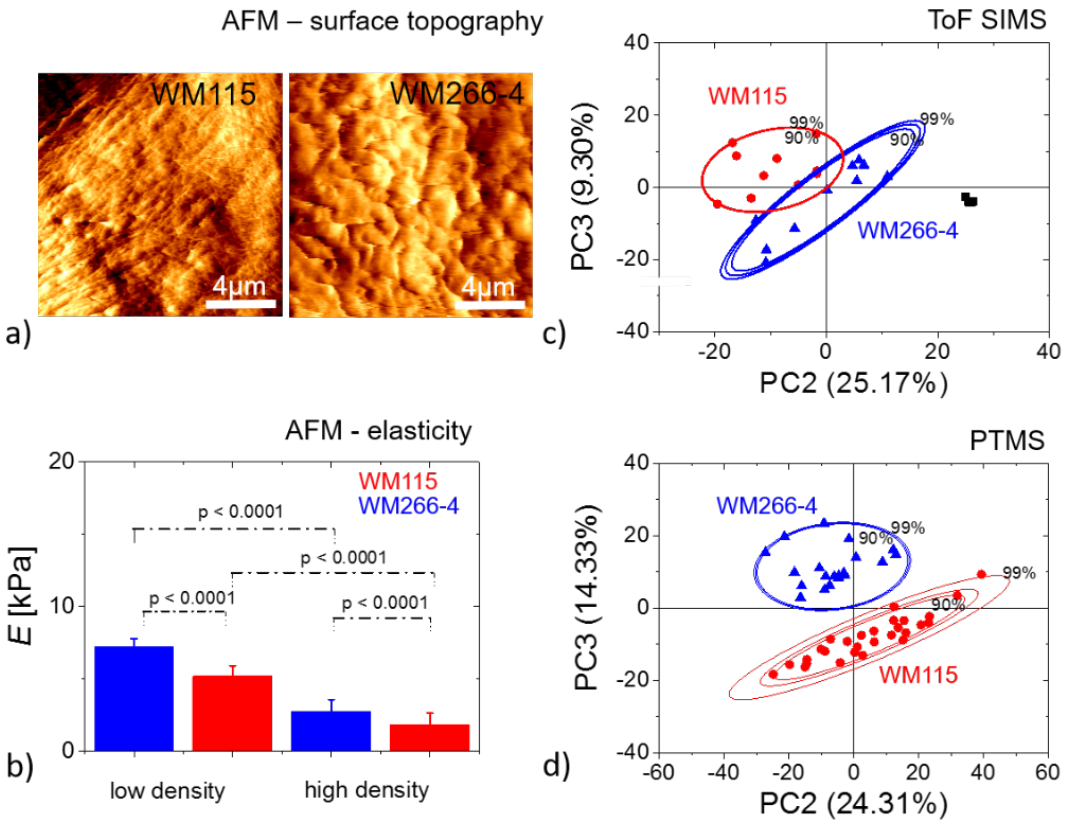

Fig. 5 *(a) Surface topography and elasticity (b) of melanoma cells. Scores plot for PC3 versus PC2 resulted from PCA of ToF SIMS (c) and PTMS (d) spectra. For each data group confidence ellipses were calculated at 90%, 95%, and 99% confidence levels.*

The considerable differences between WM115 and WM266-4 cells coincide with differences observed using AFM. Surface topography images show that the cytoskeletal network of WM115 cells is better organized (cortical filament structure) whereas WM266-4 cells are more rough and show characteristic flexible ridges (or ruffles). It was also shown that the larger deformability of metastatic WM266-4 melanoma cells correlates with the presence of flexible ridges. The observed changes were accompanied by altered surface properties. **These findings confirmed the hypothesis that cancer progression causes alterations in the morphology and deformability of cells accompanied by changes in their surface properties** [Analyst **141** (2016) 6217-6225].

Animal models of civilization diseases (i.e. cardiovascular, neurological, or cancer) were studied using different MRI techniques. Within the framework of the project "Endothelium in diseases of civilization: from basic research to innovative endothelium-targeted pharmacotherapy" led by the Jagiellonian Centre for Experimental Therapeutics, we have strived to develop appropriate MRI methods best suited to characterise pathological processes of atherosclerosis, heart failure, liver inflammation, and non-alcoholic fatty liver disease, in animal models. **Comprehensive, multi-parametric MRI protocols were developed** for assessing the endothelial function of large vessels and vessel wall permeability, as well as of heart and liver morphology and function, for use at the preclinical level [NMR Biomed., **29** (2016) 833-840; NMR Biomed., 29 (8), (2016) 1088-1097; Magn. Reson. Mater. Phy. (2016) Online First].

A decrease of the endothelial function was observed together with an increase of vessel wall permeability in mice on a fatty liver diet and confirmed in atherosclerotic mice. A significant improvement of the endothelial function was observed in response to reference therapy, confirming the method applied is of appropriate sensitivity for application in monitoring therapy procedures [Pharmacol. Rep. **67** (2015) 765–770].

Examination of the murine heart using a multiparametric MRI protocol was based on high spatio-temporal resolution *cine* measurements in basal and pharmacologically-induced stress conditions, MR

Tagging, and left atrium assessment. The most promising applications were in the detection of cardiac function improvement in spontaneously trained, genetically modified mice developing heart failure (Tgαq*44) and in the detection of subtle changes in regional cardiac activity in a model of advanced atherosclerosis (transgenic mouse apoE/LDLR-/-) [Nature Sci. Rep. **6** (2016), art. no. 24714; NMR Biomed., 29 (2016) 833-840].

Two models of liver damage were considered: acute inflammation induced by concanavaline A administration, and the progressive process of diet-induced steatosis.

The use of perfusion-related techniques MR-DCE (Dynamic Contrast Enhancement) and ASL (Arterial Spin Labelling) allowed for **a complementary assessment of microvascular changes in the developed model of acute hepatitis**. Significant decrease in parameters characterizing circulation was observed as well as their correlation with the level of changes in tissue damage (Fig. 1). Further analysis performed with the use of the multicompartmental model of the liver delivered interesting results describing changes in contrast agent transport between compartments related to tissue pathology. On the basis of the results obtained, the suitability of the model for preclinical research, and potentially also for therapy monitoring, was shown.

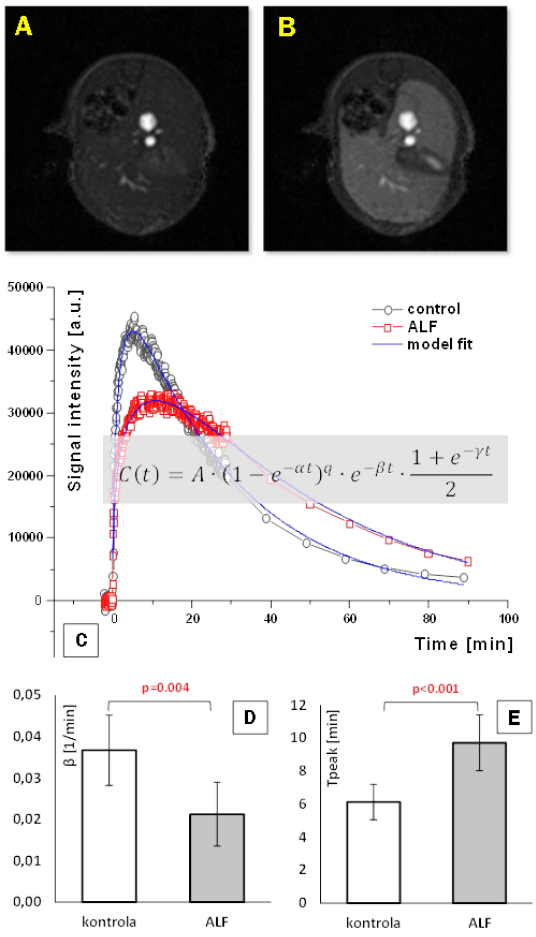

Fig. 6 *MRI DCE (Dynamic Contrast Enhancement) measurements in the mouse liver in a model of acute inflammation (see text).*

In Fig. 6. MRI DCE (Dynamic Contrast Enhancement) measurements in the mice liver in a model of acute inflammation are shown by representative images of the liver before (A) and after (B) hepatrotropic contrast agent administration (Primovist®, Bayer-Schering, Germany). MRI liver signal intensity assessed from consecutively collected images (C) fitted by the use of empirical model allows for quantification of the uptake and washout phases. Statistically significant differences in the DCE curve decay (D) and increase (E) between control and inflamed livers were shown in the concanavaline A model of acute hepatitis.

Viscoelastic properties of the liver were investigated by analysing the course of deformation under the pressure of heart beat as assessed by the MR Tagging technique. Detailed analysis of strain tensor-derived parametric maps allowed for a more reliable delineation of the shape and extent of the deformation area. Significant changes between fatty and control livers in many texture and spatial moments-based parameters were shown together with an assessment of viscoelastic properties from tissue model fits. It appears that there is a possibility of using this technique to test the liver properties and damage.

We investigated in an animal model the degeneration of myelin, which is associated with various neurological disorders, e.g. Multiple Sclerosis [J. Neurosci. Meth., 232 (2014) 30-35; Mult. Scler. J. 20 (2014) 920; Mult. Scler. J. 22 (2016) 413]. Orally administered copper chelator cuprizone leads to reproducible demyelination in the mouse brain white matter (WM), particularly in the corpus callosum (cc), and, to some extent, in the grey matter (GM). We assessed the feasibility of applying an optimized segmented Magnetization Prepared Rapid Acquisition Gradient Echo (MP-RAGE) pulse sequence and a cryo-coil at 9.4T for quantitative assessment of the demyelination processes in the brain of cuprizone-treated mice.

0Sixteen C57BL/6J mice: eight control, and eight fed with 0,2% cuprizone-containing diet for 6 weeks, were imaged using a 9.4T/21cm horizontal bore Bruker Biospec MRI scanner equipped with a Bruker CryoProbe. The 3D MP-RAGE pulse sequence was used for *in vivo* and *ex vivo* brain imaging. MRI with a set of different Inversion times (TI) were collected first in order to optimize the WM/GM contrast. An optimized MP-RAGE pulse sequence was used in the *in vivo* experiment with 22 horizontal 0.3 mm thick slices, while for the *ex vivo* experiment 48 horizontal 0.1 mm slices were collected, with planar resolutions of 70 x 59 μm, and 59 x 47 μm, respectively. Histogram analysis of the resulted images was performed, in order to quantify the number of voxels corresponding to WM and GM. Histological analysis for myelin (Sudan B) was also performed for comparison.

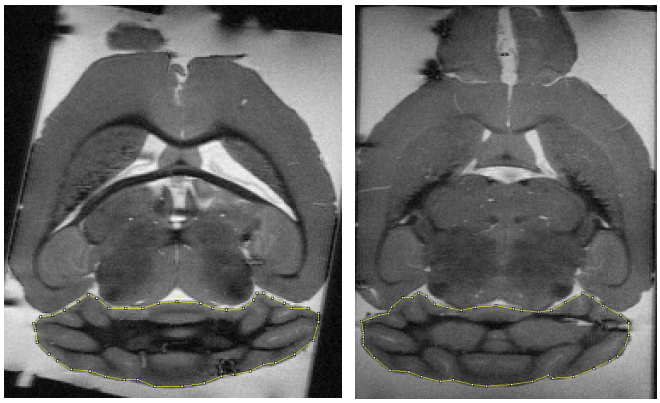

Fig. 7 *Horizontal MP-RAGE images of control (left) and cuprizone-treated (right) mouse brains ex vivo. Demyelination was detected in the corpus callosum, cerebellum and cortex.*

We showed differences between control and cuprizone-treated animals over different areas of the brain. The most significant differences were observed in the corpus callosum and cerebellum areas (Fig. 7-9). More subtle effects were detected in the cortex.

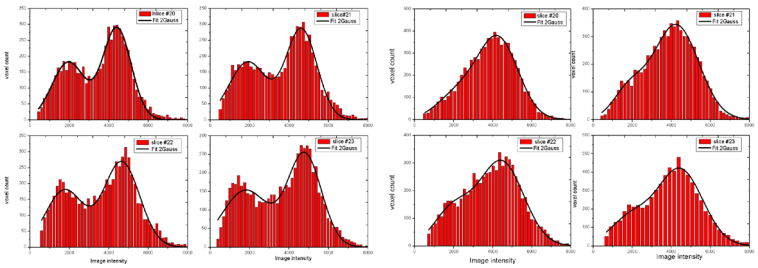

Fig. 8 *Bimodal histogram analysis of the cerebellum in control (left) and cuprizone-treated (right) mouse brains.*

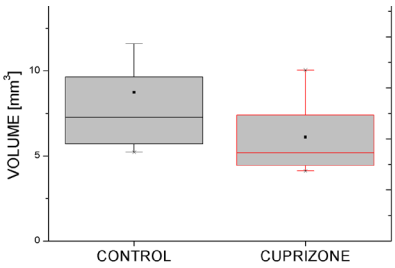

Fig. 9 *Myelinated cerebellum volume in control and cuprizone-treated mouse brains.*

Molecular MR imaging using targeted contrast agents can enhance the detection of glioma cells if an optimum pulse sequence is used. In collaboration with the University of Calgary, University of Victoria and University of Ottawa, targeted contrast agents based on iron oxide, as means for detecting high-grade gliomas have been studied using the mouse model [BMC Medical Imaging, **13** (2013) 20-27; J. Nanomaterials, 2013 (2013) 1-12; J. Neurosci. Meth., **226** (2014) 132-138].

We compared the contrast-to-noise ratio (CNR) using spin-echo (SE), gradient echo (GE), and GE with flow compensation (GEFC), and also by susceptibility weighted imaging (SWI) in T2 and T2* contrast-enhanced molecular MRI of glioma (Fig. 10). We used a nude mouse model. U87MGdEGFRvIII cells (U87MG), derived from a human tumour, were injected intracerebrally. A 9.4 T MRI system was used and MR imaging was performed on day 10 after tumour inoculation. CNR was measured prior, 20 mins, 2 hrs and 24 hrs post intravenous tail administration of glioma-targeted paramagnetic nanoparticles (NPs). GEFC provided higher CNR post contrast agent injection, compared to GE and SE. Post injection CNR was the highest with SWI and significantly different from any other pulse sequence.

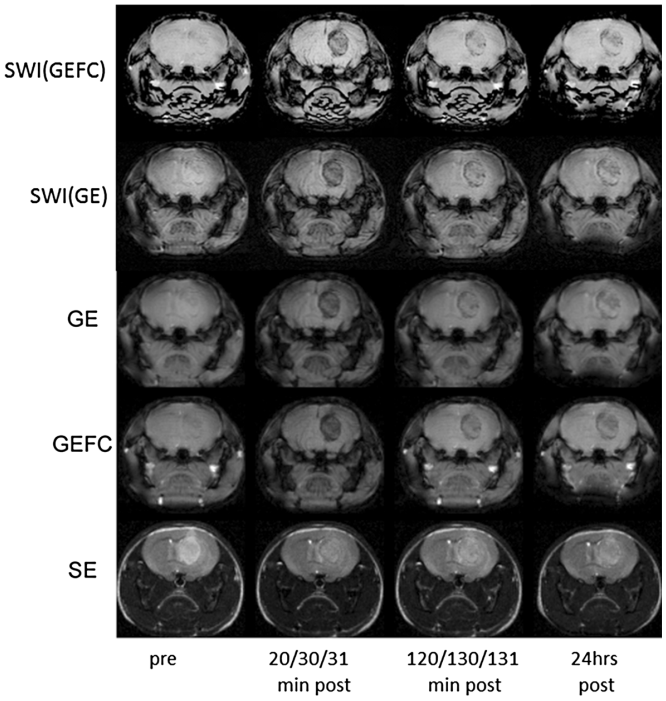

Fig. 10 *Contrast-to-noise ratio (CNR) using spin-echo (SE), gradient echo (GE), GE with flow compensation (GEFC), and susceptibility weighted imaging (SWI) in T2 and T2*.*

Hence, **we conclude that the use of flow-compensated pulse sequences, besides SWI, should be considered in molecular imaging studies.**

MR images of a tumour-bearing mouse using GE, GEFC, SE as well as SWI(GE) and SWI(GEFC) at the following time points after intravenous tail injection of targeted contrast agents: for SE: prior to, 20 mins, 120 mins and 24 hrs post; for GE: prior to, 30 mins, 130 mins and 24 hrs post; for GEFC: prior to, 31 mins, 131 mins and 24 hrs post; TR/TE = 50/7 ms for GE and GEFC. TR/TE = 5000/60 ms for SE. FOV = 2 × 2 cm^2 for each MRI. Note the increased negative contrast in GE and GEFC images after contrast agent injection. [BMC Medical Imaging, **13** (2013) 20]

The concentrations of CFCs and of sulphur hexafluoride (SF_6) in the atmosphere are at the ppt level. **The CFCs are synthetic and stable, contributing to ozone depletion in the stratosphere. The CFCs and SF_6 also play a part in enhancement of the greenhouse effect.** Stimulated by international agreements (Montreal Protocol, 1987) the measurements of CFCs and SF_6 in air began several years ago. "Clean" measurement stations were situated at locations distant from urban areas, gathering data within the AGAGE (Advanced Global Atmospheric Gases Experiment, http://agage.eas.gatech.edu/) world programme. One of such stations is Mace Head (Ireland, 53° N, 10° W), which has participated in AGAGE since 1987 and in the European InGOS (Integrated non-CO2 Greenhouse gas Observing System, www.ingos-infrastructure.eu) programme since 2011. **Similar research has also been conducted in Central Europe, in the urban area of Krakow (Poland, 50° N, 19° E) since 1997.** Based on these data, the effectiveness of the Montreal Protocol legislation, implemented in Poland [The Journal of Laws No. **52**] could be assessed [Acta Phys. Pol. A, **125** (2014) 895-897].

Figure 11. summarizes the measurements of selected halogenated compounds in the atmosphere over Krakow and Mace Head. Atmospheric mixing ratios reflect the impact of local, regional and global emissions of these

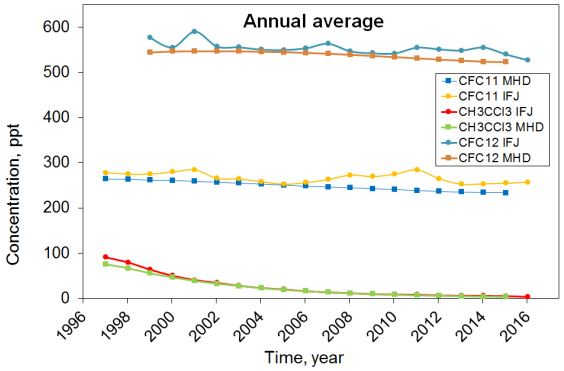

Fig. 11 *Annual averages of atmospheric mixing ratios of CFC11, CFC12 and CH3CCl3 measured in Krakow over the period 1997-2016, compared with Mace Head data.*

gases. It is apparent from the figure that the measured trace gases generally follow a decreasing trend which is particularly evident for CH_3CCl_3.

During the 19 years over which CFCs air measurements were performed in Krakow twelve working standards were used. Each of them was calibrated against a primary laboratory standard (USA Scripps). It was assumed that the concentration of individual compounds in the primary standard does not vary in time. To check whether this is indeed true, we recalibrated our primary standard twice (in 2013 and 2015). For this purpose the MHD-H184-2012 standard (from Mace Head) was used. Unfortunately, we found that the concentration of the primary standard had changed. The changes (in 2015) for the individual compounds, shown in percent of the start value, are as follows: +14,0% CFC-11, –15,4% CFC-113, –34,4% CHCl3, +9,0% CH3CCl3, –68,3% CCl4, +2,9% SF6 and +0,8% CFC-12.

Although the polar regions are not industrialized, numerous contaminants originating from human activity are detectable in the biota and abiota components of the Arctic and Antarctic environments. Improved knowledge of the degree of contamination over the polar regions is essential in the present era of global changes. We systematically studied the presence of artificial radionuclides (^{137}Cs, $^{238, 239, 240}$Pu and ^{241}Am) in terrestrial and marine environments of the High Arctic and Antarctic, originating from airborne sources. Samples were collected from remote areas, poorly investigated up to now: over western Spitsbergen, a selected region of western Arctic, western Greenland, the South Shetland Archipelago and the Antarctic Peninsula. Radionuclide levels and activity ratios of ^{238}Pu/$^{239+240}$Pu, ^{241}Am/$^{239+240}$Pu, $^{239+240}$Pu/^{137}Cs were determined by gamma or alpha spectrometry. Additionally, the atomic ratios of ^{240}Pu/^{239}Pu were assessed by ICPMS (ING PAN, Kraków). The measured activity and atomic ratios point to global fallout as the dominant source of radionuclides in the Arctic and Antarctic [Appl. Geochem (2013), **28**:100-108; Environ. Sci. Poll. Res. (2014), **21**:12479-12493]. Cryoconites occurring on glacier surfaces are the secondary source of the enhanced anthropogenic radioactivity found in the proglacial zone and marine environment. As the glacier terminus melts, the contaminated material from cryoconites is deposited in soils and marine sediments. **Activity concentrations of ^{137}Cs and Pu isotopes in cryoconites exceed respective activity concentrations in peats, mosses, lichens and organic soils** [Chemosphere (2016), **160**:162-172]. Some radionuclides and some heavy metals have a tendency to accumulate in the biota and then to transfer along the trophic chain. **In several lichen samples from Alaska ^{134}Cs was present, which points to Fukushima as a noticeable additional source.** In the southern hemisphere, the intensity of global fallout was lower than that in the northern hemisphere, which is reflected by lower activities of $^{239+240}$Pu and higher activities of ^{238}Pu in the Antarctic cryoconites, mosses, lichens, soils and birds, mammals. The enrichment in ^{238}Pu is due to the relatively higher, but more localized input of ^{238}Pu from the accidental re-entry of the SNAP 9A satellite in 1964 over Madagascar. We also evaluated levels of natural radionuclides (^{210}Pb, U, Th and Ra) in cryoconites, mosses, lichens, soils, birds and mammals [J. Radioanal. Nucl. Chem. (2016), on line, 1-11].

Improved radiation protection of nuclear medicine medical staff working with ^{131}I and of family members of patients treated this radio-pharmaceutical. The radiation safety of medical staff working at nuclear medicine facilities should be as high as possible. However, when performing their duties, they may be exposed to radioactive iodine in a partially uncontrolled manner, through administering iodine in the form of tables or solutions, or when taking care of patients to whom the isotope has been administered. To assess the magnitude of this additional exposure, **we performed ^{131}I activity measurements in the thyroids of nuclear medicine staff.**

We have also made a similar study among patients treated with ^{131}I, including their families. Assuring psychological comfort is essential for patients fighting cancer. They need to be assured that their 131I therapy is safe for them and for their families when they return to their homes after ^{131}I treatment.

The WBC (whole body counter) is the main research tool in this study. The WBC applied in this project is a unique piece of scientific equipment, in Poland and worldwide, with only two such devices available in Poland. Additionally, **gaseous and aerosol fractions of ^{131}I were measured in air inside hospital rooms by means of a method developed earlier for environmental studies** [Atm. Environ. (2014), **91**: 137-145].

The concentration of helium in groundwater is a good environmental tracer for groundwater dating in hydrogeology. Recently we modified our system for simultaneous measurements of helium, neon and argon from one groundwater sample (Fig. 12). This method allows groundwater ages

to be determined over a wide range, from hundreds to millions of years. Proper use of environmental tracers for dating purposes requires the knowledge of the recharge temperature of the system and of the excess air. Both parameters can be determined by measuring the concentration of argon and neon in groundwater. In our work (J. Najman and I. Śliwka, Acta Phys. Pol. A, 130 (2016) 737-742), the cryogenic method of enrichment with activated charcoal at abated pressure conditions was applied. Helium, neon and argon are analysed using two gas chromatographs (GC1, GC2) equipped with capillary (K1, K2) and packed columns (K3, K4, K5) and three thermo-conductive detectors (TCD). **The chromatographic method was applied to groundwater dating from Busko Zdrój, Tarnowskie Góry, Krzeszowice, Nałęczów and Nowy Targ aquifers.** The GC1 detection levels for helium, neon and argon are $14{\cdot}10^{-8}$ cm^3STP/cm^3, $1{,}9{\cdot}10^{-8}$ cm^3STP/cm^3 and $3{,}1{\cdot}10^{-6}$ cm^3STP/cm^3 respectively, and that of GC2 for helium is $1{,}2{\cdot}10^{-8}$ cm^3STP/cm^3.

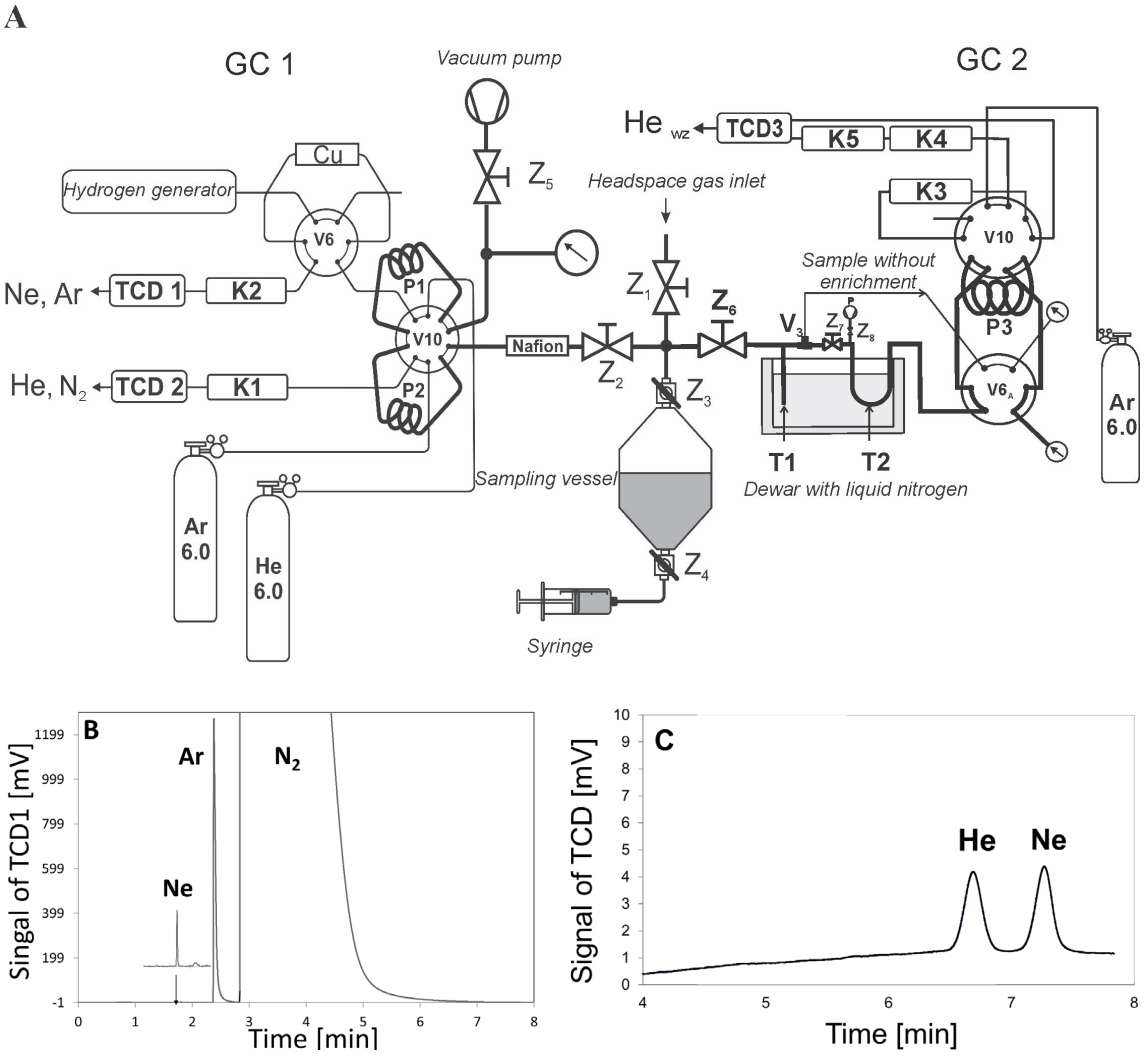

Fig. 12 ***A*** *– Design of the chromatographic measurement system for simultaneous analysis of He, Ar, Ne and He again, using the enrichment method. This system is implemented in two gas chromatographs GC1 and GC2.* ***B*** *– Chromatogram of Ne and Ar standard analysis using the GC1 system.* ***C*** *– Chromatogram of He standard analysis using the enrichment system GC2.*

The Jan A. Czubek Laboratory of Neutron Sources at IFJ PAN was created in 2014. The ING-14 pulsed neutron generator [Nucl. Instr. Meth. A, **797** (2015) 210-215] and two newly built plasma-focus (PF) devices [Nukleonika, 61 (2016) 413-418] are the principal research tools of this Laboratory, dedicated mainly for fusion plasma diagnostic projects [Physica Scripta, T **161** (2014) 014074]. The

Fig. 13 *The Plasma-Focus PF-24 device at IFJ PAN.*

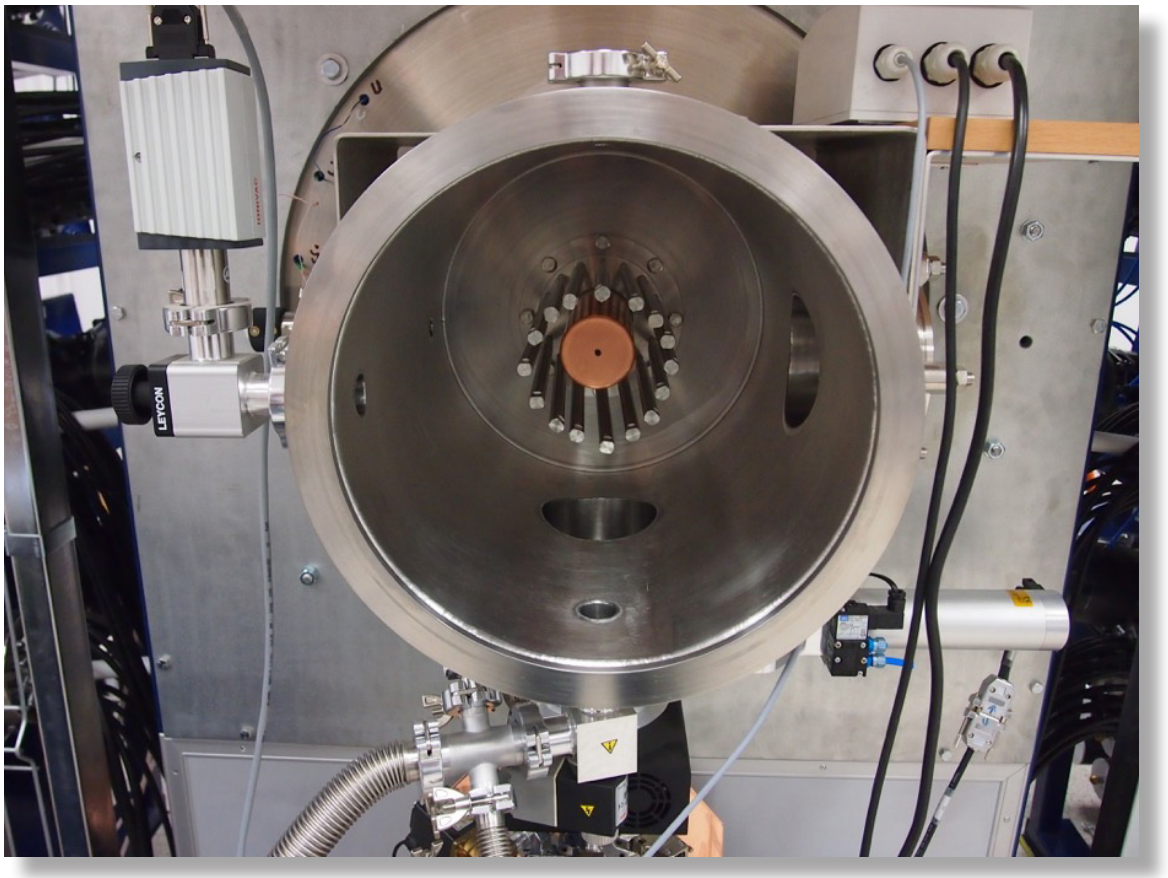

Fig. 14 *The discharge chamber of the PF-24 device, showing the system of electrodes.*

newly constructed Plasma-focus devices generate high temperatures and dense deuterium plasma and are intense sources of 2.45 MeV neutrons. The PF-24 (Fig. 13 & Fig. 14) and PF-4 were constructed with maximum bank energy of about 100 kJ and 15 kJ, respectively and with fast current rise time of about 2 μs. The neutron yield produced in the D-D reaction ranges between 10^8-10^{10} neutrons/discharge. The ING-14 produces 14 MeV neutrons from the D-T reaction with the yield of $5x10^9$ n/s in pulsing mode. The sources will be used to test new measurement methods of fusion products which include neutrons. For this purpose **a unique fast-neutron pinhole camera based on small-area (5×5) mm^2 BCF-12 scintillation detectors with nanosecond-order time resolution has been designed,** optimized using MCNP calculations and constructed [Eur. Phys. J. Plus **130** (2015) 145]. The pinhole camera has been designed to investigate the spatial and temporal distributions of DD neutrons from the PF-24 source.

Geophysical probes, based on neutron/gamma sources, have proven to be important and useful tools in shale gas exploration. Over this research area, we cooperate with the Department of Geology, Geophysics and Environmental Protection of the AGH University of Science and Technology, within the **'Blue Gas – Polish Shale Gas'** national project. The main question to be resolved within this project is how to conduct nuclear measurements in shale formations to obtain the best possible petrophysical information on the geological deposits. The properties of shale rock and of typical rock formations are substantially different. The shale rock parameters of (complex composition, very low porosity) fall outside the range of the current methods of interpretation, valid for typical rock formations. Thus, a new methodology is required. Our main task was focused on **numerical simulations of the characteristics of neutron/gamma drilling profiles for mixed shale rocks. The results obtained (curves) are extremely useful in subsequent geophysical interpretation.**

In a simulated layout consisting of a nuclear probe model, a borehole, and a model of the rock media, numerical experiments were planned and executed out. With the use of the well-known computer program MCNP5 (Monte Carlo N-Particle Transport Code), the responses of particular probes in the given rock environment were calculated.

The actual rock model consists of many different rock layers of different thicknesses. This model was built using ceramic materials exploited in the Zielona Góra calibration facility (Geofizyka Kraków S.A.) additionaly supplemented with thin layers simulating material properties characteristic of the Polish shale.

Within this work the detector responses of five geophysical probes (three variants of the neutron-neutron tool – see Fig.15, the typical gamma-gamma density tool, and the neutron-gamma spectroscopy tool) were represented numerically. 2D images of the neutron flux distribution around the borehole were constructed. This kind of chart (map) shows the origin of the neutrons registered in the detectors, and the space range of the well-logging tool can be precisely visualized. Examples of maps for detectors of the NNTK probe are presented in Fig.16. All results have been delivered to the Polish Consortium Blue-Gas [Prace naukowe INIG-PIB **209** 2016 553-556 and 557-564].

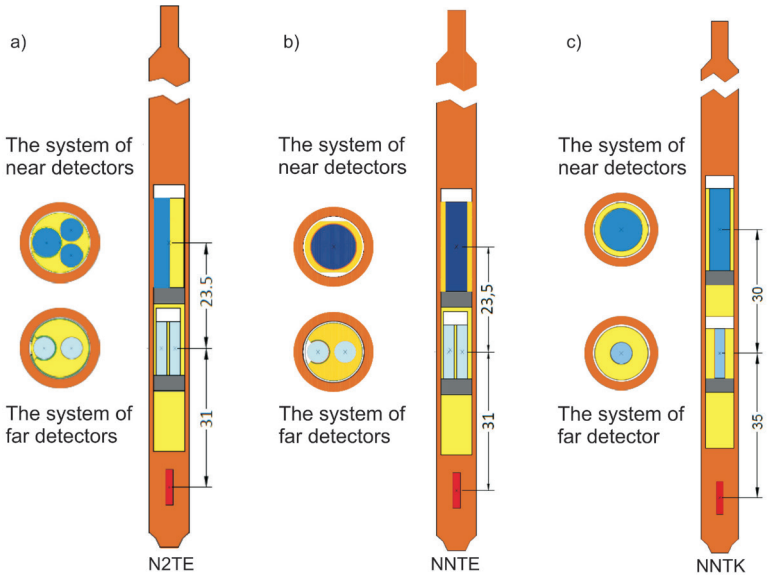

Fig. 15 *An example of the neutron well-logging tool geometry as used in the MCNP simulations.*

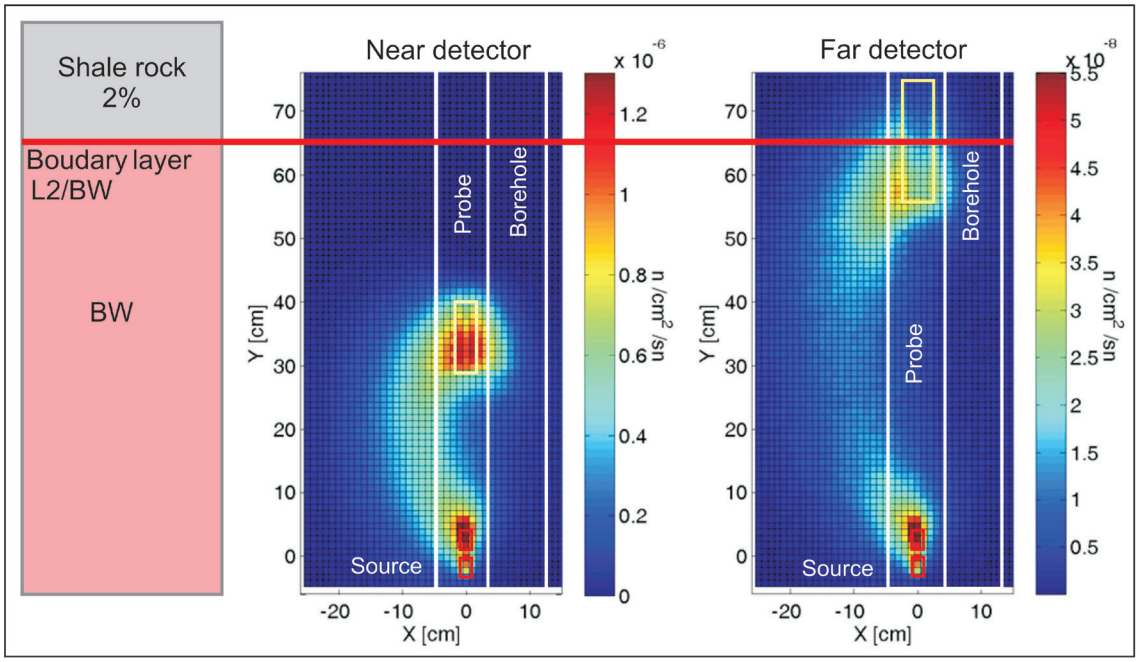

Fig. 16 *An example of 2D neutron flux distribution images for the NNTK tool in the modelled rock media.*

The grant ***Conceptual design and interface specifications of High Resolution Neutron Spectrometer for ITER (HRNS)*** was awarded in 2014 to a consortium consisting of IFJ PAN (consortium leader) and Uppsala University, with ENEA in Frascati and INF CRN in Milan, (Italy), as third parties. Apart from the NZ54 Department, the Division of Scientific Equipment and Infrastructure Construction (DAI) is significantly contributing to this project. The ITER project aims at building a fusion device which is to demonstrate the scientific and technical feasibility of fusion power. The ITER project plans to generate thermonuclear fusion reactions based on either deuterium-deuterium (DD) or deuterium-tritium (DT) fusion reactions in plasma, producing neutrons of 2.5 MeV or 14 MeV respectively. Neutron measurement systems, called neutron diagnostics, will be installed at ITER to collect information on neutron emission from the plasma and to establish some parameters describing certain features of the plasma. HRNS is a part of that set of the ITER neutron diagnostics.

HRNS is dedicated to measure time resolved neutron spectra for both DD and DT plasmas, mainly to determine the fuel ion ratio in the plasma core over the full range of ITER's operating scenarios in fusion power (neutron yield). The HRNS system is composed of a set of four differently designed neutron spectrometers to achieve the extended dynamic range required by ITER. These are the Thin Foil Proton Recoil Spectrometer (TPR), the Diamond Mosaic Detector (NDD), the Conventional Forward-Scattering Time-of-Flight (ToF) and the Back-Scattering Time-of-Flight (bToF) spectrometers. The first review of the project was presented in 2016 at the 29th Symposium On Fusion Technology.

The DAI engineers and technicians played two important roles in developing the engineering aspects of this work:

- System Design Engineer – whose role is to define the architecture, components and interfaces for the system to satisfy the specified requirements. He also acted as coordinator and integrator of the engineering work contributed by other members of the consortium. His work also called for defining the system classification (safety, seismic, quality, etc.) and analysis of loads acting on the detectors – inertial, electromagnetic, thermal and nuclear.
- CAD Officer – the main CAD design of the detectors proposed by the physicists was done at DAI. Use of the CATIA engineering software package together with the ENOVIA online collaborative environment needs the experience, credentials and training required by ITER Organization. The DAI staff fulfil these requirements.

While the grant called for conceptual design, several engineering analyses and quite detailed designs were made. A system to stabilize the ambient temperature of the HRNS and its 160 photomultipliers

was proposed. The operating conditions of different equipment within high magnetic field were analysed and an effective screening system proposed.

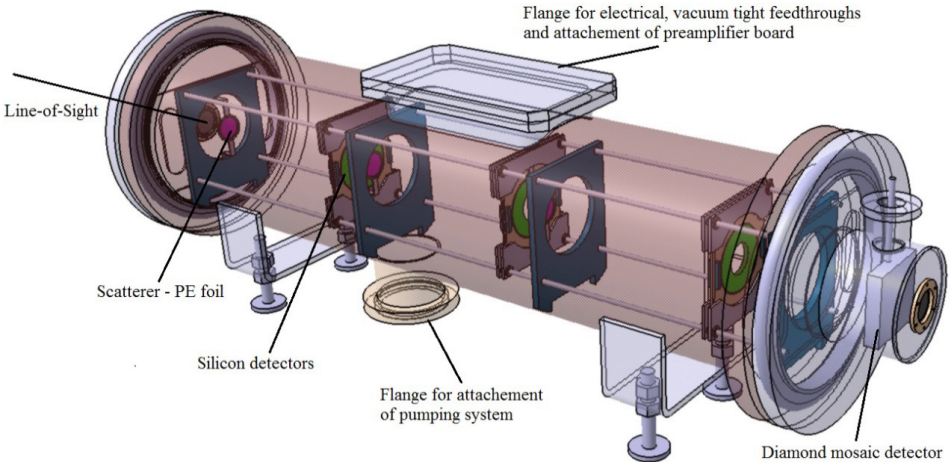

Fig. 17 *A vacuum container housing the NDD and a triplicate set of TPR detectors (in magenta – PE converter, in green – silicon detector). The collimated neutron beam enters from the left. Engineering design by DAI IFJ PAN.*

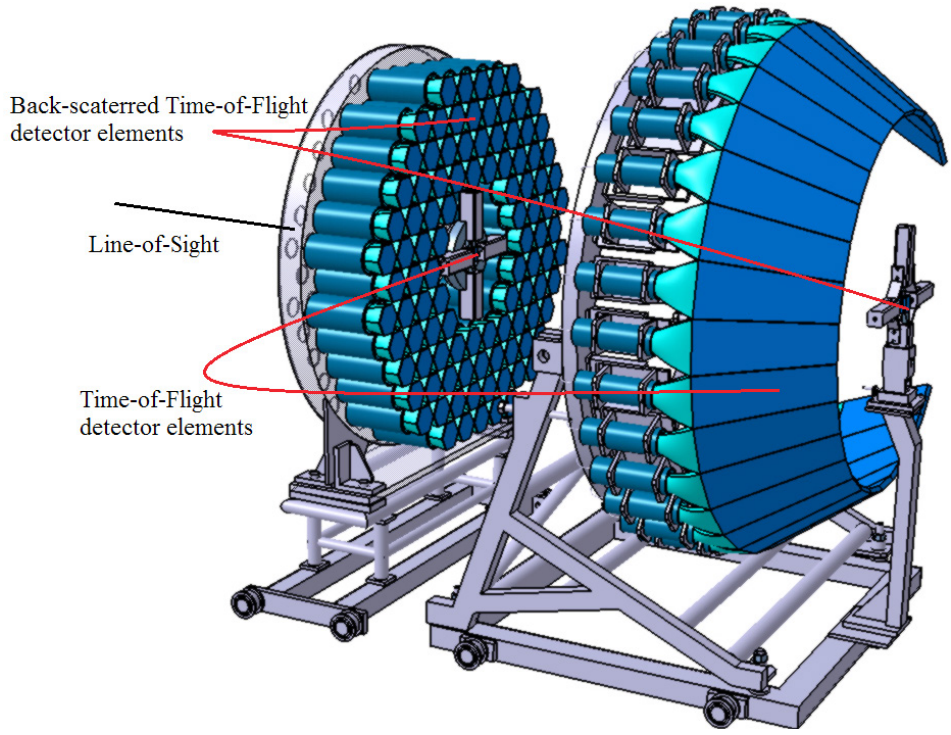

Fig. 18 *Isometric view of ToF and bToF spectrometers. The collimated neutron beam enters from the left. Engineering design by DAI IFJ PAN.*

An area of highly ordered arrays of magnetic dots and antidots was produced by nanosphere lithography [Nanotechnology **26** (2015) 425301]. The magnetic nanostructures were fabricated by depositing Co/Pd multilayers on polystyrene masks. Changes of preparation conditions allowed us to obtain arrays of separated magnetic islands as well as arrays of antidots with adjustable sizes down to 30 nm, of periods between 200 nm and 800 nm. This allowed us to observe the transition between two different

magnetization reversal mechanisms appearing on the border between the dot and antidot regimes. Such **studies were performed for the first time in a patterned system with perpendicular magnetic anisotropy, highly ordered over a large area, where both dots and antidots were created by the same method. We have shown that coercivity reaches a maximum value in an array of antidots of separation length close to the domain wall width. In such a case, each area between three adjacent holes corresponds to a single domain configuration, which can be switched individually** (Figure 19). On the other hand, small hole sizes and a large volume of material between holes results in domain wall propagation throughout the system, accompanied by strong domain wall pinning at the holes.

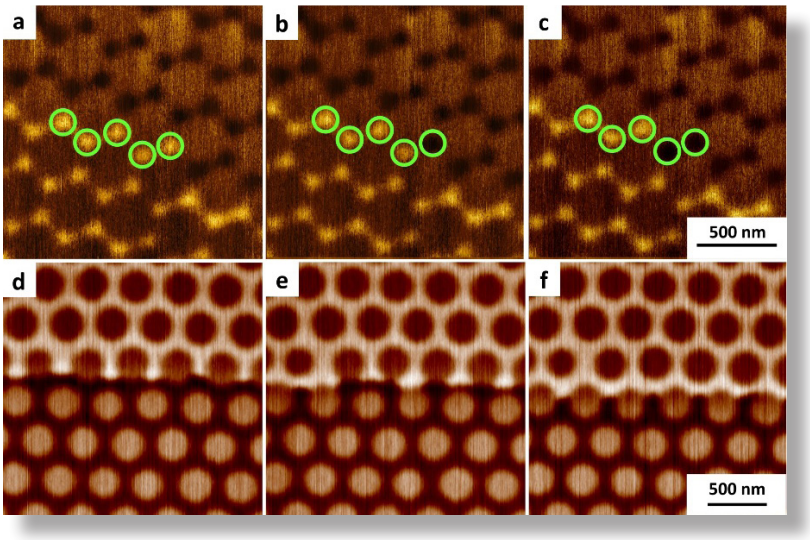

Fig. 19 *Sequential reversal of individual domains in an array of antidots with a period of 438 nm (a-c) and domain wall propagation for 320 nm dots with a period of 438 nm (d-f), obtained using a conventional recording head. Green circles mark single domains switched one after another (experiment performed with the Scanning Magnetoresistive Microscope at the University of Augsburg, within a cooperation between DAAD and MNiSW)*

The basic research performed on fabricated templates was complemented with applied studies of nanostructured sensors. Metallic bismuth due to its high conduction electron mobility is a very good candidate as a **thin film magnetoresistive sensor of magnetic field**. However, it is necessary to anneal the films to obtain good signal-to-noise ratio. Annealing at elevated temperatures leads to the dewetting process, creation of Bi islands on the film surface, and loss of film continuity. In order to avoid this problem, Bi was vapour-deposited in nanomembranes of anodic alumina. **The matrix of metallic nanowires embedded in alumina was then annealed, showing a magnetoresistance effect of 35% at 1.5 T at room temperature, approximately 2 times larger than that for flat films.**

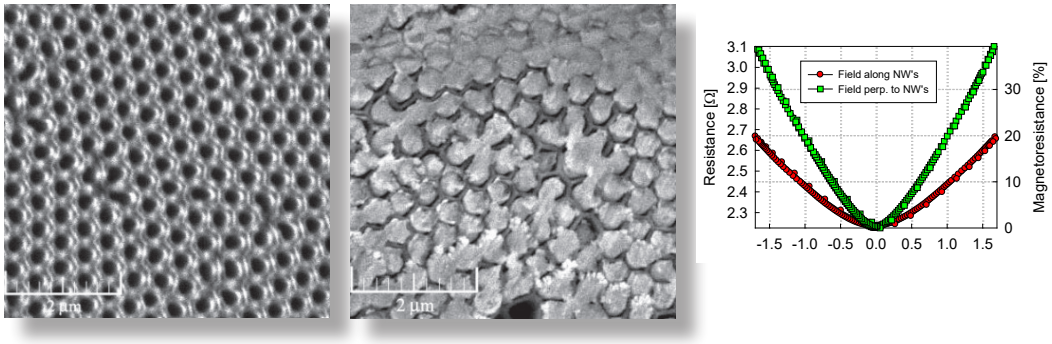

Fig. 20 *Scanning electron microscope image of (a) anodized alumina template, and (b) template filled with Bi nanowires. The plot (c) shows the magnetoresistance measured at room temperature along the nanowire direction, and perpendicularly to the nanowire axes.*

VI. DIVISION OF THE CYCLOTRON CENTRE BRONOWICE

The Cyclotron Centre Bronowice (in *Polish* – Centrum Cyklotronowe Bronowice, CCB) is a part of the Institute of Nuclear Physics of the Polish Academy of Sciences (IFJ PAN). The CCB is presently a major Polish accelerator facility, a modern nuclear physics research laboratory and a world-class proton radiotherapy centre. It is the first of its kind in Poland and one of only a few in Europe. The activities of the CCB are focused around two cyclotrons which now operate at IFJ PAN – the "old" in-house developed AIC-144 isochronous cyclotron (accelerating protons to the energy of 60 MeV), and the "new" Proteus C-235 cyclotron with a proton beam of variable energy (between 70 and 230 MeV), installed in 2013.

Over the years 2011 - 2015 the 60 MeV proton beam of the AIC-144 cyclotron was used to irradiate patients with cancer of the eyeball. The in-house developed beam delivery system and treatment room facility were all designed and constructed by engineers, technicians and software developers at the IFJ PAN – to become the first proton radiotherapy facility to operate in Poland. In developing the clinical part of this project, the team of IFJ PAN physicists and engineers closely collaborated with radiation oncologists at the Centre of Oncology in Krakow and with ophthalmologists at the Department of Ophthalmology and Ophthalmic Oncology (Collegium Medicum of the Jagiellonian University – CMUJ). By December 2015, 128 ocular patients of the CMUJ were irradiated at the AIC-144 facility, under contract with the Polish National Health Fund.

The fixed horizontal beam line and the limited range in tissue of the 60 MeV protons from the AIC-144 cyclotron precluded any applications of this beam in cancer radiotherapy apart from ocular treatments. In 2010 the IFJ PAN successfully applied and received a grant of about 30 M€ to purchase and install a modern IBA (Ion Beam Applications, Belgium) Proteus C-235 cyclotron to supply proton beams to an experimental hall and to a new eye treatment facility. Following the ground-breaking ceremony on March 18, 2011, the C-235 cyclotron was delivered from Belgium, installed on May 11, 2012 and began operation in December 2012. The C-235 cyclotron is able to accelerate protons to the energy of 230 MeV and is equipped with a degrader and energy selector which allows the energy of the proton beam to be varied continuously over the range 70 – 230 MeV. Basing on our earlier experience gained from the AIC-144 ocular radiotherapy project, a new eye treatment room was designed, fully equipped and commissioned by the physicists, engineers and technicians of our Institute. Finally, working together with IBA, the new eye treatment unit was commissioned and approved, in conformity with CE Medical standards. The first ocular patient was irradiated at the new facility on February 14, 2016.

While the application of cyclotron-produced proton beams for ocular radiotherapy was our immediate goal, the choice of the modern IBA C-235 cyclotron was dictated by

the possibility of applying its variable-energy proton beams for proton radiotherapy at all sites using a rotating gantry and Pencil Beam Scanning (PBS) technology, as well as for basic and applied research in nuclear physics, radiobiology, medical physics and radiation detectors. The success of the C-235 cyclotron project enabled the management of the Institute to apply for financing of a much broader project involving the construction of a building for medical applications of the C-235 beams, together with housing and installation of two rotating gantries with PBS therapy units able to treat tumours at all treatment sites, as well as building a modern, well equipped experimental hall for basic and applied research in nuclear physics. Commencing in 2013, two state-of-art rotating gantries were also purchased from IBA. They successively underwent installation, approval, and final commissioning in September 2015. This medical centre was officially opened on October 15, 2015. However, it took one year (until July 1, 2016) for the Polish Ministry of Health to publish an ordinance which formally enabled Polish medical centres to perform a limited number of proton radiotherapy procedures under public funding. The proton radiotherapy contract between IFJ PAN and the Centre of Oncology, Krakow Division (COOK) was signed on September 30, 2016. The first patient with a base of scull tumour was irradiated at the CCB on November 4, 2016.

The Cyclotron Centre Bronowice consists of two Departments: of the AIC-144 Cyclotron and of the Proteus C-235 Cyclotron, and of four Sections: of Dosimetry, of Treatment Planning, of Quality Assurance, and of Administration. Currently, within about 60 members of the CCB staff at the IFJ PAN are medical physicists, medical doctors, engineers, technicians, and Ph.D. students. We believe that the CCB – a unique in Poland, state-of-art proton radiotherapy installation located within the IFJ PAN – a leading nuclear physics research institute, together offer the unique possibility of combining cutting-edge proton radiotherapy with expertise in accelerator physics and with extensive basic and applied research capability in hadron radiotherapy, nuclear physics, radiation physics, clinical dosimetry, medical physics, radiobiology, microdosimetry, and materials engineering.

CYCLOTRONS AT CCB

The AIC-144 Cyclotron

The AIC-144 cyclotron is an isochronous cyclotron designed and constructed at IFJ in the early 90's to accelerate light ions (protons, deuterons and alpha particles) for research in nuclear physics. Its design, with a single dee, is unconventional. This cyclotron was used until 2010 mainly for the production of rare radioactive isotopes for scientific purposes. Later, its construction was modified and optimised to produce a 60 MeV proton beam at a current of 80 nA, stable to within 5%, for purposes of proton radiotherapy. The AIC-144 cyclotron is currently operated as a user facility for research and development in radiation physics, dosimetry, medical physics and radiobiology. Two beam lines are currently available: at the AIC-144 ocular proton therapy room and at the AIC-144 experimental room. In their vicinity, several rooms are available for preparing experiments in physics and biology. The cyclotron is operated by the AIC-144 Department engineering team of 11 accelerator engineers, technicians and support personnel, closely collaborating with engineers of the Proteus C-235 facility.

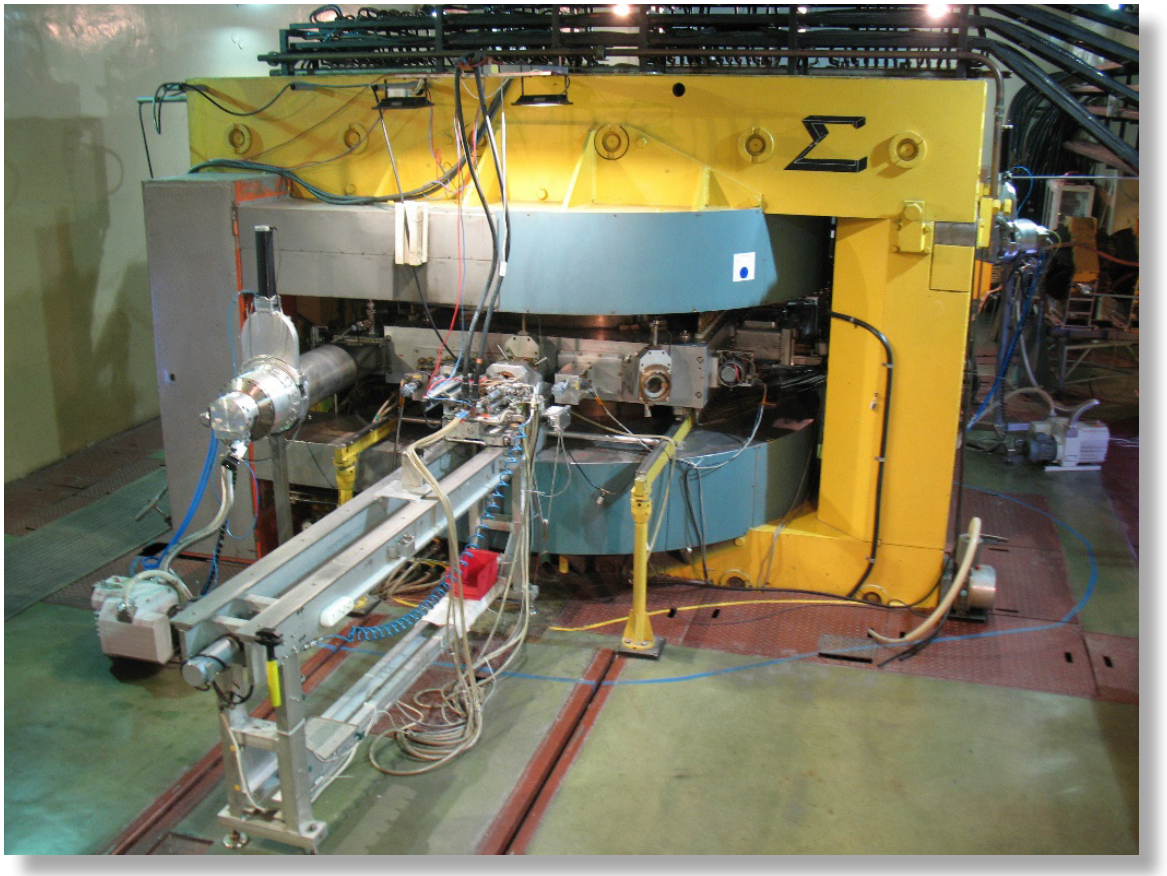

Fig. 1 *The AIC-144 isochronous cyclotron. Shown are the main magnet, magnet coils, the vacuum vessel and the ion source – at the centre (copyright: J. Sulikowski).*

The Proteus C-235 Cyclotron Facility

The new building of the Cyclotron Centre Bronowice houses the technical part and the medical area. The technical part contains the cyclotron vault and an experimental hall, together with preparation laboratories for experiments in physics and biology. The medical area provides the space necessary for the radiation therapy facility, including two scanning gantry therapy units, and for the required diagnostics and preparation of radiotherapy patients.

Fig. 2 *A view of the CCB building, December 2016 (copyright: M. Ptaszkiewicz).*

The Proteus C-235 cyclotron was designed and produced by IBA (Ion Beam Applications S.A., Belgium) specifically for medical applications. It is an isochronous cyclotron with a compact conventional magnet, able to accelerate protons to an energy of 230 MeV. Protons of this energy have a range of some 32 cm in water, which enables their radiotherapy applications at all sites in the patient. An energy degrader and selector, allowing the beam energy to be downgraded continuously to 70 MeV, is an integral part of this installation. The basic parameters of the Proteus C-235 cyclotron are: weight – 220 tons, outer magnet yoke diameter – 4.34 m, magnetic field – up to 3.1 T, maximum current in the main coil magnet – 800 A, operating frequency – 106 MHz, radially-dependent dee voltage amplitude 50-100 kV, PIG-type internal source, extraction efficiency – 70%, external beam current at 230 MeV –500 nA, total operating power consumption – 1.3 MW.

The Proteus C-325 Cyclotron Department which maintains and operates this cyclotron employs ten engineers. The variable energy beams of the Proteus C-235 cyclotron are directed to the physics experimental hall, to the C-235 eye treatment room and to two gantries.

The Experimental Hall, of floor area 100 m^2 and a height of 5 meters, uses a single horizontal proton beam line of variable energy, mainly for basic research in nuclear physics. Two preparatory rooms for physical experiments and two rooms for biological experiments are available in close vicinity to this experimental hall.

At the western, medical part of the new CCB building, the **proton treatment units** and auxiliary medical rooms are located. The medical part consists of three treatment rooms, one with a horizontal 70 MeV proton beam line for eye treatment, and two rooms equipped with rotating gantries, which allow the patient to be irradiated from any direction (0^0-360^0). Both gantries are equipped with dedicated IBA nozzles which are able to apply fields of up to 30 cm x 40 cm using proton Pencil Scanning Beams. The patient is positioned with the aid of a robotic positioner, orthogonal X-ray imaging sets and a Vision-RT optical verification system. For treatment of paediatric patients, anaesthetic columns and units are installed with access to anaesthetising gases. Imaging for treatment planning is conducted using a Siemens Somatom AS Open wide-bore computer tomography (CT) scanner which enables fast scanning using a dual-energy protocol. The CT room also contains lasers for virtual simulation and an

Fig. 3 *The Proteus C-235 isochronous cyclotron at the Cyclotron Centre Bronowice, IFJ PAN (copyright: K. Guguła).*

optical patient positioning verification system for alignment and gating purposes. In the CT room there is also full access to anaesthesiology procedures. A dedicated room has been prepared for paediatric patients, with a mobile anaesthesiology unit, allowing out-of-the-room patient preparation. After treatment the paediatric patients are transferred to a wake-up room equipped with monitored intensive-care beds. Patient-specific immobilization devices, such as thermoplastic masks, cushions or vacuum bags, are prepared in a dedicated modelling room equipped with a movable patient couch, alignment lasers, a water bath, vacuum pumps and other accessories. The patient treatment facility has been fully operational since October 2015. Up to 500-700 patients a year can be treated here, depending on their site of treatment and treatment schemes.

Fig. 4 *Positioning of a head phantom at the gantry room at the Cyclotron Centre Bronowice (copyright: T. Kajdrowicz).*

Fig. 5 *Preparation of a Computed Tomography scan of a head phantom at the Cyclotron Centre Bronowice (copyright: T. Kajdrowicz).*

Development of the Proteus C-235 cyclotron-based proton ocular radiotherapy facility

The basic advantage of proton ocular radiotherapy is in its exceptional sub-millimetre accuracy, unattainable by conventional radiotherapy using external photon beams. The C-235 ocular proton radiotherapy facility has been in-house developed at IFJ PAN and incorporated within the IBA Proteus C-235 therapy system.

The 230 MeV proton beam from the C-235 cyclotron installed at CCB in 2012 is degraded to an energy of 70 MeV and delivered to a specially designed eye therapy room where it is suitably formed and monitored. The eye therapy facility is equipped with several in-house – developed beam forming elements. After its preparation, the beam line allows a small tumour volume in the patient's eyeball to be irradiated at dose rates ranging between 6 – 32 Gy/min. The proton beam range in water (90% at the distal edge) is 31.5 mm, the distal fall-off (90%–10%) is less than 1.8 mm and lateral penumbrae measured in air (90%–10%) do not exceed 2 mm. These parameters are in line with other ocular radiotherapy centres worldwide.

The input beam energy is individually selected for the patient by a range shifter. Passive spreading of the Bragg peak is achieved by rotating wedge modulators also individually designed and machined for each patient. The beam dose is continuously monitored by PTW beam monitors and a four-segment ionization chamber. The patient is immobilized and positioned to a precision of 0.1 mm using a Patient Positioning System equipped with a BFI robotic eye therapy chair with a fixed isocentre position. Precise positioning of the patient's eyeball, which relies on X-ray images of fiducial markers attached earlier to the treated eyeball and on patient's active cooperation, is achieved by a Varian RAD-14 Diamond X-ray system using silicon flat panel detectors. The beam control system and the autonomous safety system are based on National Instruments hardware and on in-house developed dedicated software, using the LabView platform. The Varian Medical Systems Eclipse Ocular Proton Planning system has been configured to plan ocular radiotherapy at the CCB.

The C-235 proton eye therapy facility has been certified as a part of the Proteus C-235 therapy system of established CE medical certificate conformity, as a class IIb device, complying with the requirements of the European Council Directive 93/42 (approval number LRQ0960676).

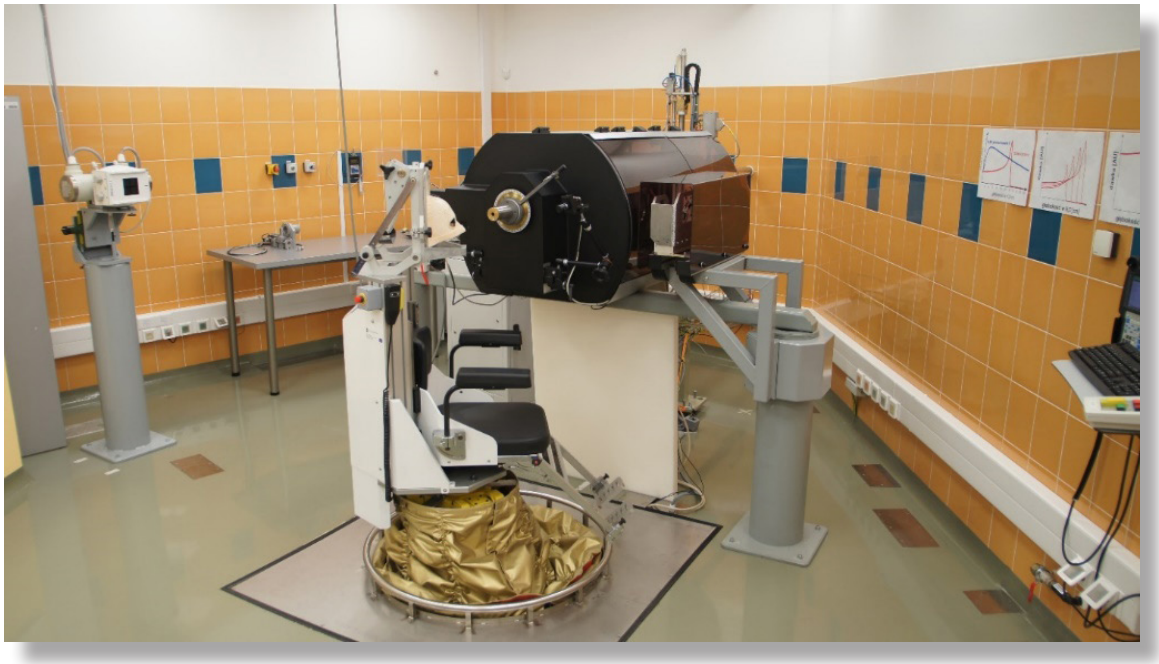

Fig. 6 *The C-235 eye-treatment room at the CCB facility (copyright: J. Swakoń).*

RESEARCH HIGHLIGHTS AT THE CCB

The main thrust of research activities of physicists, medical physicists and engineers at the CCB is in improvement of concepts and technology of proton radiotherapy and in development and applications of novel methods of dosimetry and of Quality Assurance procedures, especially for clinically applied proton beams.

In currently applied clinical proton radiotherapy it is generally assumed that the effectiveness, per dose, of tissue damage is independent of the beam's energy spectrum. Hence, a constant "clinical" value of Radiobiological Effectiveness (RBE) of 1.1 is applied to convert physical dose into biologically relevant "effective dose". However, due to the high ionization density at the end of each proton track in the beam, this assumption may lead to unexpected side-effects at distal beam ranges. The aim of this work was to gain a better understanding of the physics of beam propagation in proton radiotherapy and of its impact on tumour response. New calculation tools were developed to readily implement proton beam transport calculations in individual patient geometry, on the basis of the patient's computed tomography (CT) images. **Proton transport in different individualised patient tissues** was calculated using the SHIELD-HIT12A particle transport code. Complex and time-consuming calculations required that a powerful PLGRID-project computing cluster be used. For a sample patient CT data set, three dimensional distributions of the delivered "physical" dose, of Linear Energy Transfer (LET), and of proton and neutron fluences, were obtained. The outcome of these studies, combined with radiobiological modelling, will provide better knowledge of the spatial distribution of biological effectiveness over the treated volume, which can then be used to optimize the treatment planning process.

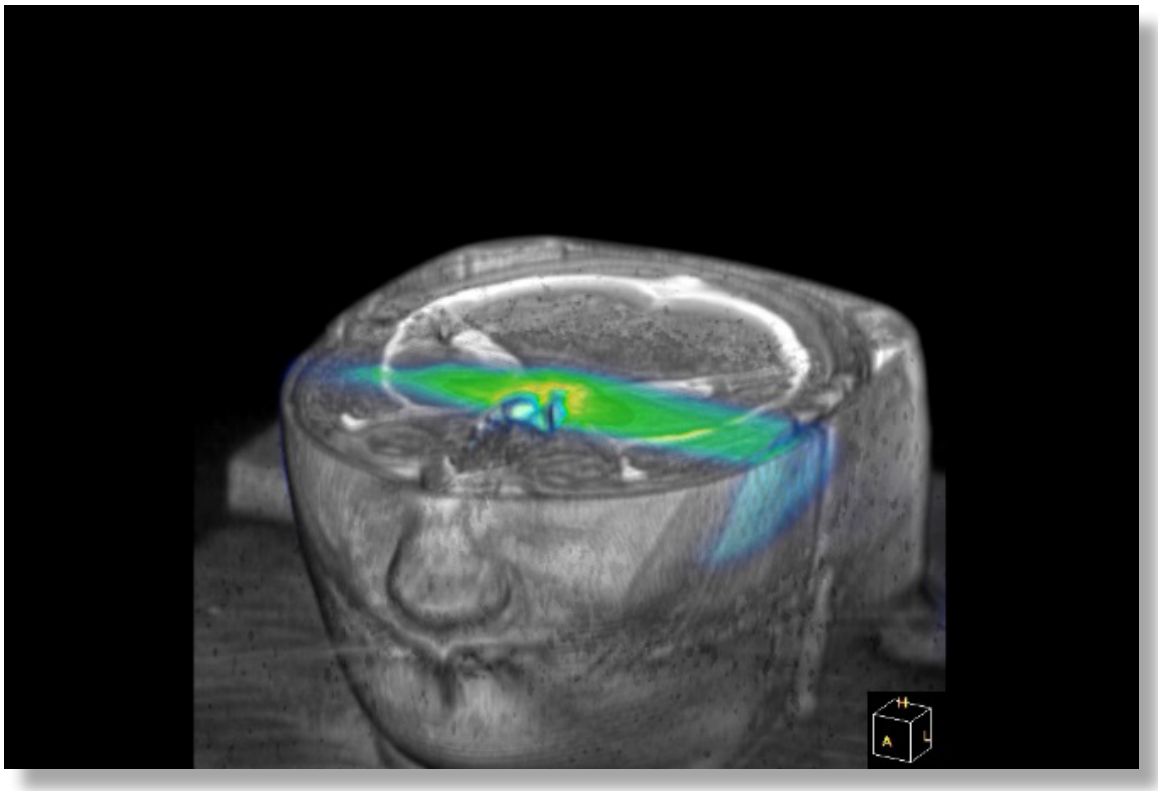

Fig. 7 *Dose distribution in the patient's head, calculated with the SHIELD-HIT12A particle transport code. The yellow region in the centre of this image illustrates the region of enhanced ionization density (LET) (image by N. Bassler and L. Grzanka,unpublished).*

A new concept in particle therapy is to apply **spatially separated, collimated narrow proton beams (i.e. proton grid therapy)** in order to reduce side effects of beam entrance at the air-body interface and simultaneously, due to proton scattering, to obtain uniform dose distributions in the target volume

inside the body. The proton grid therapy concept arose from Microbeam Radiation Therapy, where extremely narrow parallel surface-like synchrotron-produced X-ray beams demonstrated good tolerance of healthy tissue and a more pronounced response of the tumour. In our studies we investigated whether it is possible to achieve a uniform transverse dose distribution over the target volume in a proton microbeam irradiation setup and simultaneously to benefit from sparing of healthy tissues (including, e.g. scull bone) by microbeams entering the skin and skull. The FLUKA Monte Carlo code transport calculations were performed using the PLGRID-project computing cluster. It was demonstrated that by minimizing the beam size to micro-scale and by increasing the distance between the beams to some millimeters, one should be able to obtain a map with micro-spots at the entrance region to limit the healthy tissue response at beam entry. At larger beam depths one should then expect the target volume to be covered by a uniform and conformal dose distribution, resulting from enhanced proton scattering at low proton energies over the Spread-Out Bragg Peak region.

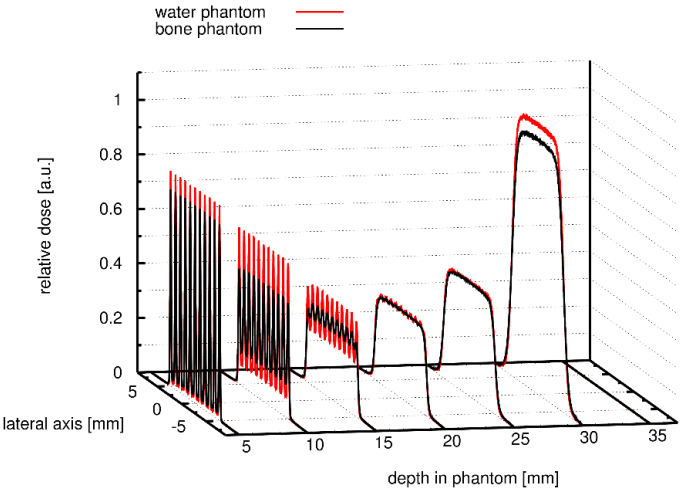

Fig. 8 *Depth-dose distribution for a set of proton microbeams (σ = 100 mm, beam separation 1 mm) constituting a 1 x 1 cm² field for a 60 MeV beam entering axially a cylindrical head phantom with or without the 5 mm bone layer at entrance (marked with black or red lines, respectively). At 30 mm depth the beams produce a laterally uniform energy deposition pattern [Phys. Medica,* ***31****, 621(2015)].*

In conventional photon beam radiotherapy, detectors used for *in-vivo* dosimetry to verify the dose applied to the patient are usually placed on the patient's body, within the treatment field. In proton beam radiotherapy, particularly when treating ocular tumours, such *in-vivo* detectors would significantly reduce the range of the beam within the patient's eyeball. To obtain additional verification of the dose applied to the patient's ocular tumour ***a special in-vivo* dosimetry system for proton ocular radiotherapy using EPR/alanine detectors** was developed. In alanine exposed to ionizing radiation some stable free radicals are generated, the concentration of which can be evaluated by Electron Paramagnetic Resonance (EPR) spectrometry. The main advantages of alanine as a dosimeter are tissue-equivalence, linear response over a large dose range (0.5-500 Gy), signal stability and its non-destructive EPR readout, enabling cumulative recording of doses in the treated tumour over consecutive exposures (in fractionated radiotherapy). In order not to disrupt the clinical setup of ocular radiotherapy, alanine detectors had to be placed at fixed locations, upstream of the isocentre - in the proton beam line but over an area outside the patient's individual beam collimator (Fig. 8). In order to relate the dose deposited in the thus placed alanine detectors with the reference dose measured at the isocentre of the ocular irradiation facility, several correction factors related to the geometry of the facility and to patient-selected sets of beam forming elements (range shifter and range modulator) were introduced. The alanine *in-vivo* dosimetry system was then tested in clinical conditions at various beam configurations, by verification against doses measured at the reference point (isocentre) using reference dosimetry. Agreement to within 3%, or better, was found, satisfying the requirements of *in vivo* dosimetry. This method will also be used in an international passive dosimetry intercomparison of ocular radiotherapy facilities, which is currently under way.

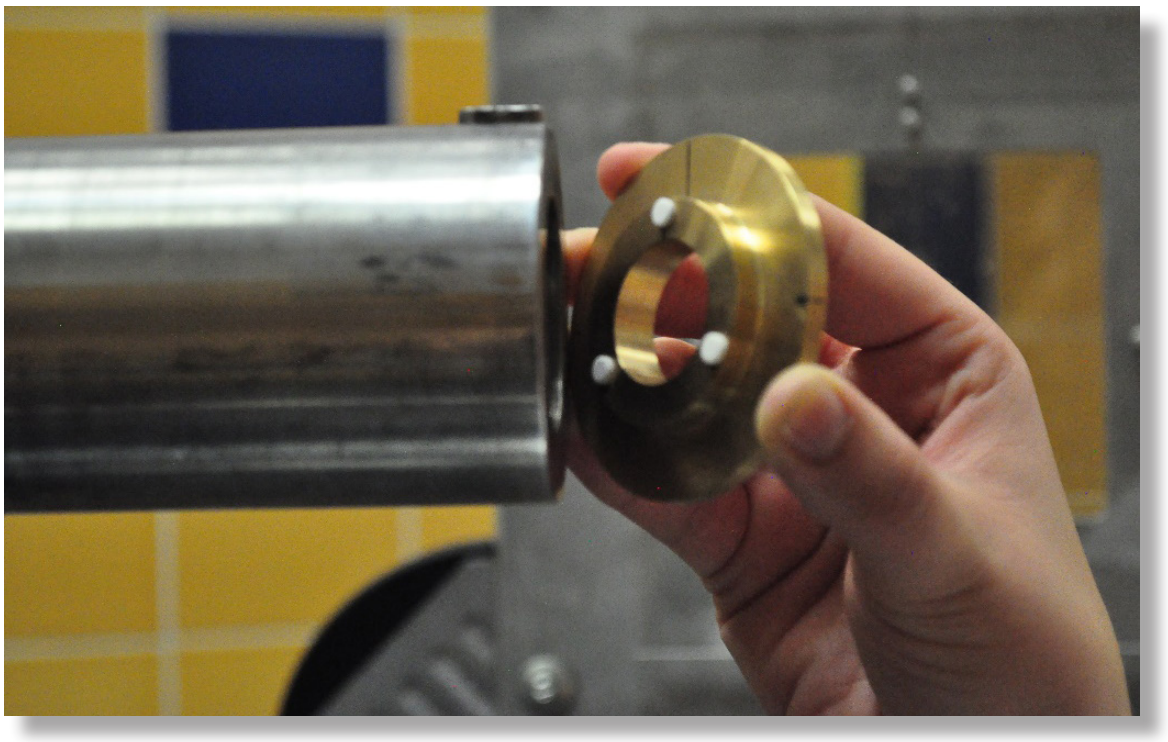

Fig. 9 *Placement of three alanine detectors (white) inside the individual patient collimator to measure the dose applied to the patient's ocular tumour, within the in-vivo EPR/alanine dosimetry system for proton ocular radiotherapy, developed at IFJ PAN (copyright: G. Mierzwińska).*

In radiotherapy, out-of-beam scattered radiation may lead to secondary cancers. The aim of this work, performed in a collaboration with the EURADOS Working Group 9 "Radiation dosimetry in radiotherapy", was to determine **secondary radiation doses and neutron spectra produced by the Pencil Scanning Beam (PBS) irradiation technique** outside the treatment fields. In years 2014 - 2016 several experimental campaigns took part at the Trento Centro di Protonterapia (Italy) and at the Cyclotron Centre Bronowice. Systematic measurements of the photon and neutron doses in a 300 x 300 x 600 mm^3 water phantom and anthropomorphic children phantoms allowed us to determine the response of a broad set of passive detectors, such as TLD, RPL, OSL and track detectors within well-defined phantom conditions. Neutron energy spectra determined around the patient using Bonner sphere spectrometers showed a high energy component, particularly in the direction of the primary proton beam. The experiment confirmed that patients treated with PBS are exposed to lower doses of radiation over areas remote from the target volume than patients treated by conventional photon beam radiotherapy. Results of these measurements will allow us to compare different methods of dosimetry and also to cross-check the obtained results.

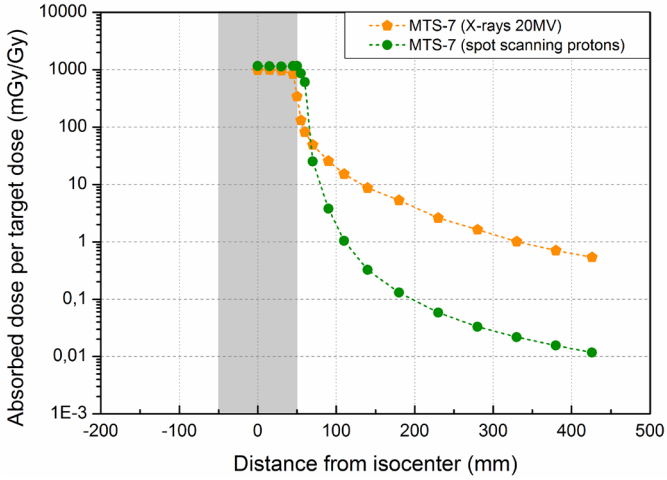

Fig. 10 *Absorbed dose per target dose (mGy/Gy) from gamma radiation measured for a 10 x 10 cm^2 field in a water phantom, using different radiotherapy techniques: photon beam (20 MV) from a Varian linear accelerator and Intensity Modulated Proton Therapy from a proton spot scanning IBA gantry, at 360° (L. Stolarczyk, unpublished).*

One of the specialised research areas in which the Institute of Nuclear Physics is particularly interested is the **development and application of different type of luminescent detectors in radiation dosimetry**. In this technique, the luminescence signal emitted from an irradiated detector, after its heating or after its exposure to laser light, is roughly proportional to the dose absorbed. Our facility for crystal growth, launched in 2011 and extended in 2014 allows us to grow crystals in the form of thin fibers and rods using the micro pulling-down technique μPD, and also as bulk crystals, using the Czochralski method. The μPD is well suited for materials research, as it enables rapid manufacture of crystal samples using small amounts of starting material. In this facility crystals can be grown within various gas atmospheres and at very high temperatures, exceeding 2000°C. Over the last few years several μPD crystals have been successfully obtained, mainly of LiF, Al_2O_3, $LiMgPO_4$, $LiAlO_2$, and various garnets. The Czochralski method was used mostly to obtain high quality, transparent LiF crystals. The main aim of growing those crystals is the search for materials for luminescent detectors of ionizing radiation, exploiting such phenomena as thermoluminescence, optically stimulated luminescence, radio-photoluminescence or scintillation. Fig. 12 presents a photoluminescence image of a highly collimated, 1.2 mm in diameter 50 MeV proton beam impinging on LiF crystal. This research is useful in the **development of 3-D dosimetry systems**.

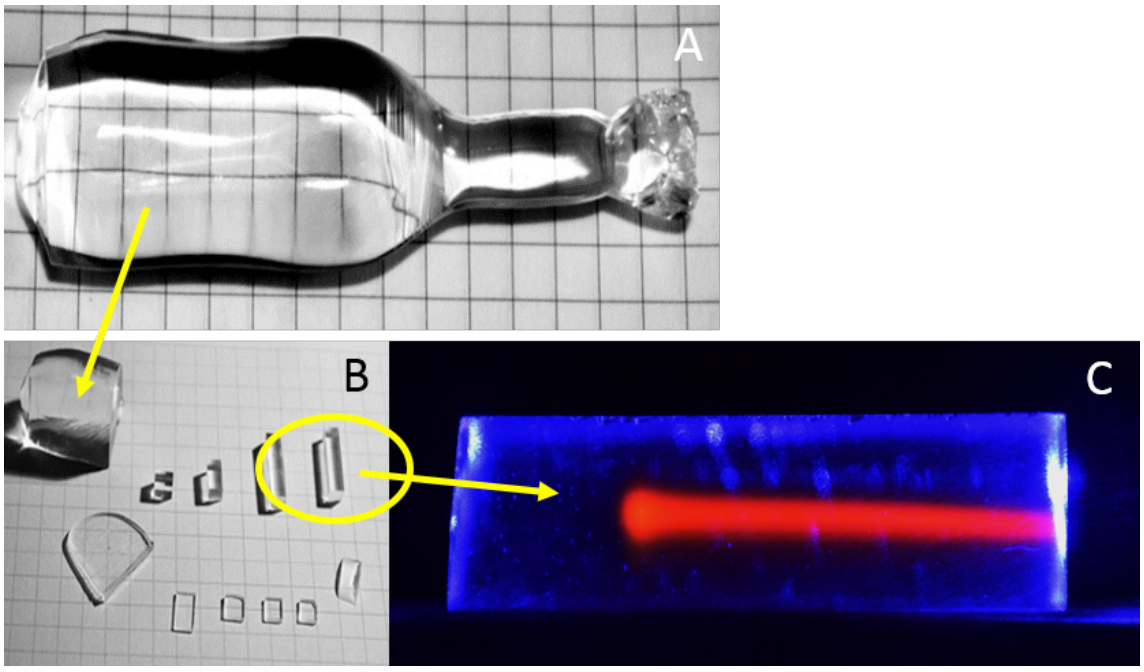

Fig. 11 *(A) Different samples of LiF crystals grown using the Czochralski method, (B) – samples cut from crystal bulk, (C) visualization of an AIC-144-accelerated 50 MeV proton beam stopping in the LiF crystal; the observed red light image was obtained by 440 nm blue light stimulated photoluminescence (copyrights: B. Marczewska).*

In proton therapy with Pencil Beam Scanning technology, high-resolution, **two-dimensional (2D) dosimetry** is needed to verify high-gradient dose distributions and for Quality Assurance procedures concerning beam properties. For these purposes, a two-dimensional (2D) thermoluminescence (TL) dosimetry system was developed at the Institute of Nuclear Physics PAN (IFJ PAN). It consists of TL detector foils, a dedicated TL reader equipped with a suitable heating system and a CCD camera and dedicated software for image acquisition and post-processing. The detector foils based on LiF:Mg,Cu,P TL material are flexible and water resistant and can be easily used in water or solid phantoms. Due to their wide range of linear dose response of up to 15 Gy, the shapes of proton spots measured with the 2D TL dosimetry system are not distorted. The system has been employed in measurements of active pencil scanning beams, PBS, at several centres in Europe. Certain variations in the symmetry of proton spots were observed.

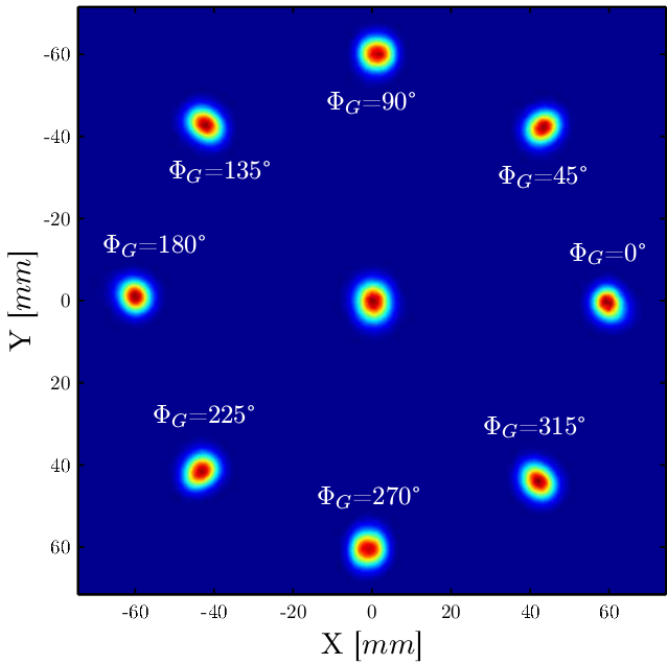

Fig. 12 *Spots of a proton Pencil Scanning Beam recorded with TLD foils at different gantry positions (angles) in one proton therapy centre in Europe. The loss of symmetry of the spot affects dose uniformity in the target volume (copyright: J. Gajewski).*

Lithium fluoride, MTS-7 and MTS-6 thermoluminescent detectors developed at IFJ PAN were also applied in **dosimetry of cosmic-rays**, which are mainly protons. In the year 2014 the analysis of data from the long-term MATROSHKA experiment (about 1500 days of measurements on an Earth orbit) was accomplished. This experiment, consisting of three phases with exposures inside and outside of the space station, provided for the first time information on cosmic radiation dose distribution inside anthropomorphic phantoms, allowing determination of organ doses and effective doses which astronauts working on orbit would receive. Within another, still running project, DOSIS-3D, the spatial and temporal distribution of doses inside the European Laboratory Columbus of the International Space Station (ISS) are being measured using MTS-7 and MTS-6 thermoluminescent and nuclear track-etched detectors. The measurements have been realized over six-month periods since the year 2012 and will be continued at least until 2018. Data gathered so far with passive radiation detectors show that the absorbed dose values inside the Columbus Laboratory follow a pattern, based on the local shielding configuration of the radiation detectors, with a minimum dose rate of 195 μGy/day and a maximum of 360 μGy/day. The absorbed dose is modulated by the variation in solar activity and by the changes in ISS altitude. Measurements in space were complemented by broad investigations of the efficiency of thermoluminescent detectors to doses of high-energy accelerator ion beams. These experimental data combined with Monte Carlo transport calculations of the cosmic radiation spectrum, enabled an evaluation of the efficiency of thermoluminescent detectors in space, depending on altitude, solar activity and shielding thickness.

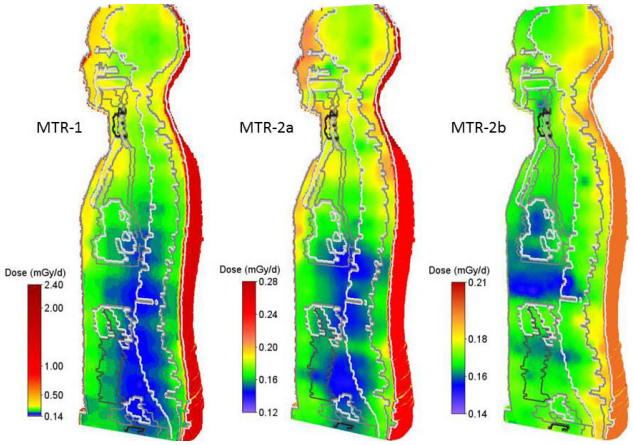

Fig. 13 *The measured dose distribution combined with the numerical voxel phantom NUNDO developed at IFJ PAN, for different phases of the MATROSHKA experiment: MTR-1 (outside ISS), MTR-2A and MTR-2B (inside ISS). The lowest doses were determined for deeply situated organs. [Radiat. Environ. Biophys.,* **53**, *719, (2014)]*

There is a growing interest in evaluating the threat to life in persons affected by radiation events and selection of those requiring medical treatment (triage). **Emergency dosimeters** for this purpose are selected among items used every day, such as electronic equipment (mobile phones), credit cards, banknotes, or plastic objects. In our research it was demonstrated that the components of mobile phones such as resistors, Integrated Circuit (IC) chips, glass screens, as well as banknotes (Fig.14) are sensitive to ionizing radiation and show good dosimetry properties, such as repeatability of signal after irradiation, linear characteristics of dose response and low limit of radiation detection starting from 0.05 Gy for IC chips, 0.08 Gy for resistors and 0.2 Gy for banknotes. Such emergency dosimeters will allow estimation of the level of potential doses in order to predict the risk of expected biological effects and the degree of threat to life (i.e. triage) and deciding whether the victim needs to be referred to a hospital for further treatment.

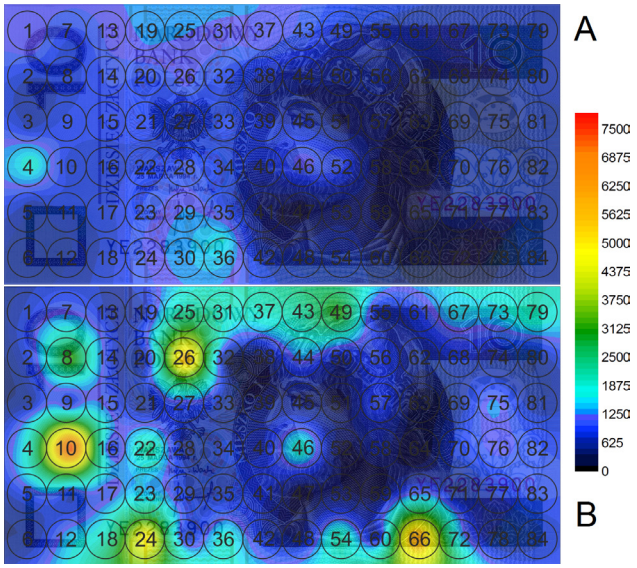

Fig. 14 *Dose mapping of optically stimulated luminescence signal of a 10 Polish Zloty banknote: (A) before and (B) after irradiation. The special fluorescent paints, used to assure the authenticity of the banknote, produce a measurable OSL signal, allowing accidental doses as low as 0.2 Gy to be determined. [Radiat. Environ. Biophys.,* **53**, *719, (2014)]*

VII. DIVISION OF SCIENTIFIC EQUIPMENT AND INFRASTRUCTURE CONSTRUCTION (DAI)

Over the years 2014-2016 the DAI engineers and technicians (a staff of about 60) have participated in many international projects. They carried out acceptance tests of the components of the **European X-ray Free Electron Laser** (E-XFEL) at DESY in Hamburg. They completed the final stages of their activities during the Long Shutdown 1 of the **Large Hadron Collider** (LHC) at CERN in Genève. They assembled one hundred composite mirrors for the Medium Size Telescope (MST) prototype and commissioned the Small Size Telescope prototype (SST-1M) at IFJ PAN for the **Cherenkov Telescope Array** (CTA) project. They also contributed projects related to the **International Thermonuclear Experimental Reactor** (ITER), together with engineering support. More details on these activities are given below.

In March 2013 a decision to open a new research topic at DAI: "physics and techniques of particle acceleration" was made by the Scientific Council of IFJ PAN. Following this decision, regular international conferences devoted to superconductivity and particle accelerators (SPAS) were to be organized by IFJ PAN to identify areas already developed and those requiring development in Poland, and to specify the infrastructure required to support this research. Two conferences were organized so far (in the years 2014 and 2016). Based on the experience gained at performing acceptance tests of the E-XFEL components, four topical groups were established: to deal with magnets and superconductivity, with RF cavities, with beam diagnostics and with control systems. The engineer staff within those groups will develop their expertise and extend the facilities at DAI in collaboration with leading laboratories in these domains, such as CERN, INFN Legnaro, or Fermi Lab. To further support these activities, the IFJ PAN cryogenic infrastructure, including the buildings and the helium liquefier, is being upgraded.

In 2016, an ISO 9001 quality management system was implemented in the DAI division. Within this system, staff positions and team structures were established and the required ISO documentation was prepared and issued.

Between 2014 and 2016 DAI continued its work within the **European X-ray Free Electron Laser** project at DESY. Tests of the cold magnets and of the current leads were performed as scheduled. With reliable infrastructure, specially constructed test stands and full commitment of the team, the required test rate of one set per week was achieved. In all, 108 tests were performed for 101 serial cold magnets and current leads. The final tests of these components were completed in March 2015.

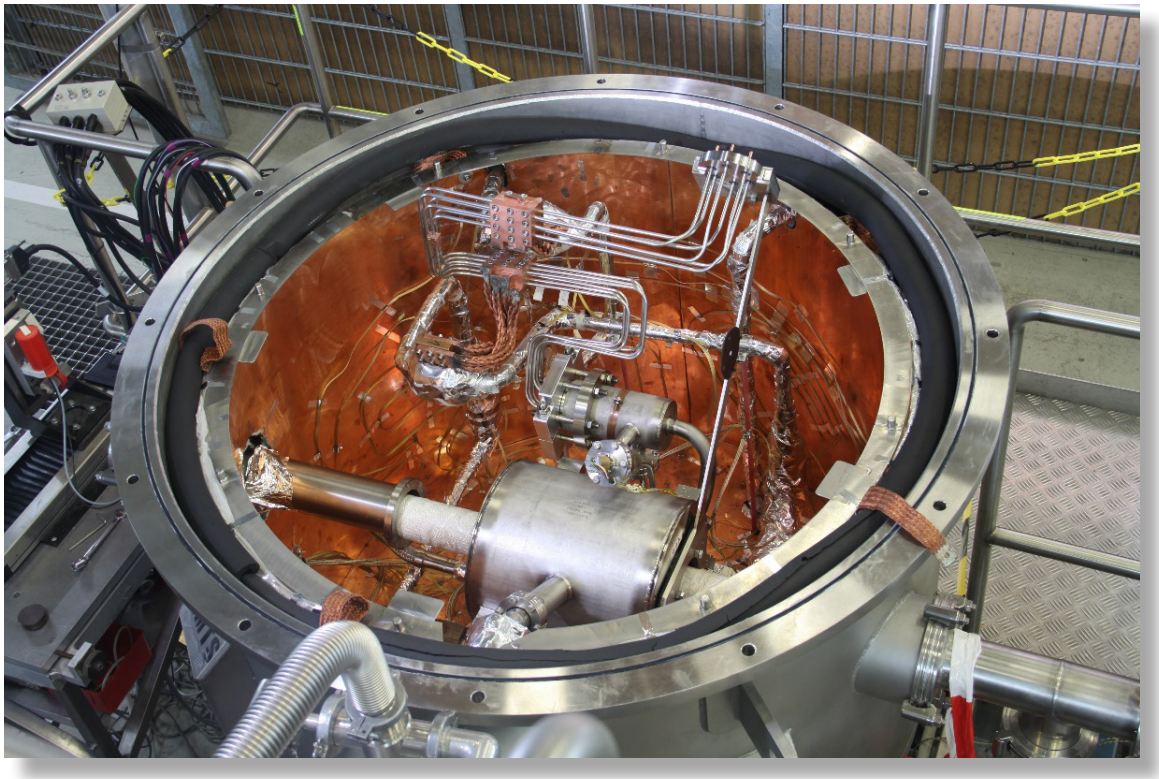

Fig. 1 *A cold magnet with the current lead in the cryostat (Image copyright: DAI).*

Tests of the serial cavities and cryomodules were performed in a hall equipped with: two vertical cryostats, preparation/storage areas for the cavity tests and three horizontal test stands, preparation/storage areas for the cryomodule tests. DAI engineers and technicians were involved in the commissioning of all five test stands. Tests of the cavities began in May 2013 and continued until the end of March 2016. During this period over 1200 tests at 2 K of 813 cavities were performed. The cryomodule tests began in May 2014 and were completed by August 2016. A total of 107 tests at 2 K of 100 cryomodules were performed.

The tests of both the cavities and cryomodules were complex processes, involving *inter alia* incoming/outgoing inspections, connection of the components to test stands, measurements at 300 K and at 2 K, leak checks, and cool down/warm up procedures. Operating five test stands in parallel was a logistic challenge. In order to reach the required test rates i.e. of eight cavities and one cryomodule per week, DAI engineers introduced many improvements to shorten the testing processes and to ensure their good supervision, e.g. semi-automatic procedures for cooling down and warming up the tested components or a new design and a prototype of a mobile clean room needed to connect the cavities with the vacuum line of the inserts. The final design of the mobile clean room was accepted by DESY experts and transferred to an external company which produced and delivered the new clean room to DESY. This improvement reduced the connection time of the cavities by a factor of three. It also greatly aided in achieving optimum performance of the hall facilities. In June 2015 a modification/optimization of the cryomodule test procedures was introduced together with DESY experts. This allowed the DESY and IFJ PAN teams to achieve a higher testing rate (1.5 cryomodule per week) in order to cope with the new challenges of the project.

Fig. 2 *The novel mobile clean room (left) and installation of the insert to the vertical cryostat (right) (Image copyrights: DAI).*

To fulfil the commitments of IFJ PAN to this project over 75 testing procedures were developed, together with dedicated data bases and professional software for measurements, quality control and reporting. The complexity of this task required that a team composed of people of various professions and skills collaborate closely. In all, about 80 people (40 engineers) were involved in the XFEL project between 2010 and 2016. Commissioning of the laser is planned in 2017.

Fig. 3 *XFEL Cryomodules at the AMTF testing hall (Image copyright: DAI).*

Over the years 2014-2016 DAI engineers continued their extensive involvement in electrical quality assurance (ELQA) and commissioning of the superconducting circuits and magnets of the **Large Hadron Collider**. These activities involved electrical measurements, follow-up of nonconformities, and daily maintenance of hardware and software. Along with ELQA came additional projects developed for CERN, such as the Low Voltage Insulation Monitoring System for warm-up and cool-down of superconducting circuits; or an automatic system for electrical tests of the cryogenic instrumentation of the current leads.

Fig. 4 *The last standard ELQA measurement during LHC Long Shutdown 1 (Image copyright: M. Brice, CERN).*

Fig. 5 *600 A Energy Extraction Switch Testers (Image copyright: DAI).*

In view of DAI's wide expertise in measurement automation, the team was asked to develop the 600-Ampere Energy Extraction Switch tester. The task involved preparation of hardware, software and setting up a database. Five complete units were manufactured and used during the LHC restart. The new measurement system greatly improved personnel safety and time efficiency during the 600-A Energy Extraction System tests. In 2014, DAI also successfully completed its engagement in the Interconnection Inspection Team for the LHC magnets, and its involvement in the supervision and coordination of an international team responsible for opening and closing of the LHC magnet interconnections.

Owing to the very satisfactory collaboration of DAI with CERN, three ELQA – related projects began in 2015:

- development and manufacture of a new Arc Interconnection Verification (AIV) measurement system, required for local electrical tests of the connections of the superconducting corrector magnets during LHC magnet replacement;
- design and production of new high voltage multichannel insulation testers needed for the LHC ELQA team,
- upgrade of ELQA software.

DAI also participates in the LHC technical stops, which are typically scheduled four times a year.

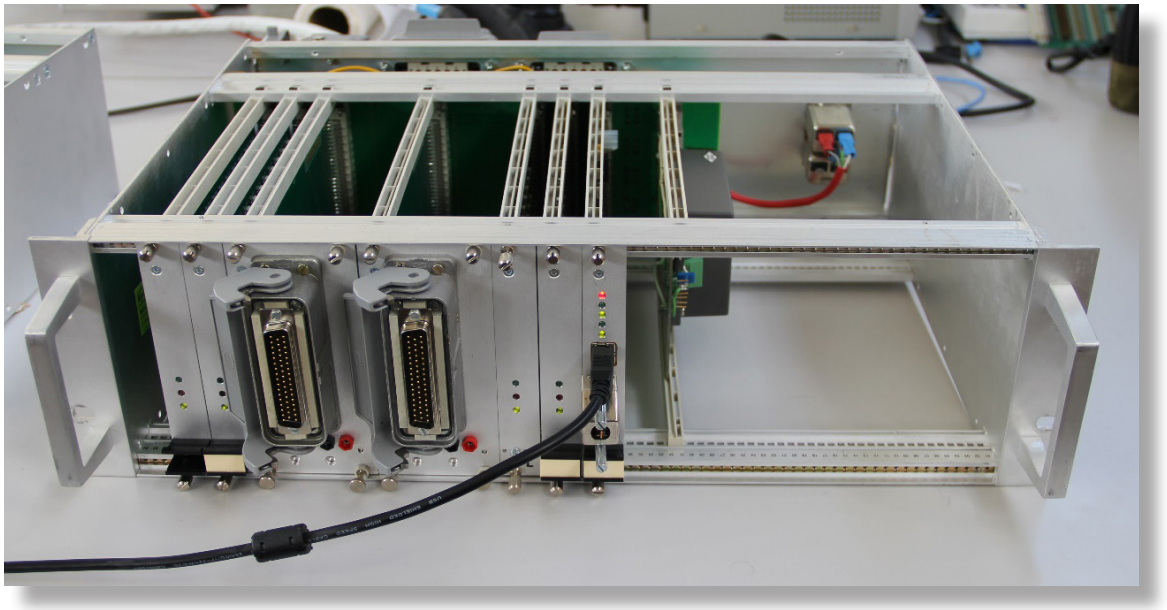

Fig. 6 *Prototype of the Arc Interconnection Verification measurement system during tests (Image copyright: DAI).*

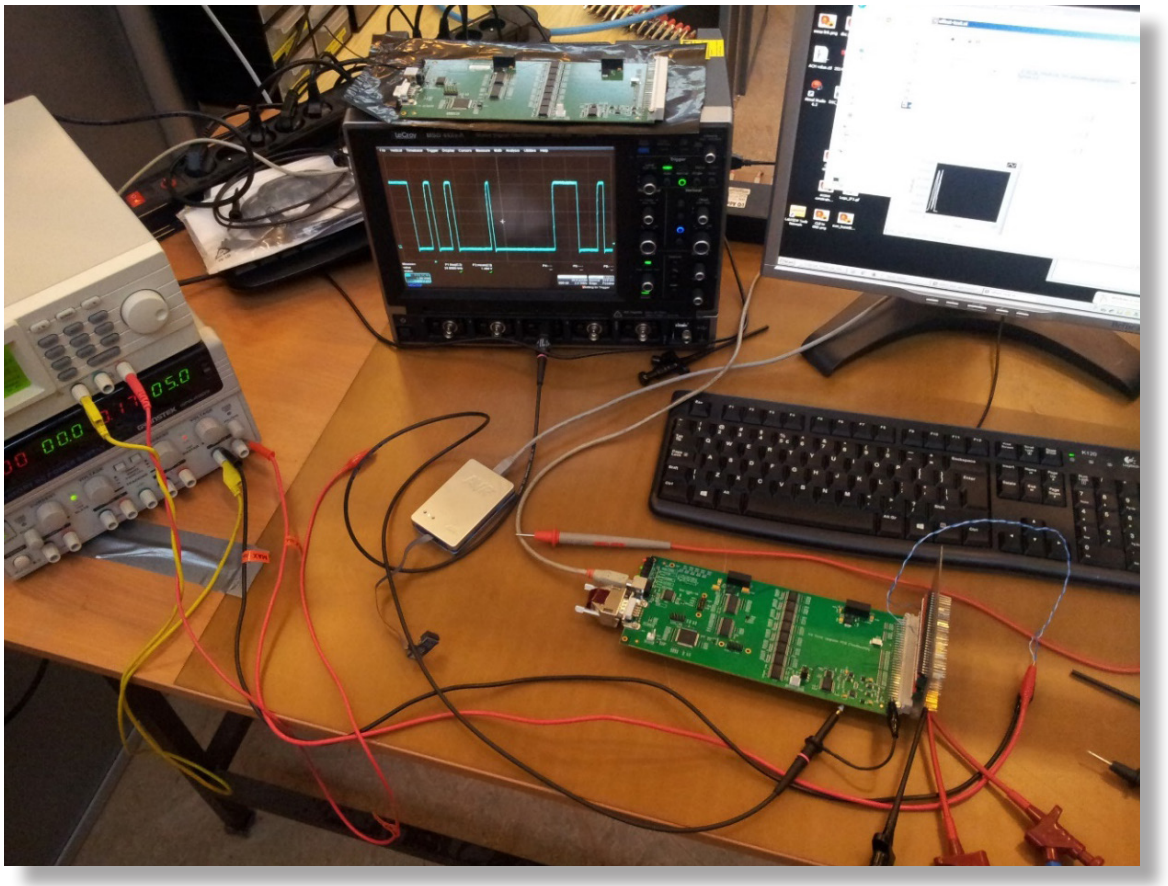

Fig. 7 *Data acquisition board for the high voltage multichannel insulation tester (Image copyright: DAI).*

A novel technology for the production of mirrors for the **Cherenkov Telescope Array** has been developed at IFJ PAN. The mirrors are designed for the medium-size telescopes (MST). They are made by cold-slumping of the front reflecting aluminum-coated panel and the rear panel interspaced with aluminum spacers. Each panel is built of two glass panels laminated with a layer of fiber-glass tissue in between for reinforcement of the structure against mechanical damage. The mirror structure is open and does not require perfect sealing needed in closed-type designs. It prohibits trapping of water inside and enables proper ventilation of the mirror to be achieved.

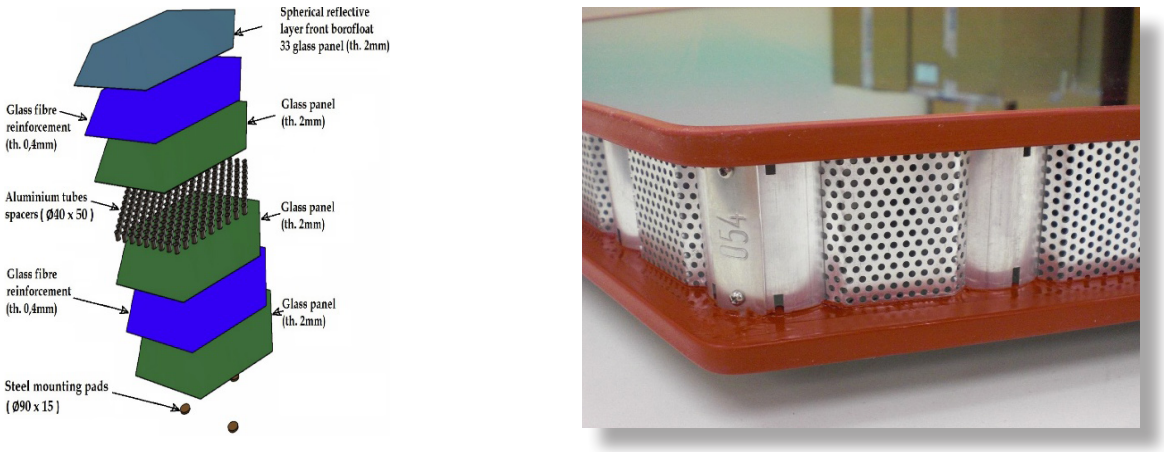

Fig. 8 *Principles of IFJ PAN technology applied to MST mirrors (left); Detail of assembled MST mirror (right) (Image copyrights: DAI).*

One hundred full-size hexagonal (1.2 m flat-to-flat, 32.14 m curvature radius) prototype mirrors for the MST have been produced during the last 12 months. The mirrors were tested on an optical test-bed at IFJ PAN. They show excellent optical properties, fulfilling CTA specifications. In particular, the point-spread function (PSF) at double focal distance is limited to 18 mm. The average deviation of the radius of curvature from its nominal value in serially produced mirrors is only by ±5 cm. The mirrors have been shipped for further optical tests to European laboratories associated with CTA. They will also undergo climate-chamber tests and will be installed in the MST prototype being constructed in Berlin. The mirror production technology is under preparation for transfer to industry where mass-production of CTA mirrors would be continued.

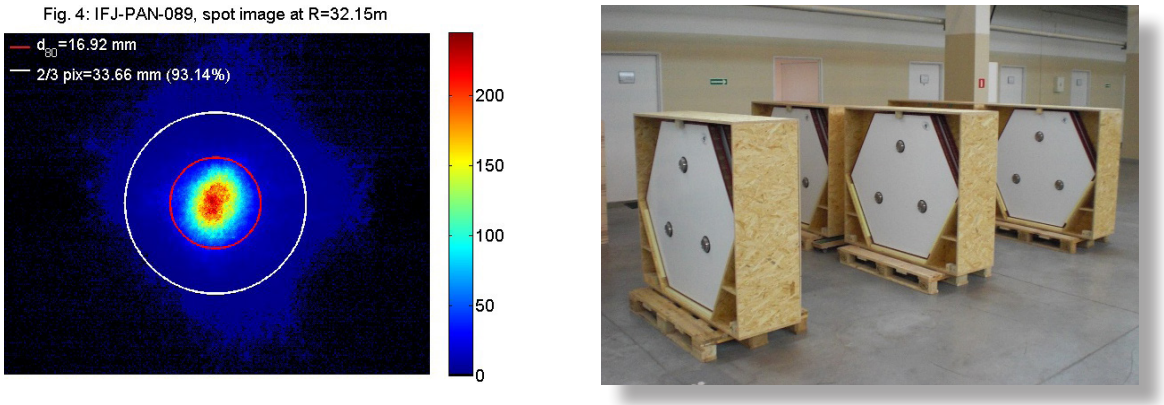

Fig. 9 *An example of measurement of an MST mirror performed at IFJ PAN (left); MST mirrors ready for shipment (right) (Image copyrights: DAI).*

A single-mirror small-size (SST-1M) telescope has been constructed by a consortium of Polish, Swiss, and Czech institutions as a prototype for one of the proposed telescopes for the new-generation ground-based **Cherenkov Telescope Array**, of a TeV gamma-ray observatory. The telescope has a 4 m diameter reflector of focal length 5.6 m,. The drive system is based on a pair of slew drives with twin servo-motors. It will be equipped with a novel fully digital camera based on silicon photomultipliers. The mechanical structure and the drive and its control system of the SST-1M telescope have been designed at DAI in collaboration with the Department of Gamma-ray Astrophysics (NZ12) and the DESY-Zeuthen team that had developed the medium-size telescope (MST). The telescope frame was produced by Ponar Sp. z o.o. in Żywiec and installed at a test site at IFJ PAN in late 2013. Over the years 2014-2016 the telescope was equipped with drive control and safety systems, cabling, a complete set of 18 hexagon-shaped mirrors with the mirror control system, and auxiliary components for mirror alignment and a telescope pointing system. The structure underwent numerous tests, including surveying measurements of structure deformations, measurements of the tensile forces in the mast's rods, full modal analysis of telescope vibrations, and tests of the control software to verify the correct functionality of the drive and safety system components, drive modes, and safety and emergency procedures. The tests performed so far prove that SST-1M is viable solution for the small-size telescope of the CTA.

Fig. 10 *The SST-1M prototype at IFJ PAN site equipped with a set o 18 mirrors and two CCD cameras (left); mirror mounts with actuators (centre); docking station (right) (Image copyrights: E.Mach, J.Niemiec ON 1)*

Since 2014 DAI has been involved in two projects supported by F4E (Fusion for Energy - European Union Joint Undertaking for the **International Thermonuclear Experimental Reactor** and the Development of **Fusion Energy**): the Radial Neutron Camera (RNC) project led by ENEA in Frascati, Italy and the High Resolution Neutron Spectrometer (HRNS) led by IFJ PAN. The RNC is one of the plasma diagnostic systems dedicated to ITER. The whole RNC project is sub-divided into parts called specific grants (SG). Over the years 2014-2016 DAI engineers were involved in three specific grants, namely SG01: Planning Phase, SG03: System Level Design for Radial Neutron Camera and SG05: High Priority Prototype Testing in support of System Level Design development of the ITER Radial Neutron Camera.

Within SG01 and SG03 DAI was involved in the review of ITER requirements, preparation of documentation as well as development and design of selected RNC sub-systems. During this phase the DAI engineers:

- prepared thermo-mechanical and electromagnetic codes and performed numerical calculations of RNC components,
- developed the design and performed numerical simulations of a prototype of a cooling system for the RNC detectors,
- developed several concepts of adjustable collimators and their drive systems.

Within SG05 DAI engineers developed the design concept of Adjustable Collimators. The Adjustable Collimator is a component to be installed inside the Line of Sight (LoS) in the so-called Ex-Port of the RNC. These adjustable collimators provide a different cross-section of the area observed by neutron detectors. The number of adjustable collimators corresponds to the available number of LoS.

Within this specific grant the DAI engineers :

- selected and developed two designs of adjustable collimators;
- prepared detailed technical specifications of adjustable collimators;
- produced a final concept design of the adjustable collimator (see Fig. 11).

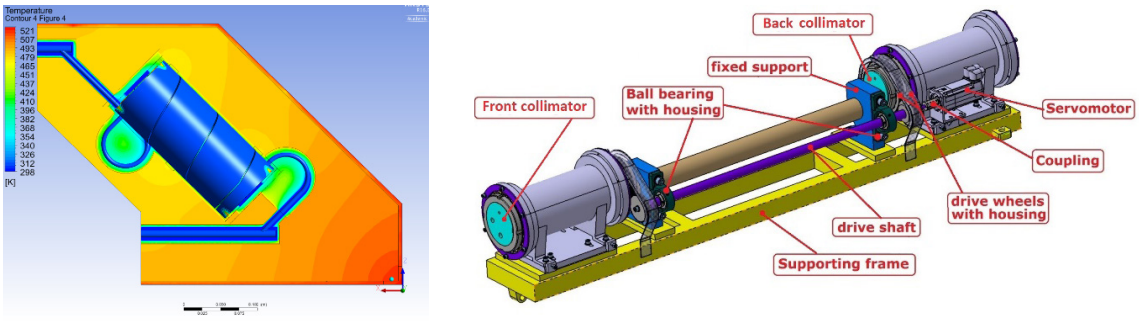

Fig. 11 *Temperature distribution in the detector cassette (left); design concept of the adjustable collimator system (right) (Image copyrights: DAI)*

The activities of DAI within the HRNS project are presented in the report of the Division of Interdisciplinary Research.

VIII. ACCREDITED LABORATORIES

The accredited laboratories at the Institute of Nuclear Physics of the Polish Academy of Sciences (IFJ PAN), apart from internal services, offer their external customers certified measurements of radioactivity and of spectra of radiation isotopes in the air, soil, or water. A regular dosimetry service is available for evaluating individual occupational and environmental exposure to radiation workers at IFJ PAN and also to external radiation workers and customers, especially in hospitals and in radiation industry. Routine calibration of all electronic radiometers which measure the activity of gamma-, alpha- and beta-ray sources, is available. To provide such services, it is mandatory that all measurement procedures are accredited to conform with the PN-EN-ISO/IEC 17025 laboratory standard. The process of accrediting all IFJ PAN measurement laboratories to this international standard commenced at the beginning of 2002, in compliance with the Polish Atomic Law and with European (EU) regulations. At present, there are four accredited laboratories at the IFJ PAN offering a broad range of radiometry services: the Laboratory for Calibration of Dosimetry Instruments (NLW), the Laboratory of Individual and Environmental Dosimetry (NLD), the Laboratory of Radiometric Expertise (NLR), and the Laboratory of Radioactivity Analyses (NLP).

LABORATORY FOR CALIBRATION OF DOSIMETRY INSTRUMENTS – NLW

wzorcowanie.ifj.edu.pl

This laboratory performs calibration of radiation survey meters in terms of air kerma rate and in terms of radiation protection quantities, using 137Cs γ-rays. Calibration is also performed in terms of surface activity (^{239}Pu and ^{241}Am α-particles and ^{90}Sr/^{90}Y, ^{36}Cl and ^{14}C β-particles). The laboratory is equipped with a gamma-ray irradiator containing three remotely interchangeable ^{137}Cs sources of nominal activities 1.96 TBq, 25 GBq and 250 MBq. Using this irradiator and a 7 m-long calibration bench, it is possible to obtain calibrated dose rates ranging between 1 μGy/h and 1 Gy/h. Each year the laboratory calibrates up to 1000 survey meters for customers from all over of Poland. Besides calibrating survey meters, the laboratory also calibrates passive individual and environmental dosimeters in terms of kerma in air, Hp(10). Hp(3) and Hp(0.07).

LABORATORY OF INDIVIDUAL AND ENVIRONMENTAL DOSIMETRY – NLD

ladis.ifj.edu.pl

The Laboratory of Individual and Environmental Dosimetry (LADIS) consists of two sections. The Section of Dose Control performs measurements of individual and environmental doses using the thermoluminescence method first developed at IFJ in the 60's of the past century. Most of the

measurement services concern individual dosimetry of workers exposed to ionizing radiation (measurements of Hp(10) , Hp(0,07), Hp(3)) and measurements of K_{air} in environmental monitoring. Currently, LADIS performs over 50000 measurements yearly for individual radiation workers and in locations at working areas or in the natural environment locations, for over 8400 institutions in Poland. The other section of the LADIS laboratory offers Quality Assurance services by performing quality control tests of medical X-ray equipment for radiography, fluoroscopy, mammography, for dental and panoramic dental systems and for computed tomography units. Following the changes in national law, in 2016 the Laboratory extended its accreditation to digital mammography, digital radiography and dental CBCT systems. Accreditation has also been extended to biological dosimetry services based on the occurrence of dicentric chromosomes.

LABORATORY OF RADIOMETRIC EXPERTISE – NLR

radon.ifj.edu.pl

The Laboratory of Radiometric Expertise continues its research activities in the following general fields: physics of natural radioisotopes, high-sensitive, low-background measurements of gamma isotopes in environmental samples, investigation of indoor radon and of factors affecting the quality of indoor air (IAQ).

The research staff of the Laboratory has participated in the following research grants:

- The influence of indoor air parameters on the dynamics of radon and its progeny concentrations', 2011-2015 (National Science Centre, contract no. 7454/B/TO2/2011/40);
- "Radon in thermal waters and radon risk in chosen thermal water spas in V4 countries"; V4 Project, 2014/2015 (International Visegrad Fund)
- "Indoor radon and health risk assessment for children and staff in kindergartens in V4 countries" V4 Project, 2015/2016 (International Visegrad Fund)
- "Technologies supporting the development of safe nuclear power" financed by the National Center for Research and Development (NCBiR). Research Task "Development of methods to assure nuclear safety and radiation protection for current and future needs of nuclear power plants", 2012-2014 (contract No. SP/J/6/143339/11)

The Laboratory offers a broad range of accredited methods of measuring radioactivity in the environment:

- measurements of concentration of natural gamma-ray isotopes (Ra-226, Th-228, K-40) in solid samples using low-background gamma spectroscopy,
- measurements of radon Rn-222 concentration in liquid samples using alpha-ray spectroscopy,
- measurements of radon Rn-222 concentration (indoor, outdoor and in soil gas) using alpha-ray spectroscopy and CR-39 track detectors.

A unique mobile laboratory (the CHIMERA Laboratory, sponsored by European Union funds), able to measure environmental gamma-ray dose rates and to perform gamma-ray spectrometry *in-situ*, as well as to measure locally radon concentration in air and in water, which is of potential application to the Polish nuclear power programme under development.

In May 2015 the Laboratory of Radiometric Expertise organized the IInd International Conference "Radon in the Environment 2015", in Kraków, Poland. This meeting gathered over 120 participants from 26 countries (including Brazil, China, India, Japan, Kuwait, Morocco, Russia). In November 2015 the Laboratory of Radiometric Expertise organized the first "European Radon Day" in Krakow, in the form of a research and training session to educate the public and local authorities on the issues of radon. Over the years 2014-2016 the staff of the Laboratory published 10 research articles in international peer-reviewed scientific journals, published 12 other reports, and delivered 20 conference presentations. Also, 444 reports of measurements and 11 expert radiometry analyses for 46 customers were issued over that period.

Staff members of the Laboratory were invited to the expert group at the National Atomic Energy Agency which developed an implementation of EU Directive 2013/59/EURATOM to the Polish Atomic Law, and to the expert group at the Ministry of Energy which developed the Polish Nuclear Power Programme.

LABORATORY OF RADIOACTIVITY ANALYSES – NLP

lap.ifj.edu.pl

The expertise within the Laboratory of Radioactivity Analyses stems from several years of research on environmental radioactivity following the Chernobyl accident in 1986. In 2008 the Laboratory was accredited by PCA (No. AB 979) to conform with the ISO 17025 laboratory standard for measurements of gamma-ray emitters, among them 137Cs, in different materials. In 2013 the PCA accreditation was extended to measurements of plutonium by means of alpha-ray spectrometry in radio-chemically prepared samples. The Laboratory is equipped with four low-background HP germanium detector gamma-ray spectrometers and with several alpha-ray spectrometers with semiconductor detectors. This accreditation assures the compatibility and high credibility of measurements within the Polish national monitoring system. Measurements of several different types of samples can also be performed for external customers.

Fig. 1 *The main office of LADIS Dosimetry laboratory.*

Fig. 2 *Presentation of individal dosemeters for whole body (red one) and for eye-lens.*

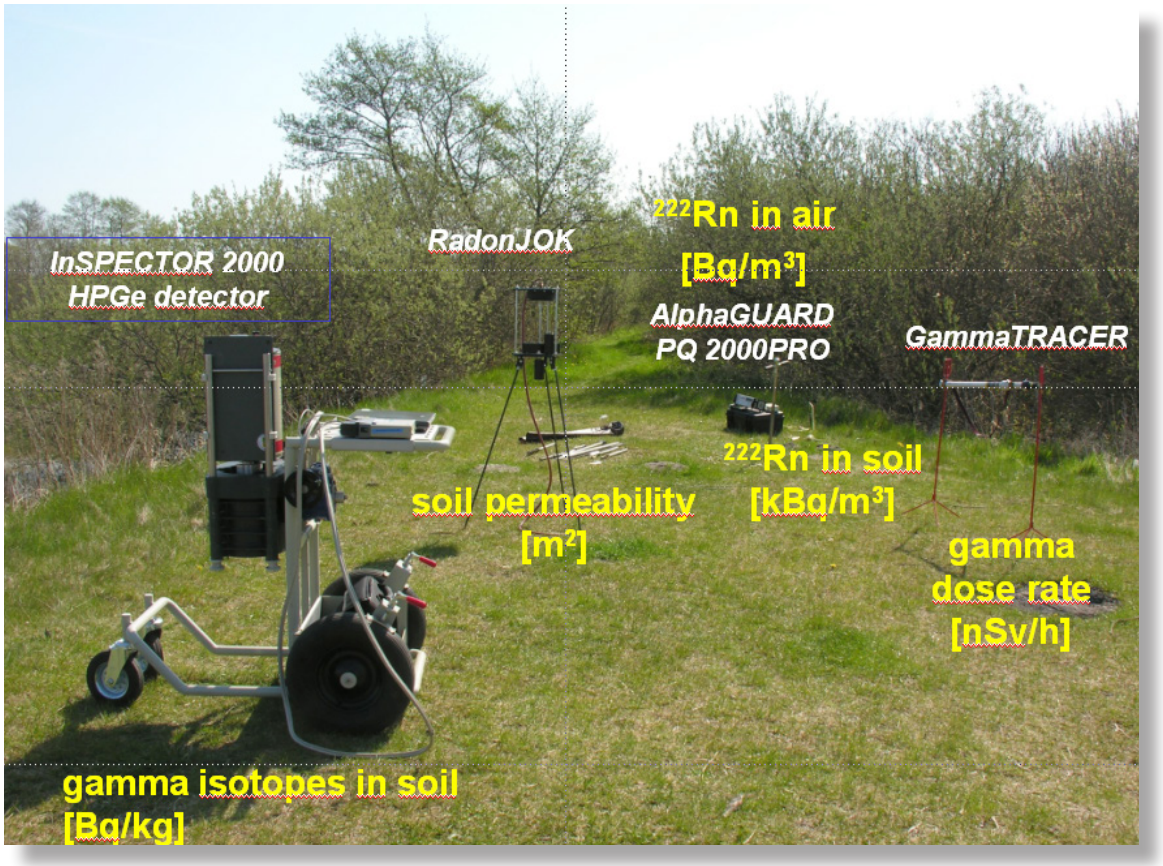

Fig. 3 *Different types of radioactivity measurements in the environment made by LER IFJ PAN.*

IX. INTERNATIONAL POST-GRADUATE STUDY COURSE

Doctoral studies at the Institute of Nuclear Physics were launched in 1984 and since that time the Scientific Council of the Institute has granted Ph.D. degrees in physics to more than 210 young scientists (47 in the years 2014-2016). Our graduates work in scientific and commercial institutions all over the world, up to now five of them have been distinguished obtaining full professor's title and more than twenty have the habilitation degree in physics (9 our former PhD students obtained it in the years 2014-2016). Realizing our PhD programme we cooperate closely with the Tadeusz Kościuszko Cracow University of Technology and with the University of Rzeszów. In 2009 we started the collaboration in the field of interdisciplinary PhD programmes linking research in physics, chemistry and life sciences. Our first common PhD-level educational project "Interdisciplinary PhD Studies: Advanced Materials for Modern Technology and Future Energy Production <ISD>" was prepared together with the AGH University of Science and Technology and the Jerzy Haber Institute of Catalysis and Surface Chemistry of the Polish Academy of Sciences. Project obtained financial support from the EU Operational Programme Human's Capital and had been successfully realized in the years 2009-2015. Within the project 15 PhD students completed and defended their theses in our Institute. In 2016, collaborating with just mentioned our long-time partners and also with the Institute of Pharmacology of the Polish Academy of Sciences, Collegium Medicum of the Jagiellonian University, Chemistry Faculties of the Jagiellonian University and the AGH University of Science and Technology and the Faculty of Material Engineering of AGH, we successfully applied for two new interdisciplinary PhD programmes named "Physics, Chemistry and Biophysics for New Materials and Technologies <FCB>" and "Interdisciplinary Research for Innovative Medicine <InterDokMed>". Both our projects won national competition and are qualified to be financially supported by the EU Operational Programme "Knowledge-Education-Development" <PO WER>. The projects will start in autumn 2017 and are scheduled for four years during which students are obliged to complete and defend their theses.

Prospective candidates to all types of PhD Studies held in our Institute are required to be university graduates with a M.Sc. degree in physics or with a M.Eng. degree in physics-related discipline of applied science. To be enrolled to the PhD studies the candidates have to pass the entrance exams in physics and English language and have to be accepted by a senior scientist (full or associate professor) who in the future will become the supervisor of the thesis. Our PhD studies are opened for foreign students and well prepared to enroll them. Currently we have 7 (10% of the total number) foreigners: 2 persons from Italy and Iran, 1 from France, Ukraine and Belorussia. Available subjects of study cover all areas of research performed at the Institute: theoretical and experimental investigations of fundamental interactions (nuclear and high energy physics) as well as theoretical and experimental investigations of condensed matter and atomic physics, astrophysics and foundations of physical theories including mathematical methods of physics. Important elements of our scientific offer, closely related to life sciences, are investigations of dynamical systems governing the behavior of complex phenomena, computer modelling of structural and dynamical properties of condensed matter, physical methods used to investigate polymers, biological and biomedical applications of Magnetic Resonance Imaging and other tomography methods, development of radioisotopes for biomedical sciences, application of radiation in medical diagnostics and therapy, ultra-sensitive detection methods applied to biology, material science and environmental studies, ion implementation in the preparation of new materials. During last years we have been used to put special emphasis on interdisciplinary research leading to possibly wide practical applications and on research done in interinstitutional and international cooperation. An illustrative example of the latter is the PhD programme "Copernicus Doctorate in Physics" agreed and signed in 2014 by our Institute and the University of Ferrara in Italy. Its aim is realization of research supervised by two tutors and leading to the PhD degree awarded by both institutions. Currently four such individual projects are going on and expected to be completed in 2017 and in first half of 2018.

In the years 2014-2016 our PhD students achieved numerous successes – Dr Agnieszka Dziurda got the LHCb Collaboration PhD thesis award for the thesis defended in 2015, Dr Justyna Bobrowska was awarded the Polish Prime Minister Prize for the best doctoral thesis defended in 2016 while Dr Paweł Janowski got in 2014 the Krzysztof Ernst Prize awarded by the Polish Physical Society for outstanding achievements in popularization of science. Our PhD students successfully applied for grants: 22 of them obtained Preludium grants for preparing PhD theses while 7 got Etiuda grants for continuing thesis-related research in foreign laboratories; both types of grants awarded by the State Scientific Council.

X. OUTREACH ACTIVITIES – PROMOTION AND EDUCATION IN SCIENCE

Over the past two years 2014-2016 the Institute of Nuclear Physics PAN has continued its efforts to acquaint students, primary and secondary schoolchildren, and the general public with science, especially in the area of physics, in a popular and instructive manner, aiming at attracting them to physics and at showing the role science plays in modern society.

Traditionally, an important element of the Institute's outreach agenda has been active participation in regular large-scale public events aimed at popularizing science by attractive forms of its presentation. Some of these events, organised every year together with other scientific institutions in the local Małopolska region and in other regions of Poland, were:

» The "Science Festival" in Krakow,
» The "Małopolska Researchers' Night",
» The Warsaw "Science Picnic of the Polish Radio and the Copernicus Science Centre",
» "Explorer's Day – The Science and Technology Festival" in Rzeszów.

Such large-scale events, typically arranged in large concert halls, stadiums or outdoors, with exhibitions and demonstrations arranged in tents, stands or exhibition booths allotted to different research institutions, attract thousands of visitors and are highly appreciated by the public. The impact of these events is further enhanced by radio or TV reporting and by reports and reviews in daily newspapers. Over the years 2014-2016, IFJ PAN regularly participated in all of the above-mentioned large-scale events.

Among other outreach activities organised by IFJ PAN in the years 2014-2016 were:

- Guided visits to selected laboratories of the Institute. Such visits are arranged throughout the year for small groups of students and schoolchildren, enabling them to visit the Institute's laboratories which are all closed to the public for safety reasons. The Institute hosted over 3300 such visitors over the past three years. In the year 2016 our Institute was visited by a total number of 1165 visitors in 45 organised groups.

- Every year, in collaboration with the International Particle Physics Outreach Group (IPPOG) and CERN, the Institute organised an International Workshop on Particle Physics for second-grade school children ("International Master Classes – Hands on Particle Physics") for hundreds of schoolchildren in several towns in Southern Poland. The number of participating students had increased from 260 in 2014 to 427 in 2016. In 2015 this workshop was supported by a grant from the Foundation for Polish Science (FNP) obtained as an award for the project „Become a Particle Physicist for one day" in the eNgage call. In 2016 partial support was granted by the Committee of Physics of the Polish Academy of Sciences. Later in the same year the Institute was asked to organise an IPPOG meeting in recognition of its active participation in this outreach programme.

- The Institute has also organised workshops for second-grade school children. The project "Play Science" took place in Bielsko-Biała in 2014 (zagrajwnauke.ifj.edu.pl) and was supported by another grant from the FNP awarded within the eNgage call. Two workshops with the same title "Particle physics", but slightly different programmes, were organised in Kraków in 2014 (warsztaty.ifj.edu.pl), and in Sandomierz in 2015 (sandomierz.ifj.edu.pl). In each workshop schoolchildren competed in solving a physical problem. The workshops consisted of several sessions held over 3-6 days, with lectures on elementary particle physics, some practical sessions involving data analysis or work with electronics, performed by participants in a competitive manner. Following these workshops, the six best and most talented schoolchildren were invited to the Institute for one month in 2015 to participate in the "Particle Physics Laboratory" summer school.

Fig. 1 *Workshop for teenagers: "Physics of Elementary Particles Sandomierz 2015".*

- The "LHC – student internship, Particle Physics Laboratory" has been organised at the Institute since 2014. This is a summer school with a student programme on particle physics. During the first week, university students attend lectures and take part in hands-on working classes. The remaining two or three weeks are devoted to different tasks usually involving analysis of data from Large Hadron Collider experiments by students under direct supervision of the scientific staff of the Institute. Usually about 50 university students take part in this programme.

- In May 2014, for the first time, an Open Day of the National Centre for Hadron Radiotherapy: Cyclotron Centre Bronowice (CCB) at IFJ PAN was organised. This gave the general public an opportunity to visit this modern therapeutic and scientific centre just after its completion. During that day, CCB hosted over 300 visitors, all of whom expressed their high appreciation of the Centre's equipment and of its medical and research programme. Since then, over the following years, CCB always attracted a large group of visitors within the yearly "Małopolska Researchers' Night".

- Within the yearly "European Radon Day" event, popular science sessions were organised at IFJ PAN in 2015 and 2016. These sessions were addressed to the local public and to local authorities. Their main goals were to make people aware of the universal presence of natural radioactivity (especially radon) in their environment, to present methods of measuring radon concentration and to inform of possible health hazards of radiation. The sessions were usually attended by about 100 participants.

The 60th anniversary of the foundation of the Institute in 2015 presented an opportunity for particularly extensive outreach activities over the years 2014-2016, with special events accompanying the "Małopolska Researchers' Night" held on the premises of IFJ PAN. Other Jubilee festivities included a one-year science promotion programme entitled "The First 60 Years of the Institute of Nuclear Physics":

- A cycle of shows entitled "IFJ for children" began at the end of 2014 and ended at the beginning of 2016. The author of these shows and their main animator was the nationally renowned radio and TV producer Wiktor Niedzicki. The shows illustrated and explained laws of physics and physical phenomena observed in everyday life, several of which involved active participation of children in the audience in experiments performed on stage. Not surprisingly, these shows met with great applause and were viewed by a total of over 7700 children and young people.

Fig. 2 *"IFJ for Children" – science show by Wiktor Nidzicki, fot. Michał Kądziołka.*

Fig. 3 *"IFJ for Children" – science show by Wiktor Nidzicki, fot. Marcin Perzanowski.*

- The show „*Stardust*" within the series "*Physics – the greatest show of the Universe*", written, directed and produced by Jerzy Gręboszz, associate professor at IFJ PAN, was widely recognised and applauded. This performance was shown in 2015 at the Kraków Congress Centre (ICE) to an audience of some 1800 persons, most of whom were schoolchildren from primary and secondary schools in Krakow.

Fig. 4 *The play "Gwiezdny pył" – Jerzy Gręboszz, ICE 2015, fot. P. Jochym.*

Fig. 5 *The play "Gwiezdny pył" – Jerzy Gręboszz, ICE 2015, fot. P. Jochym.*

Fig. 6 *The play "Gwiezdny pył" – Jerzy Gręboszz, ICE 2015, fot. S. Kwieciński.*

- To celebrate its 60th anniversary, two popular science publications were published by the Institute: a book entitled „Telephoto. A view of science", and a booklet describing simple physics experiments, entitled „New Wictor's laboratory. Tricks for children (and adults)". Both publications were authored by Wiktor Niedzicki. These books were freely distributed at all science promotion events organised by the Institute, and were also sent out to schools and to anyone interested.

At the Institute, each year there is a considerable effort to prepare an interesting programme for the "Małopolska Researchers' Night" event. At the Institute's premises a broad popular science programme is organised, showing how scientists explore and change the world. In tents, situated over the green areas of the Institute, the latest achievements of the Institute in all major areas of our research are presented and are well received by the audience. In addition, visitors can enter selected laboratories at the Institute. A telebridge specially prepared for the occasion allows visitors at the IFJ PAN to observe experiments conducted

at the Large Hadron Collider (LHC) at CERN (Geneve). Visitors may also attend special lectures, some spectacular demonstrations of physics experiments, or "Physics tricks" which often explain physical phenomena governing everyday life observations. Competitions for the audience and an urban field game "Physics paper chase", with winners rewarded by small gifts, accompany these shows and lectures.

Fig. 7 *Physics Tricks – show during..., fot. S. Kwieciński.*

Fig. 8 *Physics Tricks – show during..., fot. Ryszard Duława.*

The spectacle "Stardust" produced and directed by Jerzy Gręboszz, with IFJ PAN scientists as its actors, was shown at each edition of the "Małopolska Researchers' Night" and was always enthusiastically received by large crowds of spectators.

To the older audience the "Physics for adults" another programme was presented, a series of shows and funny stories. The auditorium was filled to the brim despite the late night hours at which this production was shown.

Every year, the "Małopolska Researchers' Night" event attracts over 1000 persons – science enthusiasts – to the IFJ PAN laboratories. Some 160 of the research staff and other employees of the Institute contribute each year to the success of this event.

Fig. 9 *Małopolska Researchers' Night 2014, fot. Ryszard Duława.*

Fig. 10 *Małopolska Researchers' Night 2016, Physics demo on superconducting levitation and other tricks in liquid nitrogen temperature, fot. S. Kwieciński.*

In 2016 the "Stardust" spectacle was also presented in Dukla (Podkarpackie region) for several hundred schoolchildren.

Over the years 2014-2016 on many occasions the outreach work in science education of several members of the Institute's research staff has been recognised by individual awards, prizes and distinctions. Dr Maciej Trzebiński (2014), Dr Michał Krupiński (2015) and Dr hab. Krzysztof Woźniak (2015) were awarded special grants in the eNgage call organised by FNP (Foundation for Polish Science). These awards included support for workshops for high school students on particle physics and optics and enabled two internet-based games to be created. The game "Optical quantum game" demonstrates the basic principles of quantum optics and photonics. The game "Quarks" explains how quarks, never observed as free particles, form hadrons which are observed.

In 2015 Dr. Paweł Janowski, E. Eng. received a medal and the prestigious Krzysztof Ernst Award from the Polish Physical Society for his individual, extensive and varied activities in popularising physical sciences.

On several occasions IFJ PAN scientists were invited by various organizations and associations (including TEDx Warsaw, the Children's University, University and school science Clubs, festivals and science picnics etc.) to deliver popular lectures on science. They also gave interviews on TV, were invited as special guests or commentators to radio programmes, and published popular articles on physics in the Internet and in Polish popular magazines. For example, Dr Michal Krupiński produced four short movies of IFJ PAN laboratories within the ADAMED Fundation programme. All of these movies are available on the SmartUp web page. Additionally, he co-authored short popular-science movies (available on You Tube), which are part of the Experimentum Simplex programme funded by the Polish Ministry of Science and Higher Education. Dr Krupiński was also invited to several popular TV programmes such as "Sonda 2" (Polish Television Program 2) or „Quarrels of Scientists" (NC+ Planete+).

ISSN: 2544-5162